FOSSIL ENERGY

DOE/BC/15111-1
(OSTI ID: 756541)

RESPONSIVE COPOLYMERS FOR ENHANCED PETROLEUM RECOVERY

Annual Report
September 1999

By
Charles McCormick
Roger Hester

Date Published: June 2000

Work Performed Under Contract No. DE-AC26-98BC15111

University of Southern Mississippi
Hattiesburg, Mississippi

National Petroleum Technology Office
U.S. DEPARTMENT OF ENERGY
Tulsa, Oklahoma

DOE/BC/15111-1
Distribution Category UC-122

Responsive Copolymers for Enhanced Petroleum Recovery

By
Charles McCormick
Roger Hester

June 2000

Work Performed Under Contract No DE-AC26-98BC15111

Prepared for
U.S. Department of Energy
Assistant Secretary for Fossil Energy

Jerry Casteel, Project Manager
National Petroleum Technology Office
P.O. Box 3628
Tulsa, OK 74101

Prepared by
University of Southern Mississippi
Department of Polymer Science
Box 5157
Hattiesburg, MS 39406

TABLE OF CONTENTS

LIST OF TABLES

LIST OF FIGURES AND SCHEMES

ABSTRACT

A coordinated research program has been initiated with the aim of developing environmentally responsive copolymers for Improved Oil Recovery (IOR). These novel polymer systems possess amphipathic microstructures which allow reversible pH-, salt, shear-, or temperature-responsiveness in aqueous media. Viscosity, fluid flow behavior, polymer interactions with reservoir rock and entrapped oil, and phase behavior can be changed by altering pH or salt concentration or by adjusting flow rates. The objectives of this work are to: synthesize responsive, amphiphilic systems; characterize molecular structure and solution behavior; measure rheological properties of the aqueous fluids including behavior in fixed geometry flow profiles and beds; and to tailor final polymer compositions for *in situ* rheology control under simulated reservoir conditions. This report focuses on a) synthesis, characterization, and photophysical studies of these polymer systems forming polysoaps or associative thickeners and b) development of procedures and an apparatus for measuring extentional flow. Polymers have been prepared from n-octyl sustituted maleic acid/ethyl vinylethers (C8MAEVE), acrylamide/11-acrylamideo-undecanoate (AMSA), and acrylic acid/acrylamide/hexyphenyl acrylamide (HPAM). A model for extensional fluid flow through beds of large mesh screens has been developed. Additionally, a rheometer using screens has been constructed for measurement of extensional flow behavior for mobility control polymers. Initial measurements have been made on controls and two copolymers recently synthesized in our labs.

CHAPTER 1: EXECUTIVE SUMMARY: BACKGROUND, OBJECTIVES, AND OVERVIEW OF RESEARCH DURING FY 1999

Introduction

A coordinated research program has been initiated with the aim of developing environmentally responsive copolymers for Improved Oil Recovery (IOR). These novel polymer systems possess amphipathic microstructures which allow reversible pH-, salt, shear-, or temperature-responsiveness in aqueous media. Conformational reordering in response to such controllable variables can result in substantial changes in viscosity and phase behavior. These characteristics are of potential utility in controlling both fluid mobility and conformance, particularly for *in situ* processes. Responsive polymers have attributes that should overcome limitations inherent in even the best conventional IOR polymers. Salt- and pH "triggers" strategically placed along the macromolecular backbone determine hydrodynamic volume and, thus, rheological behavior. Viscosity, fluid flow behavior, polymer interactions with reservoir rock and entrapped oil, and phase behavior can be changed by altering pH or salt concentration or by adjusting flow rates. Polymers are targeted to act alone or with surfactant to significantly alter fluid flow through porous media. Both viscosity of the fluid and permeability of the substrate to the aqueous phase can, in principle, be altered.

Research Objectives

The objectives of this work are to: synthesize responsive, amphiphilic systems; characterize molecular structure and solution behavior; measure rheological properties of the aqueous fluids including behavior in fixed geometry flow profiles and beds; and to tailor final polymer compositions for *in situ* rheology control under simulated reservoir conditions. This report focuses on the first phase of our research emphasizing synthesis and the development of photophysical techniques and rheological means of following segmental organization at the structural level.

Responsive Polymers: Synthesis, Characterization, and Behavior in Aqueous Media

A. N-Octylamide Substituted MAEVE Polymers. Our initial work targeted terpolymers prepared from maleic anhydride (MA) and ethylvinyl ether (EVE) which were subsequently reacted with n-octylamine and then hydrolyzed. We postulated that these polymers might be capable of playing the key roles of viscosifier and surface active agent in mobility control. Such polymers might be formulated without conventional surfactant, avoiding the problem of dispersion of surfactant and polymer inevitable with conventional flooding systems.

Chapters 2 and 3 detail synthesis and solution behavior studies demonstrating that n-octylamide MAEVE polymers can indeed behave as viscosifiers and polymeric

surfactants or "polysoaps" depending on terpolymer microstructure and concentration. Photophysical probes were utilized to assess "polysoap" behavior as well as responsiveness to pH and electrolyte (NaCl). The potential utility of these partially hydrolyzed n-octyl MAEVE systems would be to (under low pH or high salt conditions) serve as surfactants to reduce interfacial tension and sequester oil in the respective polymeric micelles. In the laboratory these systems can be "triggered" to change to extended chains for viscosification by lowering salinity or by increasing pH.

B. Poly(acrylamide-co-sodium 11-acrylamidoundecanoate); AMSA Polymers. A second polymer system also having potential as a polysoap and visocifier was studied (Chapters 4 and 5). Copolymers of acrylamide (AM) and sodium-11-(acrylamido)undecanoate (SA) were prepared, characterized, and their solution properties determined. Again, using viscosity and fluorescent probe techniques, we demonstrated concentration, salt, and pH dependence of the polysoap-to-polyelectrolyte transition. Fluorescence quenching and non-radiative energy transfer studies indicated that salt-induced chain contraction enhances organization into mixed polymeric micelles. Although responding as "smart" polymers to these environmental stimuli, efficient behavior in IOR might be limited by conformational constraints inherent in polymer microstructure.

C. Terpolymers of Acrylic Acid (AA), Acrylamide (AM), and N-[(4-hexyl) phenyl]acrylamide (HPAM). Copolymers of acrylic acid (AA) and acrylamide (AM) have been modified by introducting 0.5 mole % of the hydorphobic monomer N-[(4-hexyl)phenyl]acrylamide (HPAM). Incorporation of HPAM allows direct analysis of composition and determination of reversible associative interactions brought about by changes in pH or ionic strength. Chapter 6 details synthetic procedures and reports the technologically important transition from closed (micellar) to open (associative) interactions as followed by viscometry and fluorescence in aqueous media.

Characterization of Flow Behavior in Aqueous Media

In Chapter 7, a mechanical system consisting of a strain lock in parallel with a dashpot was used to model the extensional flow behavior of polymer molecular coils in dilute solutions. The model was applied to polymer solution flow through both beds of solid spheres and screens. It was predicted that the difference between screen and sphere bed interstitial channel geometries would alter the resistance of a polymer solution when propagating through these porous media. Porous media that have extensive converging and diverging channel geometries produce higher fluid extension rates during polymer solution flooding. These fluid flow conditions allow polymer coils to continually extend and recover. This recurring coil strain deformation converts fluid kinetic energy to heat and thereby reduces polymer solution mobility. This enhances oil displacement efficiency.

In Chapter 8, the construction of a screen extensional flow rheometer is discussed. This rheometer was used to determine the resistance of several dilute polymer solutions during flow through a set of screens. Most of the polymer coils did not extend at the low fluid extensional rates typically found during reservoir flooding. These polymer solutions would not be acceptable for flooding. However, AMBA and DAAM copolymer coils did extend at low fluid extensional rates. These polymers have the extensional rheology characteristics favorable for polymer flooding

Chapter 2: Nonradiative Energy Transfer Studies of pH- and Salt-Responsive Associations in Hydrophobically Modified, Hydrolyzed Maleic Anhydride-Ethyl Vinyl Ether Copolymers

Synopsis

A series of labeled, hydrophobically modified polymers based on the alternating copolymer of maleic anhydride and ethyl vinyl ether (MAEVE) has been synthesized to specifically address the issue of differences in domain organization of closed, polysoap systems and open, associative thickening systems. Modification was achieved by reaction of primary amines with MAEVE in an organic solvent and subsequent hydrolysis in aqueous base. This unique method allows stoichiometric modification with hydrophobic and fluorescent groups. Intramolecular associations predominate in a wide range of environments. The extent to which these interactions occur is effectively probed by monitoring nonradiative energy transfer (NRET) between naphthalene and pyrene groups covalently bound to the polymer chain. Intrapolymer NRET quantum efficiency increases with decreasing pH as the chain contracts to a globular conformation. Interpolymer NRET is independent of salt concentration, but intrapolymer NRET steadily increases with [NaCl] as the shielding of charge-charge repulsions constricts the coil. In extremely acidic and basic environments, interpolymer NRET increases as electrostatic repulsions are shielded or eliminated. A mechanism has been proposed whereby the compaction of labeled polymer micelles results in an enhancement in interpolymer aggregation due to the formation of hydrophobic micellar surfaces.

Introduction

In the past decade there have been a number of investigations in photophysics and photochemistry focusing on water-soluble polymers with pendent hydrophobic aromatic groups.[1,2,3,4,5] Amphiphilic polyelectrolytes functionalized by hydrophobic groups are of great interest because of their scientific and technological significance.[6] It is possible to elucidate the relationship between macroscopic and microscopic properties with photophysical techniques due to the sensitivity of "reporter" chromophores attached to the polymer chain. Changes in polymer conformation, microenvironment, and chain dynamics are reflected by the photophysical response.[7]

Maleic anhydride and some vinyl monomers are known to copolymerize to yield highly alternating structures.[8] These copolymers exhibit pH-responsive behavior in aqueous media. Hydrophobic vinyl mer units may aggregate to form organized domains with hydrophobic cores and charged interfaces. The hydrophilic maleic acid groups promote water-solubility.[9,10] Morishima and Webber studied the photophysical behavior of poly (maleic acid-*alt*-vinyl naphthalene)[11,12,13,14] and poly (maleic acid-*alt*-vinyl carbazole)[15,16] and observed pH-dependent fluorescence behavior. Naphthalene excimer emission was shown to vary with pH as was the

intensity of carbazole fluorescence emission. Energy transfer from carbazole[15,16] and naphthalene[11-14] to anthracene has also been studied.

Thomas and Strauss demonstrated that maleic acid/vinyl copolymers form a compact structure at low pH in aqueous solution via intramolecular hydrophobic association.[17,18,19] Such copolymers that aggregate intramolecularly to form micellar structures have been termed "polysoaps." Fluorescence quenching studies can be designed to effectively establish the domain size as a function of pH.[18,20] Strauss and coworkers have shown that the pK_a of poly (maleic acid-*alt*-butyl vinyl ether) is at a maximum at the transition from globular to open.[18,19,21]

Nonradiative energy transfer (NRET) is a useful technique for probing intramolecular associations and structural changes in polysoaps. The photophysical phenomenon of NRET between a donor and an acceptor covalently attached to a polymer has been termed "photon harvesting" by Webber *et al.*[3] and the "antenna effect" by Guillet *et al.*[22,23,24] NRET studies, for example, have been used to probe intramolecular associations in polysoaps[9-20] as well as conformational changes and associations between polymer chains in intermolecularly associating systems.[24,25,26,27,28,29,30,31]

In this study, we consider the issues associated with structural effects on hydrophobic domain organization into intramolecular (closed) and intermolecular (open) aggregates. Elucidation of the mechanism of domain formation in these systems may allow precise tailoring of copolymers and terpolymers for use as polymeric surfactants and associative thickeners. The ability to trigger changes from "polysoap" to polyelectrolyte organization would be of enormous technological utility in enhanced petroleum recovery processes. Poly (maleic anhydride-*alt*-ethyl vinyl ether) (MAEVE) copolymers were covalently labeled with naphthalene (NRET donor) and pyrene (NRET acceptor) chromophores. Previous efforts have focused on variation of the vinyl ether to control polymer hydrophobicity,[19,21,32,33] but our research group has developed a homogeneous solution technique to stoichiometrically vary the incorporation of a hydrophobic moiety in the structure (Scheme 1).[34,35] With this technique, copolymers can readily be tailored from the same parent polymer to obtain a series of polymers with identical degrees of polymerization and varying hydrophobicity.

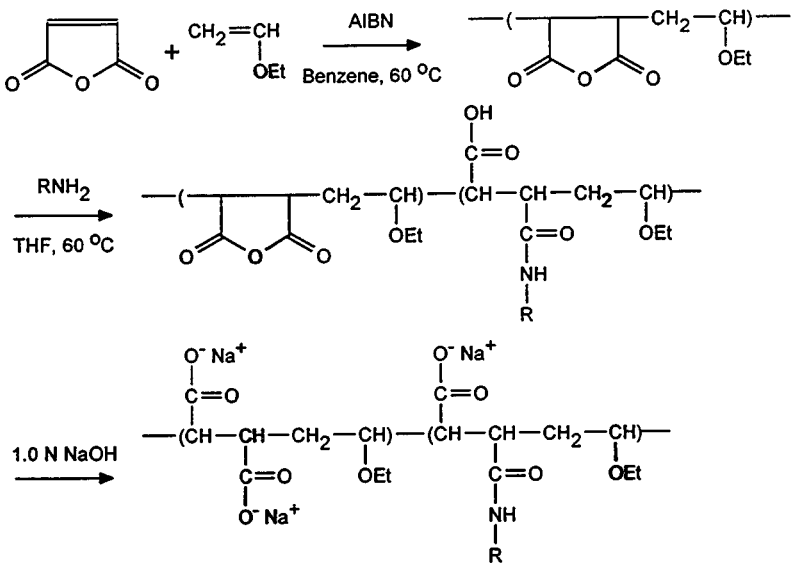

R = Octyl (C8), N1, N8, P2, P8

Scheme 2.1 Synthesis of Hydrophobically Modified Poly (Sodium Maleate-*alt*-Ethyl Vinyl Ether)s.

Viscosity, light scattering, and pyrene probe studies by our group have shown that there is a direct correlation between hydrophobicity and coil compaction. The intrinsic viscosity of hydrophobically modified, hydrolyzed MAEVE copolymers in aqueous solution has been observed to drop precipitously as substitution with octyl or dodecyl groups is increased from 20 to 30 mole %.[35] This transition parallels the polyelectrolyte-polysoap transition in quaternized poly(4-vinylpyridine)s reported by Strauss.[36] As hydrophobicity increases, intramolecular hydrophobic associative forces predominate over electrostatic forces; as a result, the polymer coil contracts, and a hydrophobic, micellar microdomain forms.

MAEVE copolymer was modified with 30 mole % octylamine prior to hydrolysis in aqueous base (Scheme 1). At this modification level, MAEVE forms a compact structure in water, as determined by rheological studies. Excimer emission studies of naphthalene-labeled MAEVE indicated that octyl incorporations up to 30 mole % allow sufficient microdomain fluidity for formation of the dimeric excited state.[35] Thus, the responsiveness of micellar domains to various environmental stimuli should be optimal. The copolymer was fluorescently labeled with 2-(1-pyrenylsulfonamido) ethylamine and 8-(1-pyrenylsulfonamido) octylamine as energy transfer acceptors; the energy transfer donors 1-naphthylmethylamine and 7-(1-naphthylmethoxy) heptylamine were also incorporated.

The naphthalene/pyrene energy transfer pair has been successfully employed by Winnik[28,29] to investigate NRET enhanced by the thermoreversible phase transition of aqueous solutions of pyrene- and naphthalene-labeled poly (N-isopropylacrylamide). Webber[37] utilized NRET studies to detect steric hindrance effects in pyrene-labeled poly (2-vinyl naphthalene). In this study, naphthalene

and pyrene chromophores are covalently attached to poly (sodium maleate-*alt*-ethyl vinyl ether). The characterization of polymers labeled with these chromophores is described herein. NRET is measured in mixed solutions of polymer singly labeled with naphthalene or pyrene to evaluate intermolecular associations, and intramolecular associations are probed by NRET studies of doubly labeled polymers. The photophysical response is determined in aqueous solution as a function of pH and electrolyte (NaCl) concentration. Results are compared with respect to changes in these parameters and in chromophore spacer length.

Experimental Section

Materials. All commercial chemicals and solvents were purchased from Aldrich Chemical Co. (Milwaukee, WI). Benzene and tetrahydrofuran (THF) were dried over calcium hydride and distilled under nitrogen. Maleic anhydride was recrystallized twice from chloroform; ethyl vinyl ether (b.p. 32-33.5 °C) was distilled twice at atmospheric pressure before use. 2,2'-azobis (2-methylpropionitrile) (AIBN) was recrystallized from methanol. Other materials were used as received. Water was deionized and possessed a conductance < 10^{-7} mho/cm.

Succinic acid N-(1-naphthylmethyl) Monoamide (1). The structures of model compounds **1-3** are shown in Figure 2.1. Into a 25 mL round-bottomed flask fitted with a magnetic stirring bar, N_2 inlet and bubbler, succinic anhydride (1.0 g, 10 mmol) dissolved in 10 mL DMF was added. A solution of 1-naphthylmethylamine (1.3 g, 8.3 mmol) in 3 mL of DMF was then added. The reaction mixture was allowed to stir for 1 hr at room temperature. The slurry was then precipitated in water and pale brown solids were recovered by vacuum filtration. The solid product was then recrystallized from boiling water after treatment with activated charcoal: m.p. 172-174 °C; ^{13}C NMR (DMSO-d_6) δ 29.2, 30.0, 40.2, 123.4, 125.3, 125.7, 126.1, 127.4, 128.4, 130.8, 133.2, 134.6, 171.0, 173.9.

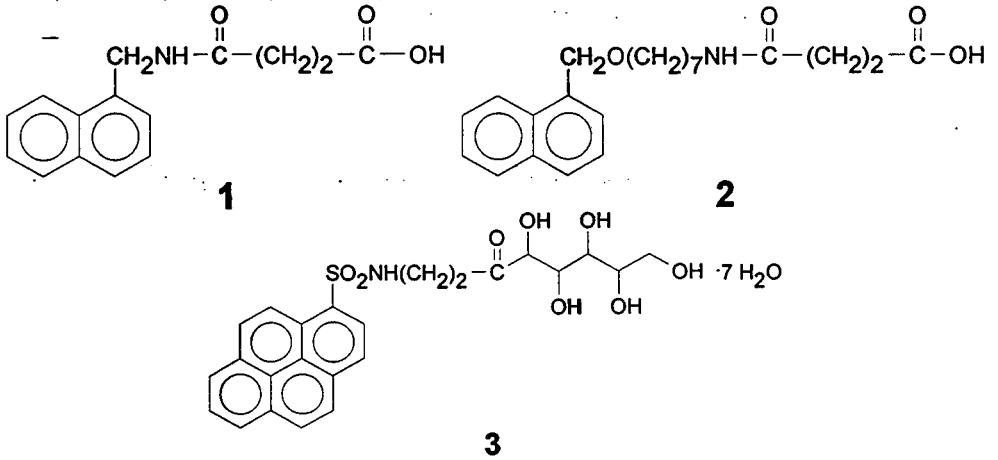

1 2 3

Figure 2.1. Model compounds **1-3**.

Succinic Acid N-[7-(1-Naphthylmethoxy)heptyl] Monoamide (2). Model compound **2** was synthesized using the methods of McCormick and Chang.[35]

N-[2-(1-Pyrenylsulfonamido)ethyl]gluconamide Heptahydrate (3). Model compound **3** was synthesized and characterized according to literature.[38]

7-(1-Naphthylmethoxy)heptylamine (N8). The structures of the chrompohores utilized for fluorescent labeling are shown in Figure 2. Labeling is accomplished by acylation of these primary amines with the maleic anhydride repeat units of poly (maleic anhydride-*alt*-ethyl vinyl ether). Label **N1** (1-naphthylmethylamine) is commercially available, and was used as received. The synthesis of **N8** label outlined by McCormick and Chang[35] was followed.

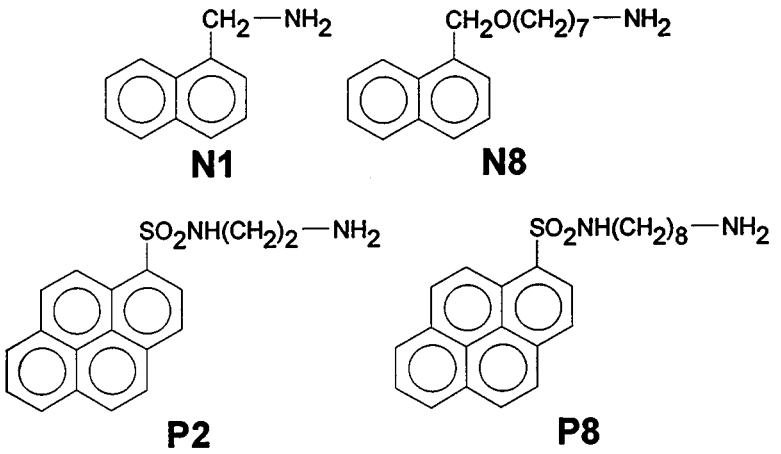

Figure 2.2. Fluorescent polymer labels N1, N8, P2, and P8.

2-(1-Pyrenylsulfonamido)ethylamine (P2) and 8-(1-Pyrenylsulfonamido)-octylamine (P8). Methods employed by Ezzell and McCormick[38] were utilized for the syntheses of both pyrene labels.

Poly(Maleic Anhydride-Ethyl Vinyl Ether) [Poly(MA-*alt*-EVE)].[35] The synthesis of the parent polymer and subsequent modifications are depicted in Scheme 1. Maleic anhydride (65.0 g, 663 mmol) was dissolved in 600 mL benzene at 60 °C in a 1 l round-bottomed flask equipped with a condenser, septa, magnetic stirring bar, and N_2 purge. After 0.20 g AIBN (1.2 mmol) was added, ethyl vinyl ether (49.0 g, 680 mmol) was immediately injected into the solution. The solution was stirred at 60 °C overnight, and the white precipitate that formed was isolated by vacuum filtration. The copolymer was purified by repeated dissolution in acetone and precipitation in diethyl ether. The M_w of poly (MA-*alt*-EVE) was 2.2×10^5 g/mol, which was measured with light scattering spectrophotometer.

Naphthalene and Pyrene-Labeled Poly (Sodium Maleate-*alt*-Ethyl Vinyl Ether)s. Solutions of octylamine (1.1 g, 8.5 mmol) and chromophore in 20 mL THF

were added dropwise into a rapidly stirring solution of poly (MA-*alt*-EVE) (5.0 g, 30 mmol) in 150 mL THF at room temperature under nitrogen. After 24 hr reflux at 66 °C, the polymers were precipitated in 1 l diethyl ether. The polymers were purified by repeated dissolution in THF and precipitation in diethyl ether.

Hydrolyses of unreacted anhydride groups were carried out in 100 mL aqueous 1.0 N NaOH. After the polymers completely dissolved, the solutions were dialyzed against deionized water at room temperature with Spectra-Por® dialysis tubing (12,000-14,000 g/mol molecular weight cutoff). When a constant, neutral pH was attained, the solutions were freeze-dried. The structure of the polymers synthesized are shown in Schemes 3 and 4. Copolymer compositions are shown in Table 1.

Table 2.1. Copolymer Compositions

Polymer	C8 Content (Mol. %)[a]	Naphthalene Content (Mol. %)[b]	Pyrene Content (Mol. %)[b]
C8	30	-	-
C8-N1	31	1.0	-
C8-P2	30	-	0.99
C8-N1-P2	30	1.2	0.99
C8-N8	32	1.1	-
C8-P8	29	-	0.96
C8-N8-P8	30	1.1	0.96

[a]From gated-decoupled ^{13}C NMR (D_2O) data.
[b]From UV absorption data.

Instrumentation. A Bruker AC-200 NMR spectrometer was used to determine ^{1}H, ^{13}C and gated-decoupled ^{13}C NMR spectra. NMR spectra were determined in either acetone-d_6 with 1% (v/v) TMS as an internal standard for unhydrolyzed polymer or in deuterium oxide with 1% (w/w) DSS as an internal standard for hydrolyzed polymers. The M_w of poly (MA-*alt*-EVE) was obtained with a Brookhaven BI-DS low-angle laser light scattering spectrophotometer. UV-VIS spectra were recorded with a Hewlett-Packard 8452A diode array spectrophotometer. Steady-state fluorescence spectra were measured on a Spex Fluorolog-2 fluorescence spectrometer equipped with a DM3000F data system.

Solution Preparation and Fluorescence Measurements. Polymer stock solutions were prepared with a concentration of 1.00 g/L at room temperature. These were allowed to stand for 24 h before dilution to a known concentration. All polymer solutions were diluted to 0.05 g/L (50 ppm) prior to fluorescence measurements. For the pH studies, 0.1 N HCl and 0.1 N NaOH aqueous solutions were used to adjust the solution pH. For the salt studies, 0.5M aqueous NaCl was added to polymer solutions.

For UV-Vis absorption measurements, water was used as a blank. All solutions were degassed by vigorous bubbling with nitrogen for 15 minutes before fluorescence measurement. All emission and excitation spectra were corrected. Slit widths were set at 2.0 mm and 1.0 mm at the fluorescence excitation and emission positions, respectively. For NRET measurements, 290 nm was chosen as the excitation wavelength. Pyrene chromophores were singly excited at 335 nm to observe pyrene fluorescence emission. Quantum yields (Φ) were calculated by integration of peak areas of corrected spectra (in wave number units) referenced to 2-amino pyridine in 0.10 N H_2SO_4 as a standard (Φ = 0.60 at 290 nm excitation wavelength).[39] Beer's law corrections were applied for optical density changes at the excitation wavelength. Corrections were also made for refractive index differences. Quantum efficiencies of naphthyl/pyrene energy transfer were determined by integration of corrected emission spectra from 310 to 370 nm (naphthyl emission) and from 370 nm to 550 nm (pyrene emission). For pyrene emission spectra excited at 290 nm in the presence of the naphthalene label, naphthyl emission was taken into account by subtraction of C8-N1 and C8-N8 spectra at identical naphthalene concentrations and environments ([NaCl], pH).

Results and Discussion

Polymer Characterization. Poly (maleic anhydride-*alt*-ethyl vinyl ether) was synthesized by a previously utilized procedure.[35] A copolymer with a completely alternating structure was obtained as confirmed by gated-decoupled ^{13}C NMR. The modifier feed consisted of 30 mole % octylamine and 1 mole % chromophore with respect to anhydride groups. From Table 1, it is readily apparent that near-quantitative chromphore incorporation onto the poly (MA-*alt*-EVE) backbone is obtained. Polymers are named according to their hydrophobe content. All copolymers contain 30 mole % octyl groups. The suffixes N and P denote naphthalene and pyrene substitution, respectively. The numbers following N and P indicate the modifying chromophore used; this number describes the number of carbons contained in the aliphatic spacer. Naphthalene and pyrene incorporation were determined by UV-Vis absorbance studies of aqueous polymer solutions. Label molar absorptivities are assumed to equal that of their model compounds (Table 2).

Table 2.2. Model Compound Molar Absorptivities

Model Compound	Fluorophore	ε ($M^{-1}cm^{-1}$)
1	Naphthalene	6780[a]
2	Naphthalene	6730[a]
3	Pyrene	24100[b]

[a]Molar absorptivity at λ_{max} (282 nm).
[b]Molar absorptivity at λ_{max} (350 nm).

Although the copolymerization of maleic anhydride with ethyl vinyl ether is a virtually alternating process,[8] substitution of hydrophobe and fluorescent label onto the polymer chain is random due to the similar reactivities of the primary amine groups on the modifiers. The random microstructure is also attributable to the homogeneity of the substitution medium. From the molecular weight of the parent copolymer, an average incorporation of 900 unsubstituted, 13 pyrene, 14 naphthalene, and 390 octyl groups per chain is inferred.

Spectroscopic Characterization. Solutions of naphthalene- and pyrene-labeled polymer were mixed with solutions of polymer C8 (unlabeled polymer) to adjust polymer concentrations (Table 3). Solutions were named according to the fluorescently labeled polymers employed. For example, C8-N1/C8-P2 is a mixed solution of singly labeled naphthalene polymer and singly labeled pyrene polymer. C8-N1-P2 is a solution of polymer doubly labeled with both naphthalene and pyrene. Polymer C8 was added to adjust all polymer concentrations to 50 ppm. The total absorbances of the polymer solutions at the excitation wavelengths (290 and 335 nm) were kept below 0.05 to avoid energy transfer by radiative processes.

Table 2.3. Solutions Prepared for Energy Transfer Experiments[a]

Short Spacer Chromophores

Solution	[C8] (ppm)	[C8-N1] (ppm)	[C8-P2] (ppm)	[C8-N1-P2] (ppm)	[Naphthalene] (μMol/L)	[Pyrene] (μMol/L)
C8-N1	25	25	-	-	0.99	-
C8-P2	25	-	25	-	-	0.95
C8-N1/C8-P2	-	25	25	-	0.99	0.95
C8-N1-P2	25	-	-	25	1.1	0.94

Long Spacer Chromophores

Solution	[C8] (ppm)	[C8-N8] (ppm)	[C8-P8] (ppm)	[C8-N8-P8] (ppm)	[Naphthalene] (μMol/L)	[Pyrene] (μMol/L)
C8-N8	25	25	-	-	1.0	-
C8-P8	25	-	25	-	-	0.92
C8-N8/C8-P8	-	25	25	-	1.0	0.92
C8-N8-P8	25	-	-	25	1.0	0.91

[a]All total polymer concentrations equal 50 ppm.

The UV-Vis absorption spectra of model compounds **1-3** are shown in 2. 3, and spectra of C8-N8, C8-P8, and C8-N8-P8 are shown in Figure 2.4.

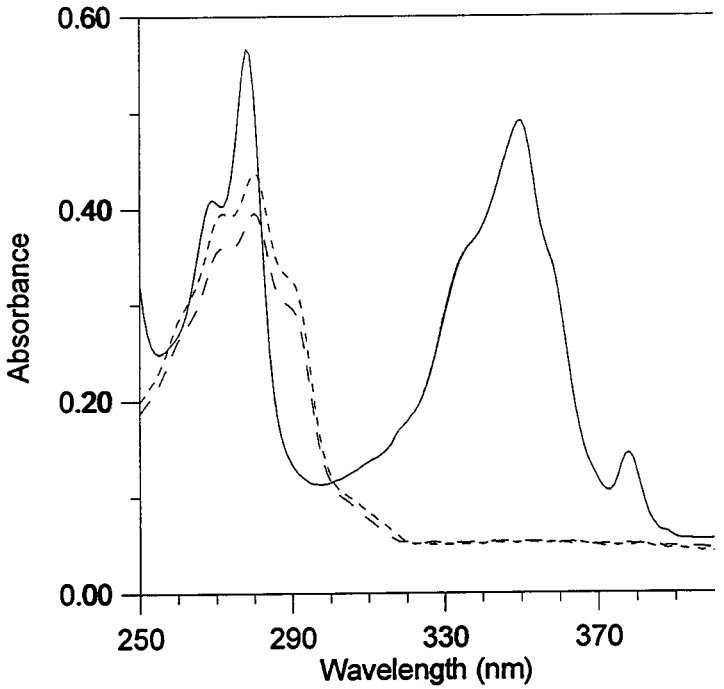

Figure 2.3. UV-Vis absorption spectra of naphthyl model compounds **1** (----------) and **2** (– – – – – –), and pyrenyl model compound **3** (——————). **[1]**, **[2]** = 50 μM. **[3]** = 20 μM.

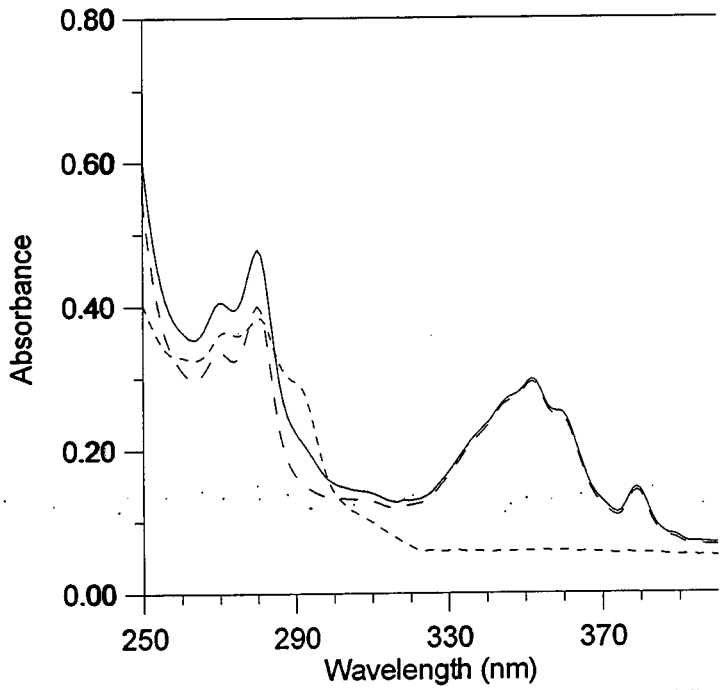

Figure 2.4. UV-Vis absorption spectra of labeled polymers C8-N8 (----------), C8-P8 (– – – – – –), and C8-N8-P8 (——————). Sample concentration: 1000 ppm. pH: 7.

A pyrene absorbance minimum is centered around 290 nm, as is an absorbance shoulder of the naphthalene chromophore. In order to maximize NRET between naphthyl and pyrene chromophores, an excitation wavelength of 290 nm is employed. This allows preferential excitation of naphthalene chrompohores in the presence of pyrene. At 290 nm, the fraction P of the total light absorbed by naphthyl chromophores in the presence of pyrene was calculated using equation 1 in which $A_N(\lambda)$ and $A_{Py}(\lambda)$ are the absorbances of naphthalene and pyrene at wavelength λ (290 nm).[40]

$$P = \frac{1 - 10^{-A_N(\lambda)}}{2 - 10^{-A_N(\lambda)} - 10^{-A_{Py}(\lambda)}} \quad (1)$$

At 290 nm, naphthyl chromophores are responsible for 50% of the total light absorbed by solutions of C8-N1 and C8-P2 at N1/P2 = 1.1; the naphthyl chromophores are responsible for 52% of the total light absorbed by polymer solutions labeled with long spacer chromophores at N8/P8 = 1.1.

Figure 2.5 shows the overlap between the UV-Vis absorption spectrum of pyrene model compound **3** and the corrected fluorescence spectra of naphthalene model compounds **1** and **2**.

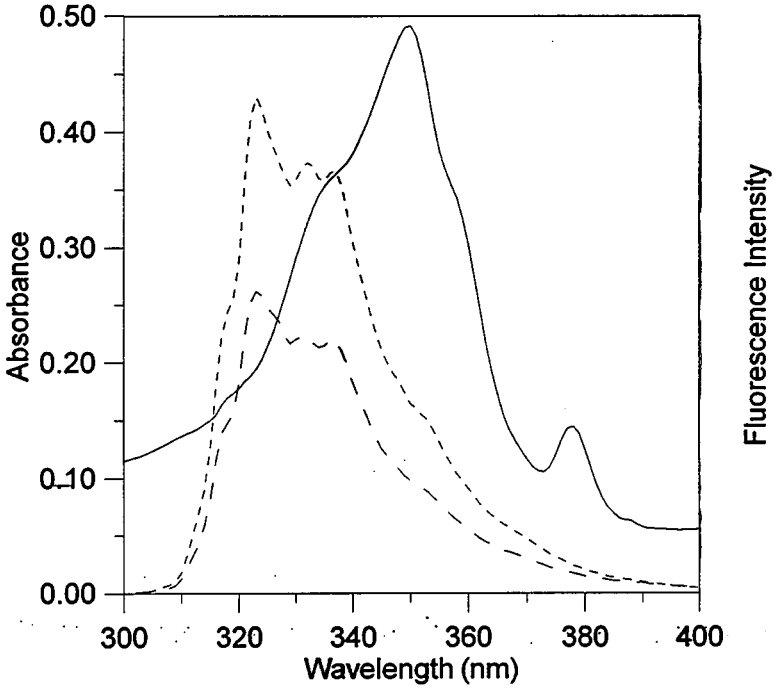

Figure 2.5. Spectral overlap of of pyrenyl model compound **3** UV-Vis absorbance (————————) with fluorescence emission of naphthyl model compounds **1** (----------) and **2** (– – – – – –). Excitation wavelength: 290 nm. pH: 7. [1], [2] = 50 μM. [3] = 20 μM.

The spectral data demonstrate good overlap between naphthalene label emission and pyrene label absorption. This overlap is requisite for nonradiative energy transfer from donor (naphthalene) to acceptor (pyrene). According to Förster,[41] the

characteristic distance R_0 between donor and acceptor at which half of the excitation energy is transferred is given by the equation

$$R_0 = \left(\frac{9000\ (\ln 10)\ \kappa^2\ \Phi_D^0}{128\ \pi^5\ n^4\ N} \int_0^\infty \lambda^4\ I(\lambda)\ \varepsilon(\lambda)\ d\lambda \right)^{1/6} \tag{2}$$

where κ^2 is a function of the mutual orientation of donor and acceptor with $\kappa^2=2/3$ for random orientation in fluid media, Φ_D^0 is the emission quantum yield of the donor in the absence of acceptors, n is the refractive index, and N is Avogadro's number. The integral depicted in equation 2 is the overlap integral, where $I(\lambda)$ is the normalized fluorescence emission intensity such that

$$\int_0^\infty I(\lambda)\ d\lambda = 1 \tag{3}$$

and $\varepsilon(\lambda)$ is the molar absorptivity of the acceptor as a function of the wavelength λ. The sixth power dependence results from dipole-dipole interactions that govern nonradiative energy transfer. The quantum yields of the model compounds are Φ_D^0 = 0.10 for naphthalene model **1**, Φ_D^0 = 0.066 for naphthalene model **2**, and Φ_A^0 = 0.73 for pyrene model **3**. These were obtained by comparison of the integrated emission intensities of aqueous solutions of model compounds excited at 290 nm with that of 2-amino-pyridine in 0.10 N H_2SO_4 (Φ = 0.60 at 290 nm excitation wavelength).[39] The overlap integral between naphthalene model **1** and pyrene model **3** was determined to be 19.05×10^{-15} cm^6mol^{-1}; the naphthalene model **2**/pyrene model **3** overlap integral is 17.08×10^{-15} cm^6mol^{-1}. In aqueous media, these data correspond to R_0 = 26.6 Å for naphthalene model **1**/pyrene model **3** and R_0 = 24.7 Å for naphthalene model **2**/pyrene model **3**.

There are several useful methods for characterization of NRET between fluorescence donor and acceptor. Morawetz used the fluorescence intensity ratio of donor to acceptor to describe NRET in polymer systems.[4] Guillet[22-24] defined the quantum efficiency of NRET, χ, as

$$\frac{\chi}{1-\chi} = \frac{\Phi_D^0\ I_A}{\Phi_A^0\ I_D} \tag{4}$$

where Φ_D^0 is the fluorescence emission quantum yield of donor on the polymer singly labeled with donor and Φ_A^0 is the fluorescence quantum yield of the acceptor on the polymer doubly labeled with donor and acceptor upon direct excitation. I_D and I_A are the integrated emission intensities of donor and acceptor, respectively, on the doubly labeled polymer. Here the fluorescence emission quantum yields of naphthalene on singly labeled polymers were used to express Φ_D^0 and the fluorescence emission quantum yields of pyrene on singly labeled polymers were

used to express Φ_A^0. Guillet[22-24] studied the naphthalene/anthracene donor/acceptor pair with an excitation wavelength of 280 nm where the extinction coefficient of anthracene is so low that its emission is negligible. However, in the studies discussed here, 290 nm is used as the excitation wavelength for the naphthyl/pyrene energy transfer pair, and both chromophores are excited at this wavelength. The expression of the quantum efficiency χ of energy transfer modified for this case is

$$\frac{\chi}{1-\chi} = \frac{\Phi_D^0 (I_A - I_A^0)}{\Phi_A^0 I_D} \tag{5}$$

where I_A^0 is the integrated fluorescence emission of the polymer singly labeled with pyrene. The quantum yields of pyrene in the doubly labeled polymers should be similar. This is supported by the similarity in pyrene emission intensities when samples are excited at 335 nm.

Figure 2.6 shows the corrected fluorescence spectra of C8-N8, C8-P8, C8-N8-P8, and C8-N8/C8-P8 in aqueous solution at 50 ppm total polymer concentration. Naphthalene excimer emission was not observed, but a small structureless emission centered at about 520 nm is observed in polymers labeled with pyrene. This band is observed when excitation wavelengths of both 290 and 335 nm are employed and arises from pyrene excimer emission. The emission intensity of naphthyl chromophores in C8-N8/C8-P8 from 310-370 nm is lower than that of singly labeled polymer (C8-N8) and of doubly labeled polymer (C8-N8-P8). Interpolymer quenching of naphthalene via nonradiative energy transfer from excited state naphthalene to ground state pyrene is responsible for this behavior.

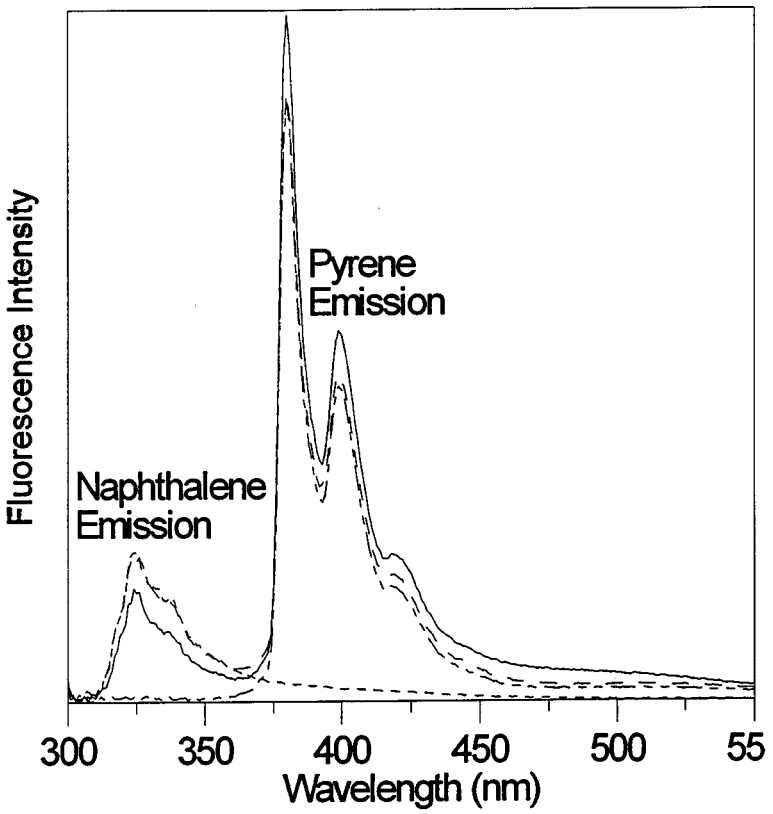

Figure 2.6. Fluorescence spectra of long spacer labeled polymers C8-N8 (- - - - - - - - - - - -), C8-P8 (— - - - - - - - - —), C8-N8-P8 (– – – – – – –), C8-N8/C8-P8 (————————). Excitation wavelength: 290 nm. Polymer concentration: 50 ppm. pH: 7

Fluorescent labels possessing short alkyl spacers do not exhibit interpolymer NRET to the extent that the long spacer systems do since the molecular motions of N1 and P2 chromophores are not decoupled from the polymer backbone to the same extent as N8 and P8. Naphthalene concentration is slightly higher in solutions of C8-N1-P2 (1.1 μM) than in other solutions of the short spacer naphthalene-labeled series. However, the intensity of naphthalene emission in solution C8-N1-P2 at 310-370 nm is less than that of C8-N1/C8-P2 (Figure 2.7). Labels associate intramolecularly at the expense of intermolecular interactions, and intramolecular NRET is more pronounced as evidenced by reduced quenching of naphthalene emission in C8-N1/C8-P2 mixed polymer solution.

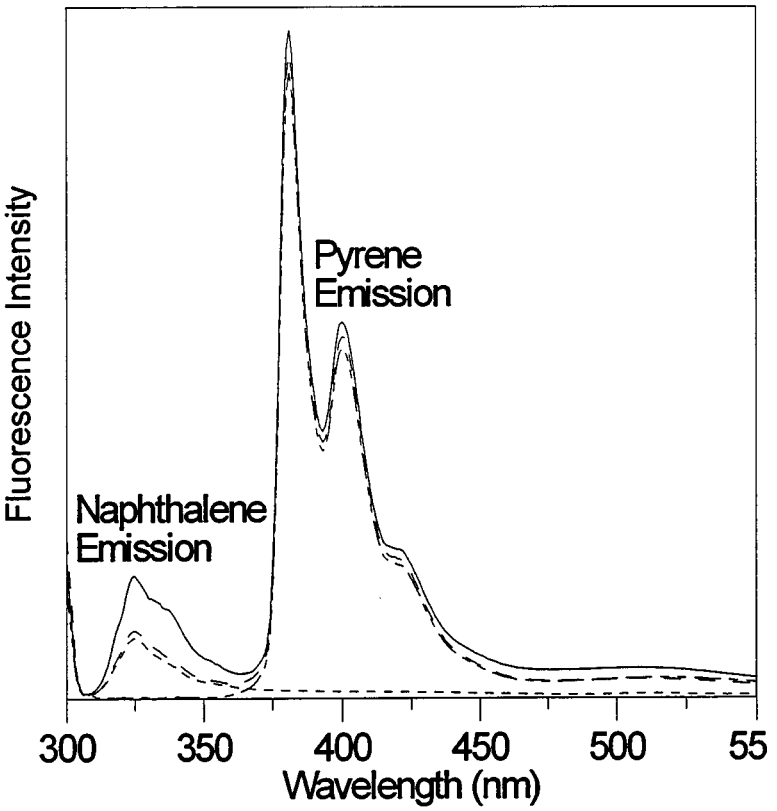

Figure 2.7. Fluorescence spectra of short spacer labeled polymers C8-N1 (----------), C8-P2 (— - — - — - —), C8-N1-P2 (– – – – – –), and C8-N1/C8-P2 (——————). Excitation wavelength: 290 nm. Polymer concentration: 50 ppm. pH: 7.

Salt Effects on NRET. The effect of sodium chloride on NRET quantum efficiency as a function of spacer length and association type is shown in Figure 2.8. NRET is most prevalent in the doubly labeled polymer series C8-N1-P2 and C8-N8-P8 (closed symbols) throughout the entire NaCl concentration range. NRET steadily increases with ionic strength. Viscosity studies indicate a reduction in coil dimensions. As this occurs, the average chromophore separation decreases and the contraction is observed as an increase in NRET.

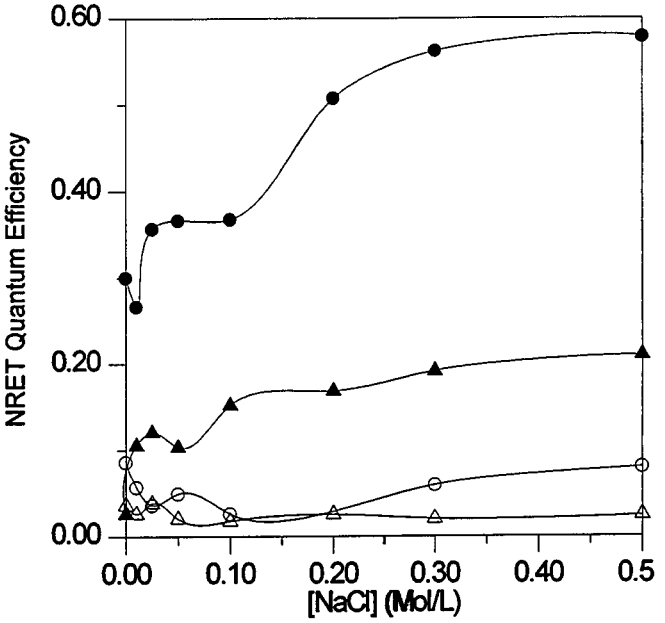

Figure 2.8. NRET quantum efficiency of C8-N1/C8-P2 (△), C8-N8/C8-P8 (○), C8-N1-P2 (▲), and C8-N8-P8 (●) as a function of sodium chloride concentration. Polymer concentration: 50 ppm. pH: 7.

A gradual NRET increase with NaCl concentration is observed for both C8-N1-P2 and C8-N8-P8 (Figure 2.8, closed symbols). Mixed solutions of singly labeled polymers show low, virtually unchanging NRET values. When NRET donor and acceptor chromphores are present on the same polymer chain, the photophysical response is more prominent. As polymer coil dimensions shrink with increasing ionic strength, the average intramolecular label separation decreases. This phenomenon is illustrated schematically in Figure 2.9.

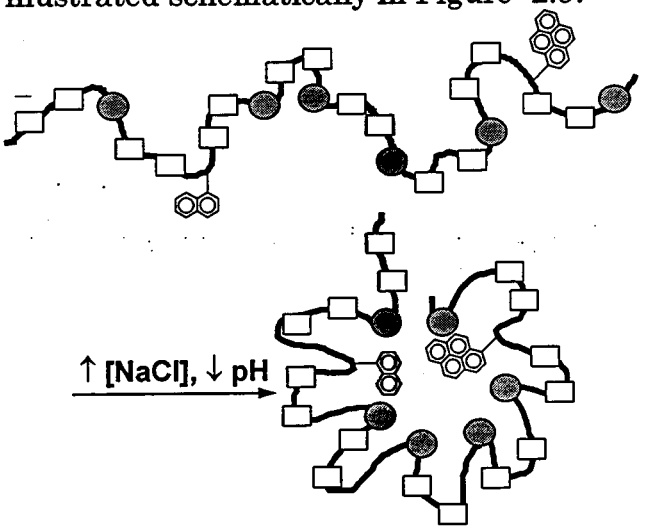

Figure 2.9. Coil contraction-triggered intramolecular NRET increase

pH Effects on NRET. The quantum efficiency of intra- and interpolymer energy transfer between naphthalene and pyrene as a function of pH is shown in Figure 2.10.

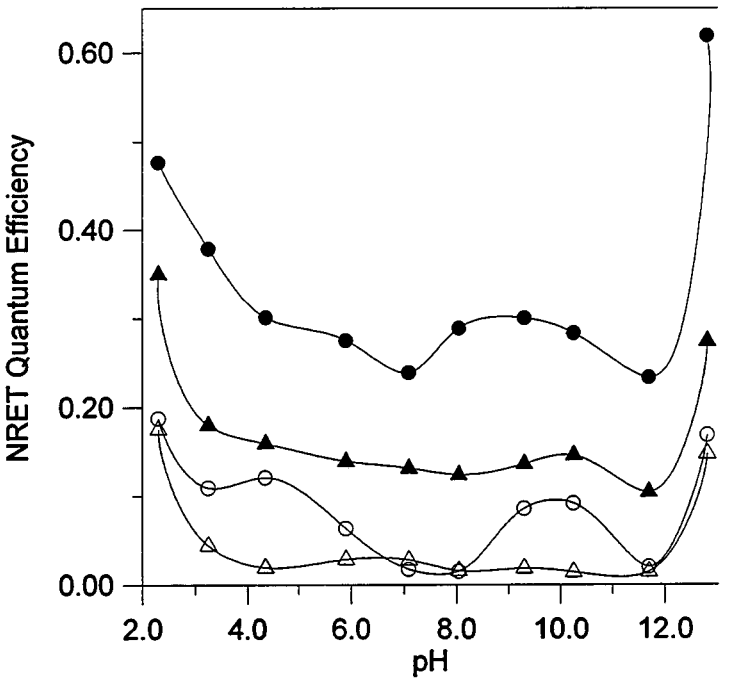

Figure 2.10. NRET quantum efficiency of C8-N1/C8-P2 (△), C8-N8/C8-P8 (○), C8-N1-P2 (▲), and C8-N8-P8 (●) as a function of pH. Polymer concentration: 50 ppm.

Energy transfer data from mixed solutions of singly labeled polymers (C8-N1/C8-P2 and C8-N8/C8-P8) are depicted by open symbols, and data from solutions of doubly labeled polymers (C8-N1-P2 and C8-N8-P8) are represented by closed symbols. For this polymer series, the molar ratio of carboxylic acid groups to hydrophobic groups is about 5.5 to 1. The acid functionality helps to impart water-solubility and pH sensitivity.

A significant feature of 2.10 is the high values of intrapolymer NRET relative to interpolymer NRET throughout the entire pH range. This is seen as an enhancement in C8-N1-P2 and C8-N8-P8 NRET quantum efficiency (closed symbols) relative to NRET in mixed singly labeled solutions (C8-N1/C8-P2 and C8-N8/C8-P8, open symbols). This suggests that intramolecular hydrophobic associations prevail over a wide pH range. The charge density along the polymer chain is a function of pH. As pH decreases, the reduction in electrostatic repulsions shrinks the polymer coil. For all polymers and solutions, the quantum efficiency of energy transfer increases below pH 5. As pH is increased, the electrostatic repulsions result in reduced intramolecular associations. The most dramatic changes in NRET quantum efficiency are observed in doubly labeled polymers C8-

N1-P2 and C8-N8-P8 (2. 10, closed symbols). NRET decreases ≥ 50% as pH is increased from 2 to 6 for both C8-N1-P2 and C8-N8-P8. As the coil is opened by coulombic repulsions, the distance between chromophores increases, and intramolecular NRET decreases. This trend is in agreement with previous studies.[34,35]

A maximum in NRET quantum efficiency occurs in mixed solutions of singly labeled long spacer polymer C8-N8/C8-P8 at pH 9-10 (Figure 2.10). This indicates an enhancement in interpolymer associations in this pH range. As the chain expands, intrapolymer associations are broken up and interpolymer interactions increase. The long alkyl spacer group decouples the motion of the naphthalene and pyrene groups from that of the polymer backbone, providing an effective mode of hydrophobe diffusion to form interpolymer aggregates. This result is supported by previous viscosity studies that indicate maxima in reduced viscosity around pH 9.5 for octylamido-modified poly (sodium maleate-*alt*-ethyl vinyl ether)s.[35] Because most or all of the carboxylic acid groups are neutralized at high pH, further base addition increases the ionic strength. The shielding of coulombic repulsions collapses the polymer coil, and an increase in intrapolymer associations is observed as an NRET enhancement in solutions of doubly labeled polymers C8-N1-P2 and C8-N8-P8 at pH > 10 (closed symbols).

At extremes in pH, intermolecular NRET increases, thus signifying the onset of an aggregative process. As pH decreases from 6 to 2, naphthalene/pyrene NRET between polymer chains in the C8-N1/C8-P2 and C8-N8/C8-P8 systems increases (open symbols). Migration of hydrophobic groups to the polymer micelle surface may account for this behavior. Strauss reported intermolecular association and gel formation in aqueous solutions of highly quaternized (38 mole % dodecyl modification) poly(vinylpyridine).[36] It was postulated that added electrolyte helps to shield Coulombic forces between pyridinium groups, and that a fraction of the surface of a polymer micelle then becomes occupied by hydrophobic groups. Polymer-polymer aggregation would then become more favorable. The elimination of electrostatic repulsions may also lead to the formation of a hydrophobic surface.

Intermolecular aggregation in polysoaps has been verified by viscosity studies.[36] Viscosity increases markedly with ionic strength, and there is a time dependence on viscosity as well. Over long periods of time, the viscosity of a freshly diluted sample decreases to an equilibrium value. This result implies a gradual breakup of polymer aggregates over time. Chang and McCormick reported similar phenomena in MAEVE copolymers modified with dodecyl groups.[35] Viscosity was found to diminish over a period of one week, and the decrease was most pronounced in the more highly substituted polymers; intramolecular organization of micellar domains with the breakup of intermolecular associations drives this response. Time-dependent aging was not observed in the rheological behavior of octyl modified MAEVE, but marked increases in intermolecular associations are seen by NRET analysis at low and high pH. Although viscometric data does not report aggregation, the photophysical response reveals that multimer aggregates do indeed form. This is shown schematically in Figure 2.11. At the

onset of interpolymer association, hydrophobic interactions occur between donor and acceptor chromophores on different polymer chains. As a result, the average distance between donor and acceptor decreases, and NRET quantum efficiency increases.

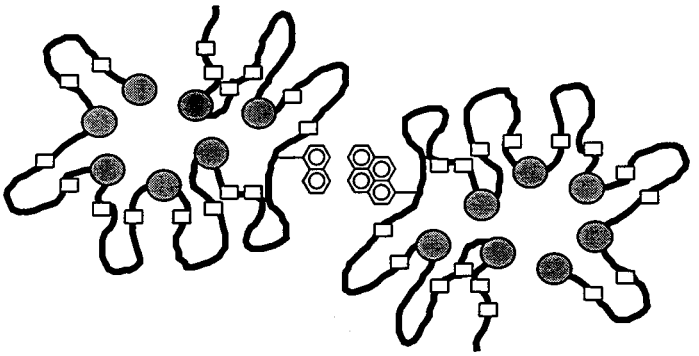

Figure 2.11. Proposed mechanism of acid-induced intermolecular NRET enhancement via exposure of hydrophobic groups to polymer micelle surface.

Ionic strength effects may account for hydrophobic micelle surface formation and aggregation. At high pH, as the electrostatic repulsions on the polymer micelle surface are shielded by added base, a fraction of the hydrophobic groups are exposed to the surface. As a result, NRET enhancement in mixed solutions of singly labeled polymers C8-N1/C8-P2 and C8-N8/C8-P8 is observed at pH > 11 (open symbols).

NRET Donor/Aceptor Ratio Effects. When the ratio of naphthalene to pyrene is changed, NRET quantum efficiency may change. Winnik has reported an NRET enhancement in mixed solutions of fluorescently labeled, hydrophobically modified poly (N-isopropylacrylamide) (PNIPAM). NRET was observable at very low polymer concentrations, and is reflective of the formation of intermolecular aggregates that were verified by quasi-elastic light scattering studies.[42] As the naphthalene/pyrene ratio is increased from 1 to 5 in C8-N8/C8-P8 mixed solutions, NRET efficiency also increases. Even at very low polymer concentrations, the highly mobile, long spacer labels can diffuse to a sufficient degree to form intermolecular aggregates. Label mobility appears to be a prerequisite for efficient NRET.

Conclusions

A series of fluorescently labeled poly (sodium maleate-*alt*-ethyl vinyl ether)s containing 30% octyl groups have been synthesized by a novel technique that allows stoichiometric control of polymer hydrophobicity. Polymers were singly labeled with 1 mole % of either naphthalene (donor) or pyrene (acceptor) chromophores for intermolecular nonradiative energy transfer (NRET) studies; polymers were also doubly labeled with 1 mole % naphthalene and pyrene for intramolecular NRET

analysis. Rheologial studies have shown that intramolecular associations predominate at the low polymer concentrations employed, but steady-state fluorescence emission studies support naphthalene/pyrene energy transfer within and between hydrophobic domains. As electrolyte concentration increases, closed associations and intramolecular NRET are enhanced due to the shielding of electrostatic repulsions that expand the polymer coil. Intrapolymer hydrophobic association and NRET are also augmented at low pH due to the elimination of electrostatic repulsive forces.

A mechanism involving the formation of a hydrophobic micellar surface has been postulated to account for the intermolecular associative behavior observed by NRET measurement at low and high pH Polymer-polymer aggregation that is not observable by viscosity studies is readily probed by NRET measurements of mixed solutions of polymer singly labeled with donor or acceptor. Chromophores separated from the polymer backbone by longer spacer lengths tend to interact to a greater extent, as reflected in the photophysical behavior of these systems. NRET enhancement with increasing [Na]/[Py] for the long spacer labeled systems supports intermolecular domain association in addition to intramolecular association at low polymer concentrations.

References and Notes

1. Morishima, Y. *Prog. Polym. Sci.* **1990**, *15*, 949.

2. Turro, N.J.; Gratzel, M.; Braun, M. *Angew. Chem. Int. Ed. Engl.* **1980**, *19*,675.

3. Webber, S.E *Chem. Rev.* **1990**, *90*, 1469.

4. Morawetz, H. *Science* **1988**, *240*, 172.

5. Nagata, I.; Morawetz, H. *Macromolecules* **1981**, *14*, 87.

6. *Water-Soluble Polymers: Synthesis, Solution Properties, and Applications*; Shalaby, S.W.; McCormick, C.L.; Butler, G.B. Eds.; ACS Symposium Series No. 467; ACS: Washington, DC, 1991.

7. *Photophysical and Photochemcal Tools in Polymer Science*; Winnik, M.A. Ed.; D. Reidel: Dordrecht, Holland, 1986.

8. *Polymer as Rheology Modifiers;* Schulz, D.N.; Glass, J.E., Eds., ACS Symposium Series No. 462; ACS: Washington, DC, 1991.

9. Morishima, Y.; Itoh, Y.; Nozakura, S. *Makromol. Chem.* **1981**, *182*, 3135.

10. Morishima, Y.; Itoh, Y.; Nozakura, S. *Macromolecules* **1984**, *17*, 2264.

11. Morishima, Y.; Kobayashi, T.; Nozakura, S.; Webber, S.E. *Macromolecules* **1987**, *20*, 807.

12. Bai, F.; Webber, S.E. *Macromolecules* **1988**, *21*, 628.

13. Morishima, Y.; Lim, H.S.; Nozakura, S.; Sturtevant, J.L. *Macromolecules* **1989**, *22*, 1148.

14. Sturtevant, J.L.; Webber, S.E. *Macromolecules* **1989**, *22*, 3564.

15. Itoh, Y.; Nakada, M.; Satoh, H.; Hachimori, A.; Webber, S.E. *Macromolecules* **1993**, *26*, 1941.

16. Itoh, Y.; Satoh, H.; Yasue, T.; Hachimori, A. Satozano, H.; Suzuki, S.; Webber, S.E. *Macromolecules* **1994**, *27*, 1434.

17. Chu, D.Y.; Thomas, J.K. *Macromolecules* **1987**, *20*, 2133.

18. Zdanowicz, V.S.; Strauss, U.P. *Macromolecules* **1993**, *26*, 4770.

19. Strauss, U.P.; Vesnaver, G. *J. Phys. Chem.* **1975**, *79*, 1558.

20. Binana-Limbelé, W.; Zana, R. *Macromolecules* **1990**, *23*, 2731.

21. Strauss, U.P.; Vesnaver, G. *J. Phys. Chem.* **1975**, *79*, 2462.

22. Ng, D.; Guillet, J.E. *Macromolecules* **1982**, *15*, 724.

23. Holden, D.A.; Guillet, J.E. *Macromolecules* **1980**, *13*, 289.

24. Guillet, J.E. and Rendall, W.A. *Macromolecules* **1986**, *19*, 224.

25. Major, M.D.; Torkelson, J.M.; Brearley, A.M. *Macromolecules* **1990**, *23*, 1700.

26. Nagata, I.; Morawetz, H. *Macromolecules* **1981**, *14*, 87.

27. Ito, S.; Ohmori, S.; Yamamoto, M. *Macromolecules* **1992**, *25*, 185.

28. Winnik, F.M. *Macromolecules* **1989**, *22*, 734.

29. Winnik, F.M. *Polymer* **1990**, *31*, 2152.

30. Schild, H.G.; Tirrell, D.A. *Macromolecules* **1992**, *25*, 4553.

31. Fox, R.B.; Price, T.R.; Cozzens, R.F.; Echols, W.H. *Macromolecules* **1974**, *7*, 937.

32. Strauss, U.P.; Schlesinger, M.S. *J. Phys. Chem.* **1978**, *82*, 1627.

33. Strauss, U.P.; Schlesinger, M.S. *J. Phys. Chem.* **1978**, *82*, 571.

34. McCormick, C.L.; Hoyle, C.E.; Clark, M.D. *Polymer* **1992**, *33*, 243.

35. McCormick, C.L.; Chang, Y. *Macromolecules* **1994**, *27*, 2151.

36. Strauss, U.P.; Gershfeld, N.L.; Crook, E.H. *J. Phys. Chem.* **1956**, *60*, 577.

37. Hargreaves, J.S.; Webber ,S.E. *Macromolecules* **1982**, *15*, 424.

38. Ezzel, S.A.; McCormick, C.L. *Macromolecules* **1992**, *25*, 1881.

39. Rusakowicz, R.; Testa, A.C. *J. Phys. Chem.* **1968**, *72*, 2680.

40. Lin, G.; Guillet, J.E. *Macromolecules* **1990**, *23*, 1388.

41. Förster,T. *Discuss. Faraday Soc.* **1959**, *27*, 7.

42. Ringsdorf,H; Simon, J.; Winnik, F.M. *Macromolecules* **1992**, *25*, 5353.

Chapter 3: Phase Transfer Studies of Structural and Environmental Effects on Domain Organization in Aqueous Solutions of Hydrophobically Modified Poly (Sodium Maleate-*alt*-Ethyl Vinyl Ether)s

Synopsis

Hydrophobically modified, water-soluble terpolymers based on maleic anhydride and ethyl vinyl ether were evaluated for their ability to act as a host for hydrophobic molecules in water. This "polysoap" behavior allows sequestering of hydrocarbons within domains along the polymer chain. Changes in pH or salt concentration trigger a conformational change leading to chain expansion. Alternating copolymers of maleic anhydride and ethyl vinyl ether were reacted with primary amines in organic solvent, then hydrolyzed in dilute aqueous base. This modification technique allows precise, stoichiometric substitution with hydrophobic groups and accessibility to a wide range of association-driven conformations in aqueous media. The degree of naphthalene (a model hydrocarbon) sequestration in solutions of hydrophobically modified poly (sodium maleate-*alt*-ethyl vinyl ether) was found to depend on hydrophobic modification, electrolyte concentration, and pH. As octyl substitution increased from 10 to 50 mole %, micellar domains formed by intrapolymer hydrophobic associations became more compact, and mobility constraints within micelles hindered phase transfer. Increasing sodium chloride concentration and decreasing pH also enhanced micellar organization. The presence of hydrophobic groups on the micellar surface in some cases was postulated to account for enhanced recruitment of naphthalene into hydrophobic domains. Data from these studies are discussed in relation to previous viscosity and fluorescence studies that confirm the conformational changes driving the transition from an extended polyelectrolyte to a compact, globular structure.

Introduction

Studies in our laboratories have focused on the associative properties of hydrophobically modified water-soluble polymers.[1,2,3] Most recently, elucidation of the domain-forming abilities of amphiphilic polyelectrolytes has been a subject of interest.[4,5,6,7,8,9] Viscosity studies of acrylamide/N-(n-decyl) acrylamide (AM/C_{10}AM) terpolymers with a charged monomer revealed that incorporation of small amounts of hydrophobe into the structure of a hydrophilic polymer dramatically alters solution properties in aqueous media.[2] A pronounced enhancement in the viscosity response occurs well below concentrations corresponding to that of the onset of chain entanglement in unmodified poly (acrylamide). Interpolymer hydrophobic association between C_{10} groups drives this response. Incorporation of a charged

monomer into a hydrophobically modified water-soluble polymer dramatically influences the nature and extent of associations. Factors including charged group placement,[2] ionic strength and pH,[1,2,4-9] and the presence of surfactants affect solution behavior.[5,7,10,11,12,13,]

Many of the copolymer systems that have been investigated tend to exhibit associative thickening properties (open associations) similar to the AM/C_{10}AM systems.[2,3] When hydrophobe content in a polyelectrolyte increases, interactions within the polymer coil (closed associations) become more prominent. The compact, globular structures assumed by these intramolecularly associating systems have been termed "unimolecular micelles,"[14,15] "polymeric micelles,"[16,17] and "polysoaps."[18,19] Intrapolymer associations are confirmed by a considerable decrease in intrinsic viscosity ([η]) and an accompanying increase in the Huggins constant (*k'*). Strauss reported a drop in the intrinsic viscosity of dodecyl (C_{12})-quaternized poly (vinyl pyridine)s from 5 dL/g to less than 0.1 dL/g as quaternization was increased from 0 to 13.6 mole %. This concentration at which this transition occurs has been termed the "critical micelle composition."[18] If the local concentration of "soap" molecules (amphiphilic groups) attached to a polymer chain is sufficiently high, micellar structures will form along the polymer chain. The unusually high Huggins k' value and tendency for gel formation observed in highly substituted dodecylpyridinium-based polysoaps indicate strong interpolymer aggregation. Strauss proposed a mechanism whereby the compact structure of the polymer micelle lends to the exclusion of hydrophobic groups from the micellar core. Interaction between hydrophobic groups on the micellar surface may then facilitate interpolymer network formation.[18]

Hydrolyzed alternating copolymers of maleic anhydride and alkyl vinyl ethers also exhibit strong intramolecular associative properties.[20,21,22,23,24,25] As the pH is decreased through the pK_a of the carboxylate groups along the polymer coil, the polymer conformation varies from a relatively open, random coil conformation to a globular structure as electrostatic repulsive forces diminish. Fluorescence studies of dansyl-labeled maleate/alkyl vinyl ether copolymers confirm the presence of hydrophobic domains at low pH, and the globular-random coil transition occurs only when the alkyl group is a butyl group or of a longer alkyl chain length.[22]

Recently, we have begun the systematic investigation of the microdomain-forming properties of alkylamido-substituted maleic anhydride-ethyl vinyl ether (MAEVE)-based polysoaps (Scheme 1) as a function of hydrophobe content, electrolyte concentration, and pH. Free radical polymerization is carried out in an organic solvent to give a perfectly alternating MAEVE copolymer.[26] Random, stoichiometric hydrophobic modification is then achieved by reaction of an aliphatic or aromatic amine with anhydride polymer repeat units in the polymer structure. Hydrolysis in dilute aqueous base affords the water-soluble polymer.[6,27]

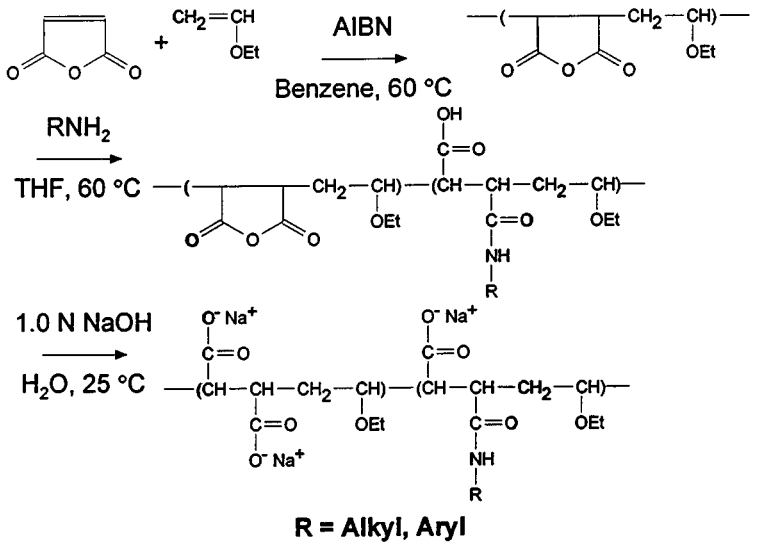

Scheme 3.1 Synthesis of Hydrophobically Modified Poly (Sodium Maleate-*alt*-Ethyl Vinyl Ether)

Partitioning of pyrene probe into hydrophobic microdomains has been confirmed by fluorescence emission studies of 4-butylphenyl modified poly (potassium maleate-*alt*-ethyl vinyl ether). The ratio of the first to the third vibronic band of pyrene emission (I_1/I_3) and the fluorescence lifetime (τ) were found to reflect the formation of a hydrophobic, micellar environment at low pH. Quasielastic light scattering studies also indicated that the effective diameter (d_{eff}) decreases with pH and increasing hydrophobe content,[9] supporting the existence of a polyelectrolyte-polysoap transition (Figure 3.1).

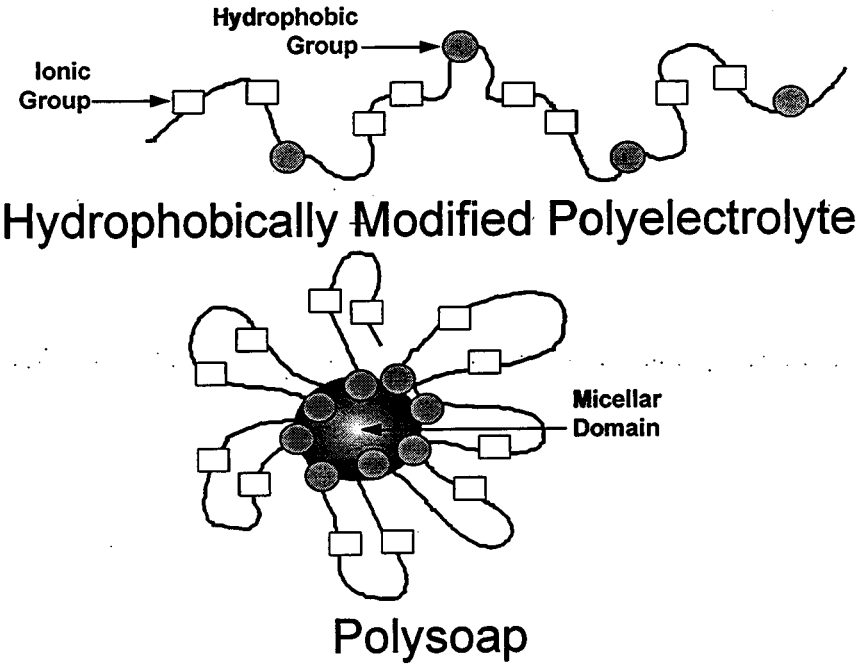

Figure 3.1 Proposed mechanism of polyelectrolyte-polysoap transition.

Although environmental and conformational changes have been reported for this class of water-soluble polymers, sequestration of small molecule hydrophobes by aqueous micellar domains formed in these systems has only been directly quantitated in a few studies.[28,29] The major objective of this study is the correlation of the aqueous phase transfer properties of hydrophobically modified poly (sodium maleate-alt-ethyl vinyl ether) with polymer micelle structure. Dissolution of a hydrophobic, polyaromatic chromophore is readily assessed via UV-Vis spectrophotometry.[28-30] Because hydrophobic modification,[18,19] along with electrolyte concentration,[6] and pH[6,9,22] affect the conformation adopted by this unique class of water-soluble polymers, sequestration shall be measured as a function of changes in these parameters. When sequestration data is compared with results from viscosity and fluorescence studies,[6] a reasonable model of the associations that drive polymer micelle phase transfer may be derived. This may ultimately lead to the development of these novel materials in phase transfer in improved oil recovery

Experimental

Materials. All reagents and solvents were purchased from Aldrich Chemical Co. (Milwaukee, WI). Acrylamide was recrystallized twice from acetone. Other materials were used as received. Water for synthesis and solution preparation was deionized and possessed a conductance < 10^{-7} mho/cm.

Hydrolyzed, Hydrophobically Modified Poly (Maleic Anhydride-alt-Ethyl Vinyl Ether) (MAEVE). The polymer utilized for subsequent hydrophobic modification and hydrolysis was previously synthesized.[6] Maleic anhydride was copolymerized with ethyl vinyl ether in benzene at 60 °C using benzoyl peroxide as initiator. After 8 hours the polymer precipitate that forms was purified by repeated dissolution in ethyl acetate and precipitation in diethyl ether. Copolymer molecular weight (M_w) determined by light scattering was 2.4×10^5 g/mol.

n-Octyl Modified Poly (Sodium Maleate-alt-Ethyl Vinyl Ether) (C8-10, 20, 30, 40, 50). The modification and hydrolysis of poly (maleic anhydride-*alt*-ethyl vinyl ether) is shown in Scheme 1. Octyl (C_8) modified polymers were previously synthesized by Chang and McCormick,[6] and substitution levels of 10, 20, 30, 40, and 50 mole % (with respect to maleic anhydride repeat units in parent copolymer) were achieved. In the results and discussion section these polymers shall be designated C8-10, C8-20, C8-30, C8-40, and C8-50; the numbers following the hyphen describe octyl group content (Figure 3.2).

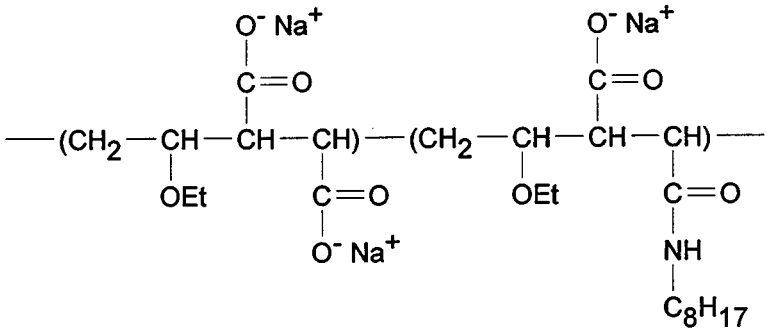

C8-#, # = 10, 20, 30, 40, 50 Mole %

Figure 3.2 Octyl modified poly (sodium maleate-*alt*-ethyl vinyl ether).

n-Octyl Modified, Pyrene labeled Poly (Sodium Maleate-alt-Ethyl Vinyl Ether) (C8-30-P8). Sodium maleate-ethyl vinyl ether copolymer modified with 30 mole % octyl groups and 1 mole % 2-(pyrenylsulfonamido)octyl groups was synthesized using the same procedure as that for the C8 series (Figure 3.3).[31]

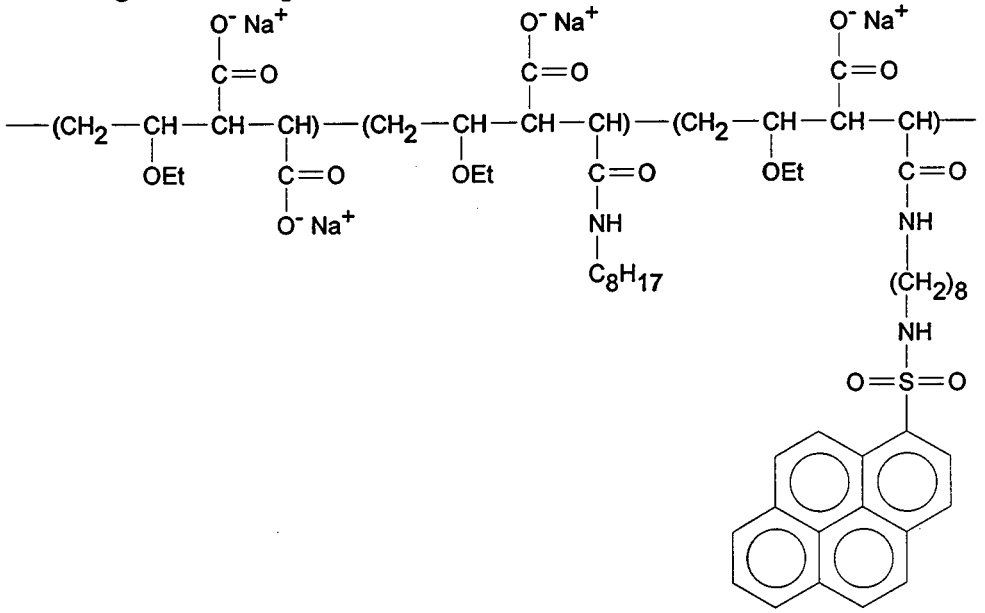

C8-30-P8, 30 Mole % C8, 1 Mole % P8

Figure 3.4 Octyl modified, pyrene-labeled poly (sodium maleate-*alt*-ethyl vinyl ether).

Instrumentation. UV-Vis spectra were recorded with a Hewlett Packard 8452A diode array spectrophotometer. Steady-state fluorescence spectra were measured on a Spex Fluorolog-2 fluorescence spectrometer and a DM3000F data system. Excitation and emission slit widths of 1 mm and right angle geometry were employed. For the fluorescence quenching studies an excitation wavelength of 340 nm was used, and emission at 400 nm was monitored.

Sample Preparation. Polymer solutions were prepared gravimetrically by dissolving the polymer samples either in deionized water or in citric acid-disodium phosphate (Na_2HPO_4) buffer. Buffered polymer solutions were prepared for the pH studies; aqueous sodium chloride (5.0 M) was added to give the desired NaCl concentration for the salt study.

Since naphthalene is only sparingly soluble in water ($2.5 \pm 0.2 \times 10^{-4}$ M), a modification of the technique employed by Zana *et al.* was utilized.[32] To a glass scintillation vial, 100 μL of a 0.33 M solution of naphthalene was added. Solvent was then evaporated with a gentle nitrogen stream. Polymer solution was immediately added, and samples were shaken for 24 h. After periods of 1 - 2 days, phase separation occured in many samples, especially in low pH and high ionic strength polymer solutions. Naphthalene concentration was quantitatively measured utilizing the UV absorbance at 312 nm ($\varepsilon = 289\ M^{-1}cm^{-1}$)[33] after 24 hours.

Results and Discussion

The preparation of hydrophobically modified poly (sodium maleate-*alt*-ethyl vinyl ether)s proceeds by a simple two step modification of the parent copolymer. A primary amine reacts with maleic anhydride repeat units along the polymer chain. This reaction is carried out in ethyl acetate. Unreacted anhydride units are then hydrolyzed to carboxylate groups by dissolution of the modified copolymer in 1 N aqueous NaOH at 25 °C. Stoichiometric formation of amide linkages is achieved without any detectable hydrolysis. An advantage of this modification process is that a series of copolymers with varying substitution can be synthesized from the same MAEVE polymer, so the degree of polymerization remains the same for the entire copolymer series. Therefore, any significant changes in aqueous solution properties may be attributable to conformational and environmental changes brought about by hydrophobic interactions.

Poly (maleate-*alt*-alkyl vinyl ether)s are known to possess good water-solubility, and when the alkyl group is sufficiently hydrophobic, a compact structure results. The globular conformation is most prominent at low pH, where chain-expanding electrostatic interactions that compete with intrapolymer hydrophobic association are eliminated. When the alkyl group of the vinyl ether is longer than C_4, a transition from an intramolelularly associating system to an extended state occurs as carboxyl groups are ionized.[34,35] As alkyl group size is increased from C_5 to C_8 in dansylated copolymers, fluorescence studies indicate that environmental hydrophobicity in the fully ionized state increases with alkyl chain length. This behavior is independent of polymer molecular weight, which suggests that short-range interactions are responsible for microdomain organization.[22]

Naphthalene Sequestration Studies. The micellar environment formed by intrapolymer association of alkyl groups can act as an effective host for hydrophobic molecules.[19,28-30] Time-resolved fluorescence quenching studies by Binana-Limbelé

and Zana indicate that micellar domains are present that can solubilize model hydrophobes such as pyrene probe. Polymer micelle aggregation number and probe-quencher diffusion are also found to be highly dependent upon the degree of ionization.[20] Hydrophobicity, ionic strength, and pH may also affect micellar domain size, as is the case for small molecule surfactant solutions.[3637-38] When polymer micelle properties change, the phase transfer properties may also vary.

A simple, quantitative method to evaluate hydrocarbon uptake by polymer micelles involves the use of an aromatic or polyaromatic hydrocarbon. Ito *et al.* studied the effects of counterion type on azobenzene and naphthylazo dye uptake.[28] Hurter and Hatton evaluated micelle-water and octanol-water partition coefficients of poly (ethylene oxide-propylene oxide) block copolymers for naphthalene, phenanthrene, and pyrene.[30] Here we investigate the sequestering abilities of octyl modified maleate-*alt*-ethyl vinyl ether copolymers utilizing naphthalene. The high molar absorptivity of chromophores such as naphthalene allows accurate, rapid quantitation by UV-Vis spectrophotometry.

Initial efforts focused on the use of azobenzene as a solute for phase transfer studies, but trans-cis photoisomerization induced shifts in absorbance and λ_{max}. Environmental fluidity has been shown to affect the rate of azobenzene trans-cis photoisomerization in hydrophobically modified, azobenzene-labeled poly (sodium 2-acrylamido-2-methylpropane sulfonate) (NaAMPS) unimolecular micelles.[39,40] A photostable chromophore such as naphthalene was found to be better suited for this study.

Naphthalene is sparingly soluble in water, and UV studies of saturated aqueous naphthalene solutions indicate a solubility of $2.5 \pm 0.2 \times 10^{-4}$ M at 25 °C. In order to maximize naphthalene dissolution and phase transfer, a previously reported technique was utilized to prepare saturated aqueous naphthalene solutions.[32] Naphthalene solution was added to a vial and solvent then evaporated. Solubilization of naphthalene by polymer micelles was confirmed by increases in UV absorbance at 312 nm (ε = 289 $M^{-1}cm^{-1}$)[33] after one hour. After several days, many polymer solutions began to precipitate. Accurate, reproducible results were obtained by measuring the absorbance after 24 h.

Because naphthalene is soluble in water, this must be taken into account when determining naphthalene partitioning into C8 polymer micelles. Normalized naphthalene sequestration is quantitated as follows:

$$\frac{[Np]}{[C8]} = \frac{[Np]_{Total} - [Np]_{H_2O}}{[C8]} \qquad (1)$$

where [Np]/[C8] describes the amount of naphthalene solubilized per hydrophobic group. [Np] is the concentration of micellized naphthalene and [C8] is the concentration of n-octylamide polymer repeat units in solution. $[Np]_{Total}$ is the total soluble naphthalene concentration determined from UV absorbance measurements, and $Na]_{H_2O}$, the solubility of naphthalene in water, is subtracted from $[Np]_{Total}$ to obtain the concentration of micellized naphthalene, [Np].

Naphthalene Uptake as a Function of Hydrophobic Substitution. Naphthalene uptake by 0.6 g/dL solutions of the C8 series as a function of substitution are plotted in Figure 3.4.

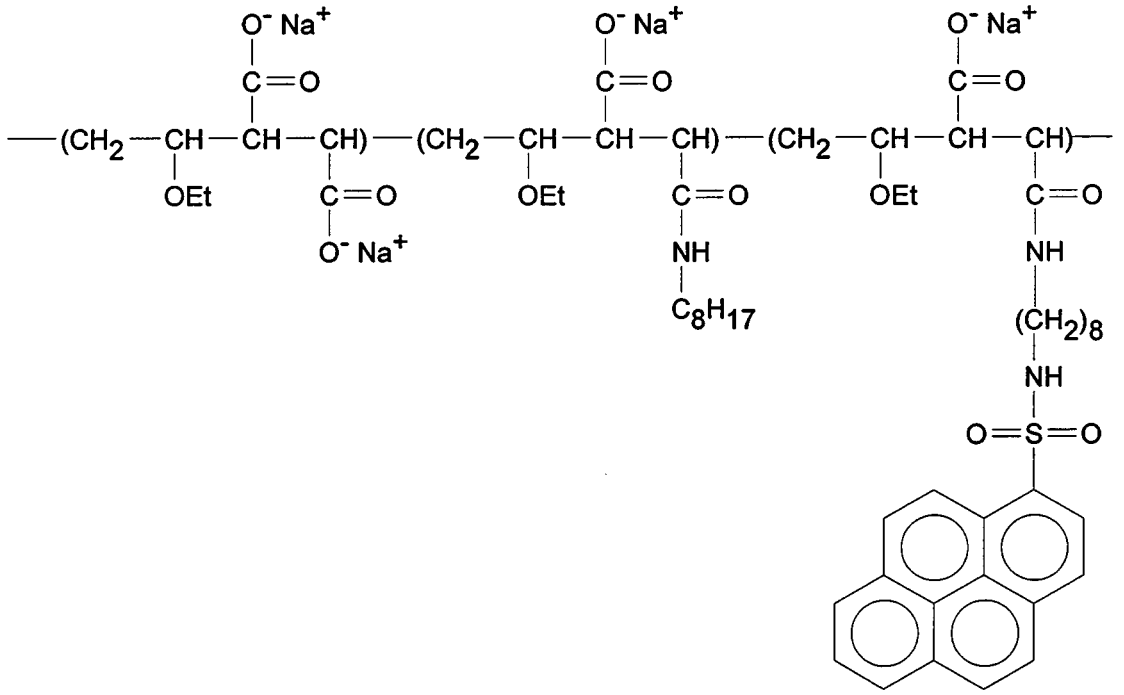

C8-30-P8, 30 Mole % C8, 1 Mole % P8

Figure 3.4 Normalized naphthalene uptake [Na]/[C8] as a function of octyl substitution for 0.6 g/dL aqueous polymer solutions in the C8 series.

A maximum in naphthalene sequestration is noticable at 20 mole % octyl substitution. We have previously shown that as C8 substitution is increased from 0 to 50 mole %, intrinsic viscosity ([η]) drops an order of magnitude from over 11 dL/g to less than 2 dL/g.[6] The decrease in [η] is most pronounced as substitution is increased from 20 to 30 mole %. This transition parallels the polyelectrolyte-polysoap transition reported by Strauss.[18]

The rise in [Np]/[C8] as substitution increases from 10 to 20 mole % is expected. The addition of octyl groups along the chain allows for a higher degree of intramolecular micelle formation. However, [η] drops only slightly in this range as hydrophobic modification is doubled. Obviously, the localized concentration of octyl groups is not sufficiently high for significant coil contraction, but there is sufficient micellization of octyl groups to form organized microdomains. As substitution increases from 30 to 50 mole %, [Np]/[C8] drops to levels below that of 10 mole % modified C8 polymer. When micellar structure becomes more organized with increasing C8 content, naphthalene uptake is appreciably hindered. The compact conformation adopted likely is a rigid, vitrified phase.

Fluorescence emission studies of labeled polysoaps support this proposed mechanism. Excimer/monomer fluorescence emission studies of naphthalene-

labeled C8 modified copolymers previously synthesized in our labs indicate a maximum in naphthalene dimer formation at 30 mole %.[6] As chain dimensions decrease with increasing hydrophobicity, naphthalene labels are brought in closer contact to each other. The probability of interaction between naphthyl groups in forming the sandwich-like dimeric excited state increases in this C8 incorporation range. With further hydrophobic substitution, naphthyl labels are "diluted" within the micellar environment.[41] The compactness of the microdomains at high modification levels can also hinder the orientation that is requisite for excimer formation.[42]

Changes in the rate of micelle formation-breakdown may also account for the reduction in solubilization efficiency. Zana *et al.* reported changes in pyrene solubilization as micellar formation and breakdown rates changed. As the residence time of a surfactant within a micelle inceases, pyrene solubilization decreases.[32] Solubilization studies by Carroll revealed that micelle formation-breakdown and adsorption-desorption of micelles at the oil-water interface dictate uptake kinetics rather than oil diffusion into micelles.[43] Obviously, when surfactant groups are bound to a polymer chain, their motion is resricted considerably. This equates to the formation of a restricted environment that hinders the motion of amphiphilic repeat units and guest molecules. Chu and Thomas have reported this phenomenon in pyrene probe emission studies of poly (sodium 11-undecenoate) (SUe) and sodium undecanoate (SUa) micelles.[16] Probe-quencher mobility in SUe polymer micelles was found to be much less than the mobility in SUa small molecule micelles.

Salt Effects. Normalized naphthalene sequestration ([Np]/[C8]) as a function of sodium chloride concentration for 0.6 g/dL solutions of C8-10, C8-20, and C8-50 is shown in Figure 3.5.

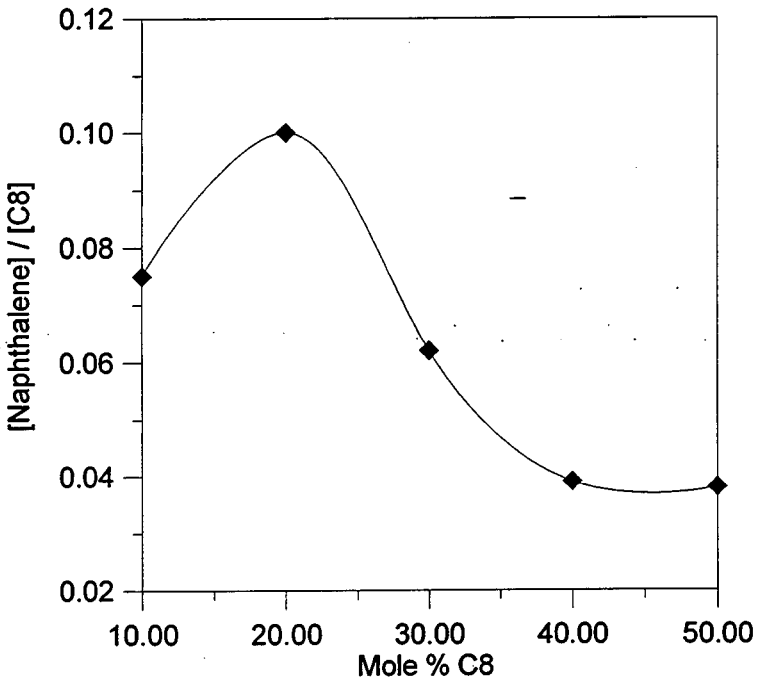

Figure 3.5 Normalized naphthalene uptake [Na]/[C8] as a function of sodium chloride concentration for 0.6 g/dL aqueous polymer solutions of C8-10, C8-20, and C8-50.

These three samples are the most representative of the possible micellar structures within this series. C8-10 forms an inadequately organized polymer micelle in deionized water, C8-20 possesses optimum organization, and the environment in a C8-50 micelle is quite rigid. No noticable trend is observed in C8-20; [Np]/[C8] values fluctuate around 0.08. However, in both C8-10 and C8-50, [Np]/[C8] is enhanced with salt-triggered coil contraction.

C8-10 possesses moderate sequestration properties in deionized water, even though a relatively open conformation is adopted. As added electrolyte shields electrostatic repulsions, the coil contracts, and hydrophobic microdomains become more organized as the localized octyl group concentration increases. Although C8-10 acts as a polyelectrolyte at low ionic strength, environmental changes that contract the chain impart a conformation more characteristic of a polysoap.

Micellar domains formed by C8-50 are highly organized, and it would seem that salt addition could further vitrify the microenvironment and inhibit phase transfer. As ionic strength increases, so does [Np]/[C8]. If an already compact structure is contracted further, an effective vehicle for water-micelle phase transfer may result. If the ionic surface of a polysoap contracts, a fraction of the micellar surface may then consist of hydrophobic groups. If a portion of the surface does indeed consist of hydrophobic groups, interpolymer hydrophobic aggregation is augmented. This has been shown to occur in poly (vinyl pyridine)s quaternized with dodecyl groups,[18] and in poly (sodium maleate-*alt*-ethyl vinyl ether) modified with dodecyl groups.[6] In both cases, when a freshly prepared stock solution was diluted, the viscosity of the dilution slowly decreased over hours, and sometimes over a period of days. This effect is not observed rheologically in the C8 series, but nonradiative energy transfer studies of mixed solutions of naphthalene- and pyrene-labeled C8-30 indicate that interpolymer aggregation does occur at very low polymer concentrations (< 0.01 g/dL) in some cases.[31]

pH Effects. Naphthalene sequestration by 0.6 g/dL solutions of C8-10, 20, and 50 at pH 4, 6, and 8 is plotted in Figure 3.6. As pH is increased from 4 to 8 in solutions of C8-10 and C8-20, slight increases in naphthalene sequestration are observed. C8-50 exhibits maximum sequestration at pH 4.

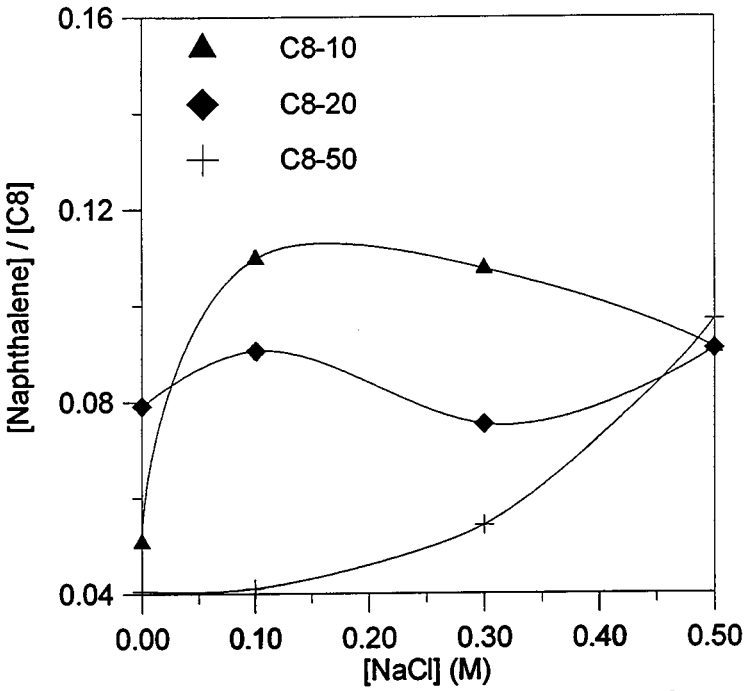

Figure 3.6 Normalized naphthalene uptake [Na]/[C8] as a function of pH for 0.6 g/dL aqueous polymer solutions of C8-10, C8-20, and C8-50.

Ionic strength effects may be responsible for the increase in [Np]/[C8] with pH for C8-10 and C8-20. Buffered aqueous solutions were prepared for this study, and these buffers consisted of mixed solutions of 0.1 M citric acid and 0.2 M disodium phosphate (Na_2HPO_4). As pH is increased by increasing the disodium phosphate-citric acid ratio, overall electrolyte concentration increases. The shielding of electrostatic repulsions may predominate over the elimination of charge-charge repulsions by acid addition as a mechanism for enhanced polymer micelle organization at these hydrophobe compositions

As pH decreases, naphthalene sequestration by C8-50 is enhanced. The increase correlates well with the proposed formation of a hydrophobic micellar surface. As carboxylate groups are protonated, the elimination of Coulombic repulsive forces allows contraction of the micellar corona. As the number of charged groups on the surface decreases, and the fraction of uncharged carboxylic acid functionalities increases, a fraction of the micelle surface may become occupied by hydrophobic groups.

Recent photophysical studies of anionic polysoaps corroborate the existence of hydrophobe partitioning into unmicellized hydrophobic portions of the polymer coil. Strauss[29] and Zana[20,44] have carried out aggregation number studies on maleate-alkyl vinyl ether polymers to further elucidate the mechanism of polysoap micellization. Zana evaluated intramolecular micelle formation in poly (disodium maleate-*alt*-decyl vinyl ether) (PS10) and poly (disodium maleate-*alt*-hexadecyl vinyl ether) (PS16). Time-resolved fluorescence quenching studies of aqueous PS16 solutions showed that probe-quencher migration between microdomains through unmicellized repeat units is possible. Fluorescence quenching studies of aqueous

poly (dilithium maleate-*alt*-hexyl vinyl ether) solutions by Strauss support the existence of quencher partitioning between micellized and unmicellized portions of the polymer coil.[29] Benzophenone quencher solubility in hexyl copolymer micelles is independent of pH, and exit rate constants for benzophenone as quencher were higher than other quenchers that possessed similar exit rate constants.

A mechanism for pH- and salt-triggered sequestration by unmicellized hydrophobic groups is depicted in Figure 3.7. As a portion of the micelle surface becomes covered with hydrophobic groups, the nonpolar surface can effectively interact with a hydrophobe in solution or with an oil-water interface. Micelle formation-breakdown would then become less important than simple hydrophobic interactions between guest molecules and readily accessible hydrophobic groups on the micellar surface.

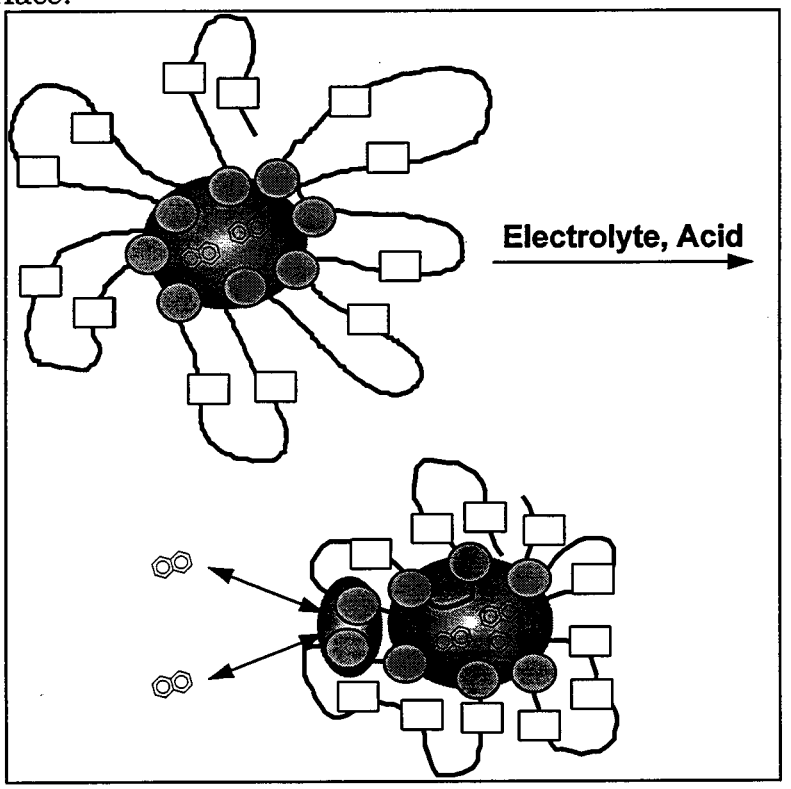

Figure 3.7 Conceptual model of naphthalene sequestration by unmicellized hydrophobic surface groups.

Fluorescence Quenching Studies. Results from naphthalene solubilization studies suggest that the environmental fluidity of micellar domains can affect the extent to which phase transfer occurs. Electrolyte concentration and pH also influence micelle organization. Fluorescence quenching studies of naphthalene- and pyrene-labeled anionic polyelectrolytes with nitromethane showed that coil shrinkage slows the diffusion of amphiphilic quencher molecules to fluorescent labels.[45,46] Dynamic diffusion-controlled quenching is described as follows:

$$\frac{I_0}{I} = 1 + K_{SV}[Q \tag{2}$$

$$K_{SV} = k_q \tau_0 \tag{3}$$

where I_0 is the steady-state fluorescence intensity of a chromophore in solution prior to quencher addition, I is the fluorescence intensity at quencher concentration [Q], K_{SV} is the Stern-Volmer quenching constant (M^{-1}), k_q is the first order quenching constant (M^{-1} s^{-1}), and τ_0 is the fluorescence lifetime in the absence of quencher. If quenching were solely dynamic or static in nature, a plot of I_0/I vs. [Q] should give a straight line with a slope equal to K_{SV}. Steady-state quenching studies of 0.1 g/dL solutions of pyrenylsulfonamidooctyl-labeled C8-30 polymer (C8-30-P8) as a function of sodium chloride concentration and pH revealed linear I_0/I vs. [Q] plots in all cases, with K_{SV} values in the range of dynamic, diffusion-controlled quenching.

The effects of sodium chloride concentration and pH on the quenching rate are depicted in Figure 3.8. Sodium chloride and buffer both have no effect on pyrene fluorescence, so changes in K_{SV} would reflect changes in the rate of label-quencher diffusion. As K_{SV} decreases, quencher mobility within the micellar environment becomes more restricted. As sodium chloride concentration increases, the Stern-Volmer quenching constant decreases. The enhancement in micellar organization induced by salt-triggered micelle contraction that increases sequestration also decreases mobility within the micelle. As pH is increased from 4 to 8, overall K_{SV} values are lower due to ionic strength effects of the citrate-phosphate buffer. A noticable increase in K_{SV} is observed as pH is increased from 4 to 8. As a more open conformation is adopted via deprotonation of carboxyl groups, label-quencher diffusion becomes more facile. These results, in conjunction with data from naphthalene uptake studies, support the presence of soaplike structures capable of sequestering hydrophobic materials, and that the fluidity of the micelles present in solution is controllable by changes in sodium chloride concentration and pH.

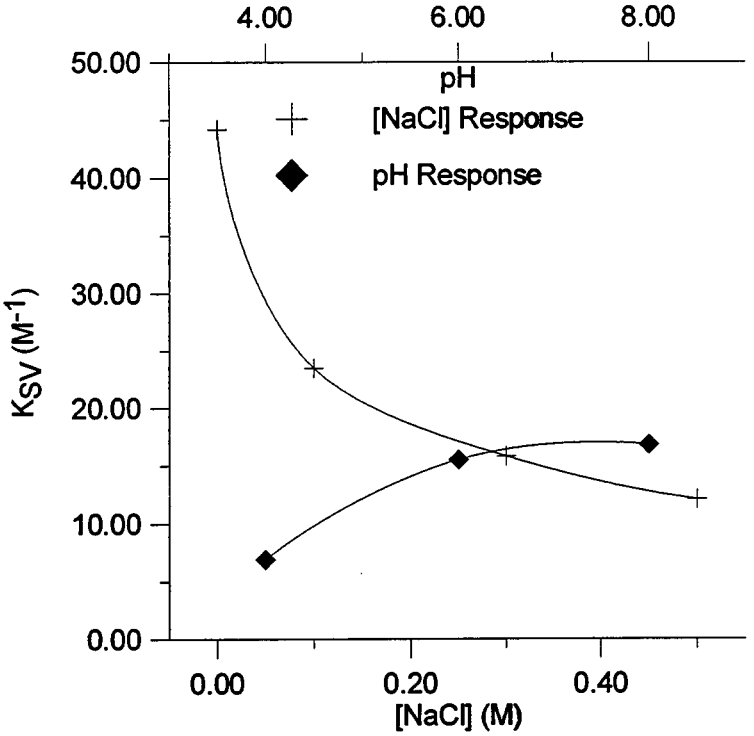

Figure 3.8 Stern-Volmer quenching constants of 0.1 g/dL aqueous polymer solutions of C8-30 polymer labeled with 1 mole % pyrenylsulfonamido octyl groups (C8-30-P8) as a function of sodium chloride concentration and pH.

Conclusions

In this study, UV-Vis analysis confirms the partitioning of naphthalene into hydrophobic microdomains formed by hydrophobically modified poly (sodium maleate-*alt*-ethyl vinyl ether)s in aqueous solution. The extent and also the mechanism of solute phase transfer is controllable by variation in polymer hydrophobicity, electrolyte concentration, and pH. As hydrophobic group substitution increases from 10 to 50 mole %, the polyelectrolyte-polysoap transition previously observed by fluorescence and viscosity studies correlates with the formation of a micellar environment that restricts the mobility of hydrophobic guest molecules. Optimum sequestration was observed at a composition of 20 mole % octyl substitution; this corresponds to a modification level just short of the polyelectrolyte-polysoap transition. With further increases in polymer hydrophobicity, sequestration is diminished by the formation of a highly compact, rigid microenvironment due to intrapolymer micellization of octyl groups. If electrolyte is added to C8 polymer solutions, micellar organization is enhanced, and similar effects are observed when pH is lowered. At the maximum level of octyl modification (50 mole %), salt- and pH-triggered micelle reorganization results in enhanced phase transfer properties.

A mechanism has been proposed whereby the shielding or elimination of electrostatic repulsive forces decreases micellar surface coverage by carboxyl and

carboxylate groups, and a fraction of the surface becomes covered with hydrophobic groups. The interaction of nonmicellar hydrophobic groups with a hydrophobic solute or an oil/water interface can increase as the formation of a hydrophobic surface creates an effective vehicle for phase transfer. Results from fluorescence quenching studies of pyrene-labeled, octyl modified copolymer support the vitrification of micellar domains with increasing salinity and acidity. Studies of this nature and the development of models for association and sequestration may ultimately aid in the design of water-soluble polysoaps for improved oil recovery and phase transfer by enabling the prediction and control of hydrocarbon uptake properties by structural and environmental changes.

References and Notes

1. McCormick, C. L., Middleton, J. C. and Grady, C. E. *Polymer* 1992, **33**, 4184.

2. McCormick, C. L., Middleton, J. C. and Cummins, D. F. *Macromolecules* 1992, **25**, 1201.

3. McCormick, C. L., Nonaka, T. and Johnson, C. B. *Polymer* 1988, **29**, 731.

4. Branham, K. D., Davis, D. L. and McCormick, C. L. *Polymer* 1994, **35**, 4429.

5. Chang, Y. and McCormick, C. L. *Polymer* 1994, **35**, 3503.

6. McCormick, C. L. and Chang, Y. *Macromolecules* 1994, **27**, 2151.

7. Chang, Y., Lochhead, R. Y. and McCormick, C.L. *Macromolecules* 1994, **27**, 2145.

8. Chang, Y. and McCormick, C. L. *Macromolecules* 1993, **26**, 6121.

9. McCormick, C. L., Hoyle, C. E. and Clark, M. D. *Polymer* 1992, **33**, 243.

10. Magny, B., Iliopoulos, I., Zana, R. and Audebert, R., *Langmuir* 1994, **10**, 3180.

11. Iliopoulos, I. and Olsson, U. *J. Phys. Chem.* 1994, **98**, 1500.

12. Iliopoulos, I., Wang, T. K. and Audebert, R. *Langmuir* 1991, **7**, 617.

13. Peiffer, D.G. *Polymer* 1990, **31**, 2353.

14. Morishima, Y., Nomura, S., Ikeda, T., Seki, M. and Kamachi, M. *Macromolecules* 1995, **28**, 2894.

15. Morishima, Y. and Kamachi, M. *Proc. Am. Chem. Soc. Div. Polym. Mat.: Sci. Eng.* 1994, **71**, 271.

16. Chu, D. Y. and Thomas, J. K. *Macromolecules* 1991, **24**, 2212.

17. Chu, D. Y. and Thomas, J. K. *Macromolecules* 1987, **20**, 2133.

18. Strauss, U. P., Gershfeld, N. L. and Crook, E. H. *J. Phys. Chem.* 1956, **60**, 577.

19. Strauss, U. P. and Gershfeld, N. L. *J. Phys. Chem.* 1954, **58**, 747.

20. Binana-Limbelé, W. and Zana, R. *Macromolecules* 1990, **23**, 2731.

21. Binana-Limbelé, W. and Zana, R. *Macromolecules* 1987, **20**, 1331.

22. Strauss, U.P., Schlesinger, M.S. *J. Phys. Chem.* 1978, **82**, 1627.

23. Strauss, U. P. and Schlesinger, M. S. *J. Phys. Chem.* 1978, **82**, 571.

24. Strauss, U. P. and Vesnaver, G. *J. Phys. Chem.* 1975, **79**, 2428.

25. Strauss, U. P. and Vesnaver, G. *J. Phys. Chem.* 1975, **79**, 1558.

26. Baldwin, M. G. *J. Polym. Sci.* 1965, **A3**, 703.

27. McCormick, C. L., Hoyle, C. E. and Clark, M.D. *Polymer* 1992, **33**, 243.

28. Ito, K., Ono, H. and Yamashita, Y. *J. Coll. Sci.* 1964, **19**, 28.

29. Zdanowicz, V. S. and Strauss, U. P. *Macromolecules* 1993, **26**, 4770.

30. Hurter, P. N. and Hatton, T. A. *Langmuir* 1992 **8**, 1291.

31. Hu, Y., Kramer M. C., Boudreaux, C. J. and McCormick, C. L. *acromolecules*, Submitted for Publication.

32. Lianos, P., Viriot, M. L. and Zana, R. *J. Phys. Chem.* 1984, **88**, 1098.

33. 'Spectrometric Identification of Organic Compounds, 4th Ed.,' Silverstein, R. M., Bassler, G. C. and Morrill, T. C., Wiley, New York, 1981, pp. 326-329.

34. Dubin, P. L. and Strauss, U. P., *J. Phys. Chem.* 1970, **74**, 2842.

35. Dubin, P. L. and Strauss, U. P. *J. Phys. Chem.* 1967, **71**, 2757.

36. Zachariasse, K. A., Phuc, N.V. and Kozankiewicz, B. *J. Phys. Chem.* 1981, **85**, 2676.

37. Lianos, P. and Zana, R. *J. Phys. Chem.* 1980, **84**, 3339.

38. Mazer, N. A., Benedek, G. B. and Carey, M.C. *J. Phys. Chem* 1976, **80**, 1075.

39. Morishima, Y., Tsuji., M., Seki, M. and Kamachi, M. *Macromolecules* 1993, **26**, 3299.

40. Morishima, Y., Tsuji, M., Kamachi, M. and Hatada, K. *Macromolecules* 1992, **25**, 4406.

41. McCormick, C. L., Hoyle, C. E. and Clark, M.D. *Macromolecules* 1990, **23**, 3124.

42. Seo, T., Take, S., Akimoto, T., Hamada, K. and Iijima, T. *Macromolecules* 1991, **24**, 4801.

43. Carroll, B.J. *J. Coll. Interface Sci.* 1981, **79**, 126.

44. Binana-Limbelé, W. and Zana, R. *Macromolecules* 1987, **20**, 1331.

45. Kramer, M. C., Welch, C. G., Steger, J. R. and McCormick, C. L. *Macromolecules*, in Press.

46. McCormick, C. L., Hoyle, C. E. and Clark, M. D. *Macromolecules* 1991, **24**, 2397.

Chaper 4: Synthesis, Rheological, and Photophysical Studies of the Associative Properties of Pyrene-Labeled Poly (Acrylamide-*co*-Sodium 11-Acrylamidoundecanoate)

Synopsis

The synthesis, rheological, and fluorescence properties of a novel water-soluble polymer based on a micelle-forming monomer are reported. Sodium 11-Acrylamidoundecanoate (SA), a surface-active monomer, copolymerizes readily with acrylamide (AM) to give high molecular weight polymer. Incorporation of the fluorescent monomer 2-(1-pyrenylsulfonamido) ethyl acrylamide into the monomer feed yields a terpolymer with associative solution properties different from previously synthesized AM/SA copolymers. The fluorescent label acts as a model hydrophobe; changes in associations that elicit a viscosity response in AM/SA copolymers also affect the emission characteristics of the pyrene label. Steady-state fluorescence emission studies reveal significant constriction of the polymer chain as pH decreases or electrolyte concentration increases. As a result, the nature of pyrene-pyrene association can be varied from inter- to intramolecular as electrolyte or acid concentration increases. Fluorescence quenching studies indicate that the salt-induced chain contraction may enhance the organization of mixed polymeric micelles formed by SA and pyrene repeat units. Emission studies of mixed solutions of labeled AM/SA copolymer with surfactants reveal a micellar bridging mechanism. The steady-state emission techniques employed confirm the pronounced pH and salt-responsiveness of AM/SA-based polymers observed in viscosity studies.

Introduction

Ongoing research in our laboratories involves the synthesis and characterization of water-soluble polymers that exhibit associative behavior in aqueous media. Of particular interest are amphiphilic copolymers containing both hydrophilic and hydrophobic monomers. The pronounced associative thickening behavior observed in these systems arises from interpolymer hydrophobic associations. For example, the viscosity profile of aqueous solutions of copolymers of acrylamide with small levels (≤ 1 mole %) n-alkylacrylamide comonomers possesses an upward curvature at a low critical overlap concentration (C*).[1] This C* occurs well below the onset of chain entanglement observed in acrylamide homopolymer. When fluorescent hydrophobes are incorporated into acrylamide polymers, the photophysical response may effectively probe solution behavior on the microscopic level. Copolymers of acrylamide with a pyrene-containing acrylamido monomer exhibit a parallel increase in excited state dimer (excimer) formation and viscosity.[2,3] Interpolymer hydrophobic associations between pyrene groups that bring about the viscosity response also induce changes in the photophysical behavior.

Ionic group incorporation improves the solubility of these systems, and solution properties can become dependent on pH and/or electrolyte concentration. Terpolymerization of acrylamide, n-decylacrylamide (C_{10}AM) and a carboxylate or sulfonate acrylamido comonomer affords a copolymer with strong associative properties.[4] The salt- and pH-responsiveness inherent to these systems is a function of ionic group type and placement. Hydrophobic associations in carboxylate-based systems are much stronger than those observed for their respective sulfonate analogs. Also, placement of the ionic group farther from the polymer backbone appears to affect the nature of the hydrophobic associations.[4]

If a hydrophobic group and a zwitterionic or ionic group are incorporated into the same vinyl monomer unit, water-solubility and surface activity can result. Sodium 11-acrylamidoundecanoate (Figure 4.1) is one such surface-active amphiphile readily polymerizable by free radical techniques.[5] Previous studies of SA homopolymer and copolymers with acrylamide (AMSA)[6,7] indicate considerable pH and salt-responsiveness; pyrene probe studies confirm the formation of micellar microdomains. SA can be described as a "tail end-attached" monomer.[8,9] The repeat units of the resultant polymer contain a carboxylate group on the end of a pendent hydrophobic group. When this geometry is assumed, the motions of the hydrophobic group are coupled to the polymer backbone, and the pendent polar group may perturb hydrophobic associations in aqueous solution. As a result, polymerized, tail-attached surfactants possess good water-solubility and poor micellization.[9] Pyrene probe studies indicate a micellar environment not quite as hydrophobic as that formed by polymerized surfactants containing polar groups closer to the polymer backbone. Similar results are observed for polymerized sodium 11-undecenoate micelles, and restriction of pyrene from efficiently organized polymeric micelles has been postulated.[10,11,12]

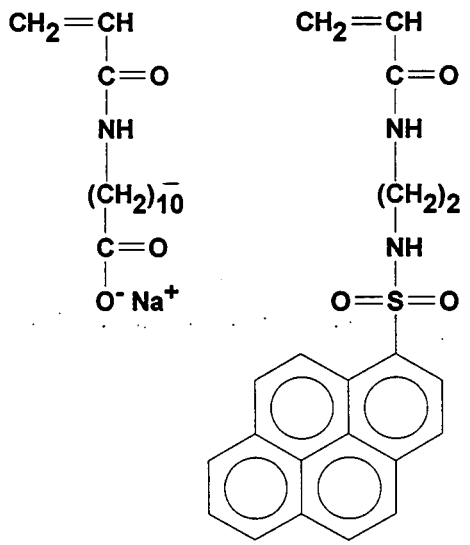

1 2

Figure 4.1. Sodium 11-acrylamidoundecanoate (SA, **1**) and 2-(1-pyrenylsulfonamido)ethyl acrylamide (APS ("Py"), **2**).

The objective of this study is the elucidation of the associative properties of a terpolymer of acrylamide (AM), sodium 11-acrylamidoundecanoate (**1**, Figure 4.1), and the fluorescent label 2-(1-pyrenylsulfonamido)ethyl acrylamide (**2**, Figure 4.1). Small incorporations of SA (≤ 10 mole %) and **2** (< 1 mole %) are sufficient to impart unique solution properties. Viscosity studies have shown that domain organization is highly dependent on pH and salt concentration, and that SA imparts this responsiveness. Fluorescence emission techniques with an incorporated label allow investigation of the solution properties on the microscopic level. Techniques such as these have previously been employed by our research group in studies of naphthalene- and pyrene-labeled water-soluble polymers.[2,3,13,14,15]

Experimental

Materials. All reagents and solvents were purchased from Aldrich Chemical Co. (Milwaukee, WI) unless noted otherwise. Acrylamide was recrystallized twice from acetone. Other materials were used as received. Water for synthesis and solution preparation was deionized and possessed a conductance < 10^{-7} mho/cm.

Sodium 11-Acrylamidoundecanoate (SA) (1). The methods of Gan[5] were employed in the synthesis of SA monomer. Purity was confirmed via NMR and melting point determination.

2-(1-Pyrenylsulfonamido) Ethylacrylamide (2). The procedure employed by Ezzell and McCormick[2] was followed to give pyrene monomer in good yield and purity according to NMR and HPLC analysis.

Pyrene-labeled AM/SA Copolymer (AMSA/Py) (3). A solution of sodium 11-acrylamidoundecanoate (1.80 g, 6.5 mmol) and acrylamide (9.00 g, 127 mmol) in 340 mL H_2O was added to a reaction flask immersed in a water bath at 50 °C. After finely ground 2-(1-pyrenylsulfonamido) ethyl acrylamide (0.51 g, 1.3 mmol) was added to the flask, the solution was degassed with nitrogen for one hour. Sodium dodecyl sulfate (Sigma, 99 % pure) (21.7 g, 75.2 mmol) was then added. At this point direct bubbling of nitrogen through the solution was stopped to prevent excessive foaming. The solution was stirred in a nitrogen atmosphere for 3 hours; after this time, most, but not all of the fluorescent comonomer had dissolved into SDS micelles. A degassed solution of potassium persulfate (50 mg, 0.19 mmol) in 5 mL H_2O was then injected into the monomer/surfactant solution. After stirring under nitrogen for three hours, the viscous polymer solution was added to 1400 mL acetone to yield 7.9 g (70 % yield) of a white precipitate. The polymer was washed with refluxing methanol for 16 hours in a Soxhlet extractor to remove residual monomer and surfactant.

Instrumentation. A Bruker AC-200 NMR spectrometer was used to determine ^1H and ^{13}C NMR spectra. Molecular weight was obtained with a Chromatix KMX-6

low angle laser light scattering photometer equipped with a 633 nm HeNe laser. Refractive index increments (d*n*/d*c*) were measured with a Chromatix KMX-16 laser differential refractometer. UV-VIS spectra were recorded with a Hewlett Packard 8452A diode array spectrophotometer. HPLC was carried out with a Hewlett Packard 1050 Series chromatograph fitted with a photodiode array UV detector and an Alltech Versapak C_{18} reversed-phase column. Steady-state fluorescence spectra were measured with a Spex Fluorolog-2 fluorescence spectrometer equipped with a DM3000F data system. Excitation and emission slit widths of 1 mm, an excitation wavelength of 340 nm, and right angle geometry were employed.

Results and Discussion

Polymer Syntheses. Gan[5] first reported the copolymerization of acrylamide with sodium 11-acrylamidoundecanoate (SA) at a monomer feed level of ≥ 30 mole %. Reactivity ratio studies indicated that SA monomer incorporation was equivalent to the molar ratio of the monomer feed. When a growing radical encounters a micelle containing polymerizable vinyl monomers, the localized monomer concentration and orientation are quite high. Rapid polymerization within the micelle occurs. This is observed as a fast overall polymerization rate yielding high molecular weight polymer. When SA is homopolymerized, high conversion and molecular weight ($M_w > 10^6$ g/mol) are obtained in a short period of time (< 1 hr). Even though a low feed level of SA is employed, high conversion within a short period of time is obtained.

Gan reported molecular weights in the 5×10^5 - 2×10^6 g/mol range. The molecular weights of AM/SA copolymers are observed to decrease to the lower limit as AM content is increased from 0 to 70 mole %.[6] The AMSA/Py copolymer in our work has a molecular weight of 1.8×10^6 g/mol. Good monomer, surfactant, and initiator purity may account for the higher molecular weight.

SA incorporation is assumed to equal monomer feed based on Gan's work and the high conversion obtained. When a copolymer of AM and SA with 90/10 AM/SA (mol/mol) in monomer feed was characterized by integration of ^{1}H NMR spectra, a copolymer composition of 10 ± 1 mole % was determined. If stoichiometric SA incorporation is assumed, 0.6 mole % incorporation for AMSA/Py is determined from UV-Vis studies (ε_{Py} = 24,100 M^{-1} cm^{-1} at 350 nm). The polymerization utilized 1 mole % fluorescent monomer in the monomer feed, but only 60 % of the monomer was incorporated. Ezzell and McCormick[2] also reported low pyrene comonomer content in acrylamide copolymers synthesized both homogeneously and in the presence of added surfactant. Incomplete pyrene monomer uptake by aqueous SDS micelles may account for this result. After pyrene monomer is added to the aqueous AM/SA/SDS solution, complete dissolution to reattain a clear monomer solution does not occur. Even after several hours stirring at 50 °C, undissolved fluorescent monomer persists.

The procedure in which an external surfactant is added to copolymerize a hydrophobic monomer with a hydrophilic monomer in aqueous solution is termed

"micellar polymerization." This technique can impart unique microstructural characteristics.[16,17,18] A "blocky" microstructure may result from the inherent heterogeneity of the medium. When such a polymerization is carried out, the propagating radical in aqueous solution adds to the hydrophilic monomers in the aqueous phase. When the macroradical encounters a micelle, polymerization of monomers within the micelle is favored as their residence time in the micelle increases. At high surfactant concentrations, this is a valid assumption, as the polymerization rate (k_p) is quite high (10^3 - 10^4 M^{-1} sec^{-1}) for acrylamide and its related monomers.[19] Since virtually all of the hydrophobic monomer, along with a fraction of the acrylamide[6,20] is partitioned into the micellar interior, a "blocky" incorporation of hydrophobic monomer is likely. Runs of hydrophobic units should be separated by long runs of hydrophilic sequences. In aqueous solution, concentration-dependent intra- or intermolecular associations of these hydrophobic segments result in micelle-like or associative behavior, respectively.

Recent studies by Zana and Candau[21,22] support the proposed microstructure of these polymers. Surface-active n-alkyldimethyl (vinylbenzyl) ammonium chlorides (n-alkyl = C_8, C_{12}, and C_{16}) were found to polymerize by a non-topological mechanism dependent upon alkyl chain length. In the case of the C_{16} surfactant, radical propagation occurs in nucleated, long-lived micelles that are more stable than unpolymerized micelles. Because the polymerized micelle is more stable than uninitiated micelles, the aggregates grow with the loss of uninitiated aggregates. With surfactants of shorter alkyl chain length, the growing radical does not possess sufficient stability to allow particle growth, and micellar breakdown provides accessibility to the aqueous environment. As the SA concentration in monomer feed increases, so does the SA micelle concentration; as a result, a higher fraction of SA "blocks" are incorporated into the resultant polymer structure. Because SA is an acrylamido monomer that polymerizes rapidly, polymerization of most if not all the SA micelle is facile. Chu and Thomas[12] reported the polymerization of sodium 11-undecenoate (SUe) micelles to give oligomers and polymers with molecular weights equivalent to the aggregation number of SUe at a given concentration. The double bond of an acrylamido group would polymerize more rapidly than SUe, and the absence of abstractable hydrogens in the SA monomer structure would eliminate chain transfer as a termination mechanism. Thus, extensive propagation within an SA micelle would effectively compete with micellar breakdown.

Viscosity and Excimer Emission Studies. When an AMSA copolymer is labeled with a fluorescent hydrophobe, the apparent viscosity response exibits a pronounced upwards curvature relative to poly (acrylamide) (PAM) of higher molecular weight (5 - 6 × 10^6 g/mol) due to interpolymer hydrophobic association of pyrenyl groups (Figure 4.2). A low critical overlap concentration ($C^* \cong 0.35$ g/dL) is observed. C^* for PAM is 0.6 g/dL. In deionized water above 0.8 g/dL, AMSA/Py solutions possess a gel-like, viscoelastic consistency. In 0.3 M sodium chloride, a viscosity reduction indicative of electrolyte-induced coil contraction is observed. Immediately after addition of sodium chloride to aqueous AMSA/Py solutions, the more highly concentrated (> 0.2 g/dL) solutions become gel-like with shear-

dependent phase behavior; when shaken, the polymer precipitates from solution. Viscosity decreases with time as monomer units reorganize to their most thermodynamically stable conformation.

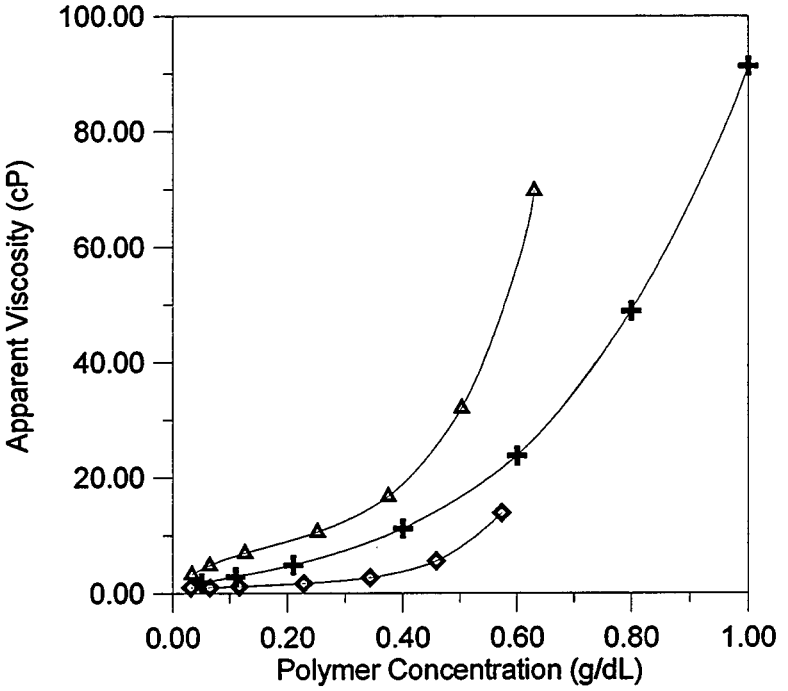

Figure 4.2. Apparent viscosity of poly (acrylamide) (5-6 × 10^6 g/mol) as a function of polymer concentration in deionized water (✚); apparent viscosity of AMSA/Py (1.8 × 10^6) as a function of polymer concentration in deionized water (▲) and aqueous 0.3 M NaCl (◆). pH: 7.

Viscosity studies provide a reasonable assessment of the bulk, macroscopic solution behavior, but a detailed analysis requires the use of a more sensitive characterization technique. Fluorescence emission studies are inherently sensitive to low chromophore concentrations and angstrom-level motions.

Our research group has investigated pyrene label excimer emission to elucidate solution behavior. As the degree of hydrophobic association increases, interaction between isolated, covalently bound pyrene groups allows the formation of dimeric, sandwich-like conformations that lead to excimer formation. Interpolymer hydrophobic association is observed as an increase in excimer relative to that of "monomer" emission. A typical fluorescence spectrum of AMSA/Py is shown in Figure 4.3. The peak maxima at 380, 400, and 420 nm arise from the fluorescence emission of isolated pyrenes (monomer emission). The broad, structureless band centered around 520 nm results from emission of excited dimeric pyrene (excimer). The intensity of excimer emission relative to that of the monomer emission (I_E/I_M) increases with polymer concentration. This response parallels the macroscopic viscosity behavior.[3,23] I_E/I_M is plotted as a function of polymer concentration in deionized water in Figure 4.4. I_E is taken as the fluorescence

intensity at 519 nm, and I_M as the fluorescence intensity at 400 nm. I_E/I_M steadily increases with polymer concentration. Intermolecular hydrophobic associations between pyrene labels that are responsible for the viscosity profile also increase the population of excited pyrene dimers, and, therefore, an increase in I_E/I_M. I_E/I_M values for a given polymer concentration are higher in salt. Viscosity studies indicate that the polymer coil shrinks as salt is added. As this occurs, the distance between pyrene groups on the same polymer chain decreases, and excimer formation becomes more favorable. As polymer concentration increases, I_E/I_M also increases in 0.3 M NaCl. This seems to indicate that intermolecular aggregation still occurs although no discernible C* in the viscosity response is observed.

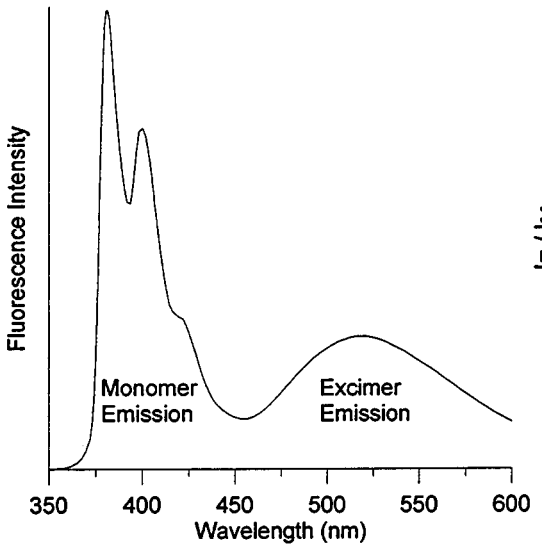

Figure 4.3. Fluorescence emission spectrum of AMSA/Py. Polymer concentration: 0.052 g/dL in deionized water. pH: 7. pyrene label concentration: 3.4×10^{-5} M, excitation wavelength: 340 nm.

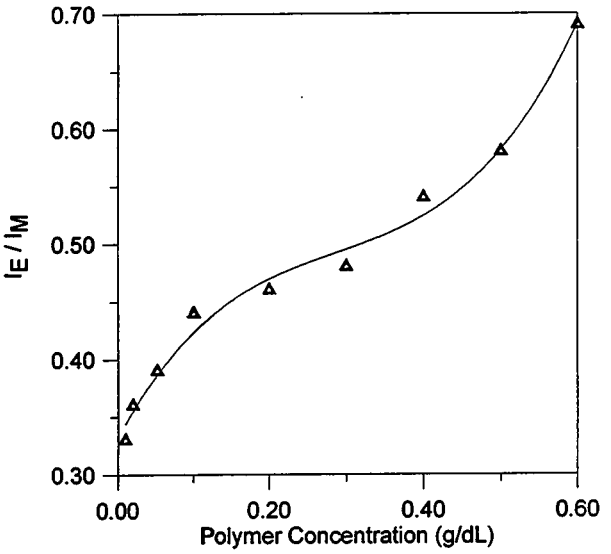

Figure 4.4. Excimer emission / monomer emission (I_E/I_M) of AMSA/Py in deionized water. pH: 7), I_E = fluorescence intensity at 519 nm, I_M = fluorescence intensity at 400 nm. Excitation wavelength: 340 nm.

Figure 4.5 illustrates the effects of added electrolyte on the degree of excimer emission below and above the critical overlap concentration (C*). Viscosity studies have shown that a decrease in pH or addition of electrolyte lower the viscosity of AMSA copolymers. Below C*, intrapolymer micellization of SA units is enhanced as charge-charge interactions between pendent carboxylate groups are shielded. Pyrene groups within the polymer coil are closer to one another, and an increase in excimer emission relative to monomer emission is observed. Above C*, past the initial onset of polymer-polymer aggregation, I_E/I_M is independent of ionic strength and polymer concentration. This suggests that pyrene-pyrene aggregation is insensitive to salt above C*. This result indicates that interpolymer association occurs primarily via interactions between chromophores.

As can be seen in Figure 4.6, pH also exerts a considerable effect on polymer dimensions. The viscosity response at pH 4 is considerably less than that at neutral pH for AM/SA copolymer due to protonation of carboxylate groups.[7] At low pH values, I_E/I_M is quite high, and excimer emission decreases precipitously as the carboxylic acid groups are neutralized. Electrostatic repulsion increases as the degree of ionization along the polymer chain increases. This causes coil expansion and increased separation of pyrenes within individual polymer chains. As pyrene groups become isolated, excimer emission decreases.[23]

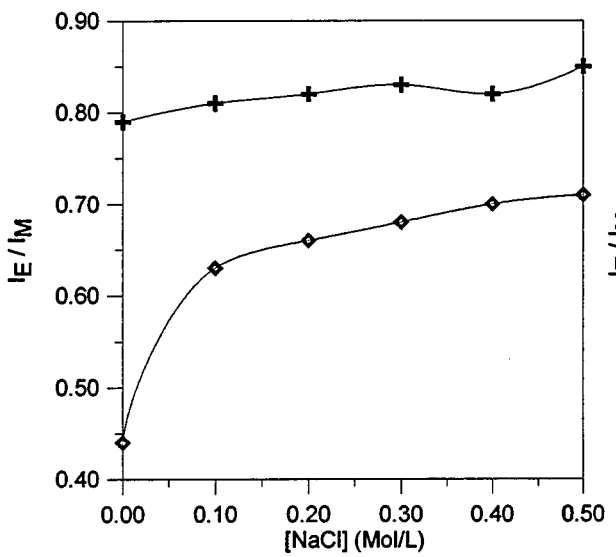

Figure 4.5. I_E/I_M as a function of aqueous NaCl concentration below (◆, 0.12 g/dL) and above (✚, 0.6 g/dL) C*. pH: 7.

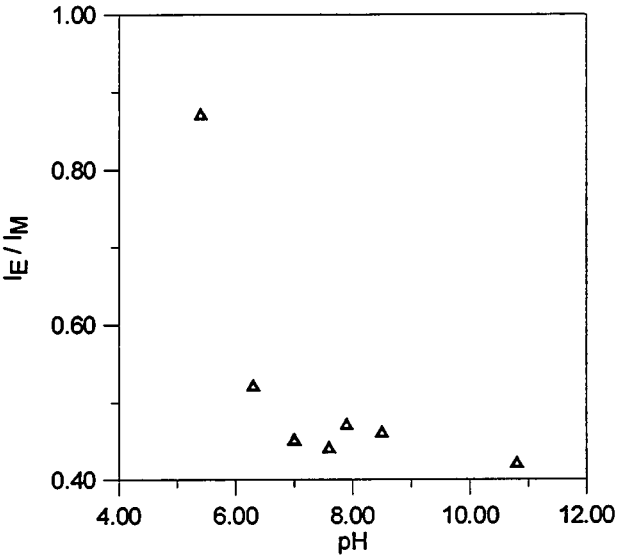

Figure 4.6. I_E/I_M of AMSA/Py as a function of pH below C*. Polymer concentration: 0.12 g/dL.

Fluorescence Quenching Studies. In order to probe ion binding and the accessibility of the pyrenylsulfonamido chromophore to the aqueous environment, fluorescence quenching experiments were carried out using the cationic, hydrophilic quencher thallium nitrate ($TlNO_3$) and the amphiphilic quencher nitromethane ($MeNO_2$). First order quenching constants were calculated using the Stern-Volmer equation.[24] Dynamic, diffusion-controlled quenching can be described as follows:

$$\frac{I_0}{I} = 1 + K_{SV}[Q \qquad (1)$$

$$K_{SV} = k_q \tau_0 \qquad (2)$$

where I_0 is the fluorescence intensity of a chromophore in solution in the absence of quencher, I is the fluorescence intensity at quencher concentration [Q], K_{SV} is the Stern-Volmer quenching constant (M^{-1}), k_q is the first order quenching constant (M^{-1} sec^{-1}), and τ_0 is the fluorescence lifetime in the absence of quencher. If quenching is dynamic, a plot of I_0/I vs. [Q] should give a straight line with a slope equal to K_{SV}.

Stern-Volmer plots for thallium nitrate and nitromethane quenching of 0.12 g/dL AMSA/Py in deionized water and aqueous sodium chloride solutions are shown in Figures 4.7 and 4.8. The linearity of the I_0/I versus [Q] plots verifies the dynamic nature of fluorescence quenching. The fluorescence lifetime of the pyrene label was found to be independent of [NaCl], so any changes in K_{SV} would signify changes in quencher-label interactions. From the average pyrenylsulfonamidoethyl fluorescence lifetime determined by Ezzell and McCormick[3] ($\tau_0 \cong 1.3 \times 10^{-8}$ sec), quenching rate constants can be calculated. The Stern-Volmer quenching constants and quenching rate constants (Table 4.1) approximate those of previously reported values.[3,25] The magnitude of the quenching rate constants signifies a dynamic, diffusion-controlled process.

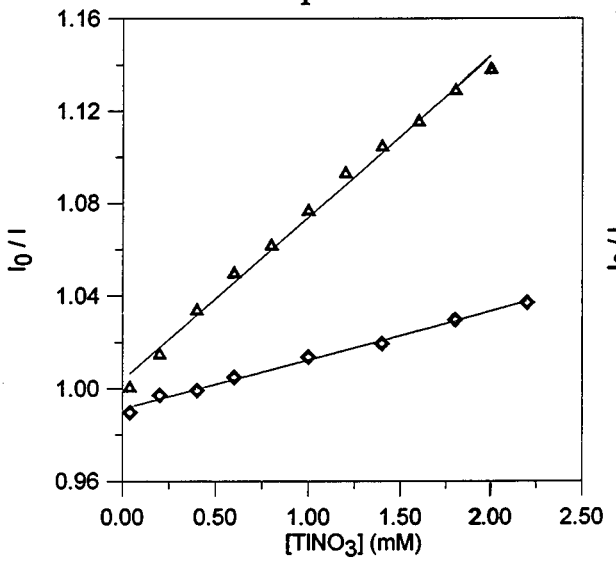

Figure 4.7. Stern-Volmer plot of 0.12 g/dL AMSA/Py quenching by thallium nitrate ($TlNO_3$) in deionized water (▲) and in aqueous 0.1 M NaCl (◆). pH: 7. I and I_0 are intensity values at 400 nm.

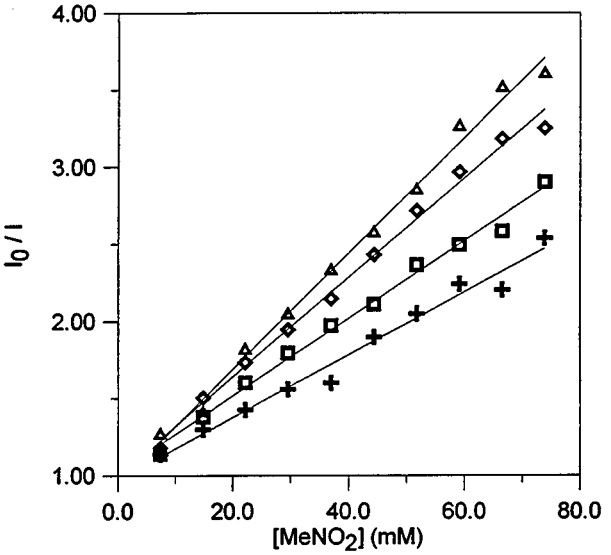

Figure 4.8. Stern-Volmer plot of 0.12 g/dL AMSA/Py quenching by nitromethane ($MeNO_2$) in deionized water and in H_2O (▲), 0.1 M NaCl (◆), 0.3 M NaCl (■), and 0.5 M NaCl (✚). pH: 7. I and I_0 are intensity values at 400 nm.

The reduction in the quenching efficiency of Tl^+ with salt addition could arise from enhanced compartmentalization of pyrene labels as added electrolyte enhances intrapolymer micellization. The reduction is due more likely to dilution of atmospheric Tl^+ counterions in the presence of added NaCl. At the low molar SA composition in the polymer, the Manning charge density parameter (ξ) is less than the critical charge density parameter ξ_c for univalent counterions ($\xi_c = 1$).[26] If counterions were condensed onto the carboxylate groups, the combination of static quenching by bound Tl^+ and dynamic quenching by atmospheric Tl^+ counterions would result in an upwards curvature in the Stern-Volmer plot. Morishima and Kamachi reported this result for phenanthrene-labeled acrylamide/sodium acrylate terpolymers with varying acrylate anion content.[25] For terpolymer containing 27

mole % sodium acrylate repeat units ($\xi = 0.67$), I_0/I vs. $[TlNO_3]$ plots yield a linear response. Higher charge density systems such that $\xi > 1$ exhibited a nonlinear Stern-Volmer response.

The effect of electrolyte addition on polymer conformation is illustrated by the data obtained from nitromethane quenching studies. Dynamic, diffusion-controlled quenching is indicated by the linear quenching response. As electrolyte concentration increases, K_{SV} decreases. It should be noted that sodium chloride does not quench pyrenylsulfonamide fluorescence. Therefore, it is valid to assume that any change in the nitromethane Stern-Volmer quenching constant with added sodium chloride arises from electrolyte-induced conformational or environmental changes and not from sodium chloride quenching. Ezzell and McCormick[3] determined that pyrene label aggregation had little effect on the quenching constant of nitromethane. For similar concentrations of a random acrylamide/2 copolymer and a similar copolymer with a more block-like microstructure, K_{SV} values did not differ significantly, despite the higher degree of excimer formation observed in the blocky copolymer. In both copolymers, K_{SV} values indicated that pyrene labels resided in a rather hydrated environment. If pyrene-pyrene aggregation were the sole association mechanism, K_{SV} values would not differ so markedly. Obviously SA micellar structure affects the diffusion of quencher to label. As salt is added, K_{SV} decreases. Hydrodynamic diameter also diminishes in this ionic strength regime. The reduction in the probe diffusion rate suggests that the rigidity of SA/Py mixed micelles increases with added salt. This phenomenon is depicted in Figure 4.9. As acid or electrolyte reduce polymeric micelle dimensions, the shielding (salt) or elimination (acid) of coulombic interactions between pendent carboxylate groups increases the extent of intramolecular hydrophobic associations

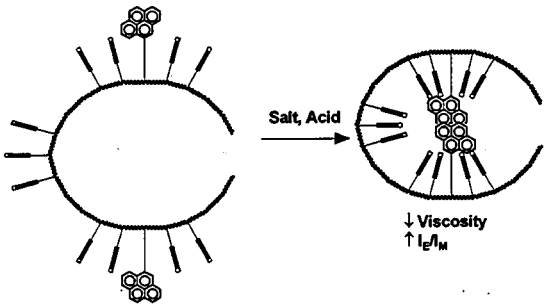

Figure 4.9. Proposed mechanism of salt/pH-triggered collapse of a fluorescently labeled, tail end-attached polymeric micelle.

Polymer-Surfactant Interactions. The addition of surfactants to aqueous solutions of amphiphilic polymers can either induce or break up interpolymer aggregation. The nature of the associations is dictated by the surfactant concentration and charge.

Additon of an oppositely charged surfactant such as hexadecyltrimethylammonium chloride (CTAC) to solutions of unlabeled AMSA copolymers results in a dramatic increase in viscosity up to a point where phase

separation occurs. When further surfactant is added, AMSA copolymers redissolve, and viscosities decrease. Goddard reported stoichiometric precipitation when anionic surfactant was added to bovine serum albumin on the acidic side of the isoelectric point.[27] Goddard proposed the existence of a second "layer" of bound surfactant ions with the ionic groups pointing outwards and the hydrophobic groups associated with the hydrophobic groups of the first layer.[28]

As CTAC concentration is increased in aqueous solutions of AMSA/Py at neutral pH, I_E/I_M increases (Figure 4.10). In the 10^{-4} to 10^{-2} M [CTAC] range, the polymer precipitates from solution. The excimer emission enhancement that accompanies increasing viscosity is consistent with an enhancement of interpolymer associations. In a study of the interaction of hydrophobically modified poly (sodium acrylate)s, Iliopoulos reported a viscosity increase and phase separation with increasing dodecyltrimethylammonium chloride (DTAC) concentration.[29] At higher DTAC concentrations, the polymers redissolve. This same trend is observed for AMSA/Py. Iliopoulos proposed a micellar bridging mechanism whereby mixed micelles of surfactant and hydrophobic groups from different polymer chains form transient crosslinks. These aggregates are held together by a combination of ionic attractive forces and hydrophobic associations. This mechanism is illustrated in Figure 4.11. Viscosity then increases as a result of interpolymer aggregation, and phase separation may occur. As further surfactant is added, the hydrophobe/surfactant ratio decreases, and the mixed micelles may contain only a few alkyl side chains due to the disruption of interpolymer crosslinks by surfactant (Figure 4.11). This is reflected in the low I_E/I_M values exhibited by AMSA/Py at the high CTAC concentrations where polymer redissolution occurs. Chang and McCormick observed a similar micellar bridging mechanism in solutions of cationic, hydrophobically modified poly (acrylamide)s and the anionic surfactant sodium dodecyl sulfate (SDS).[30]

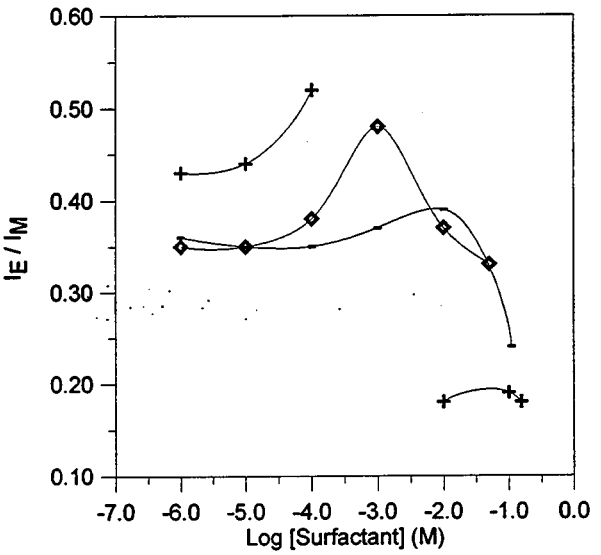

Figure 4.10. I_E/I_M of 0.12 g/dL AMSA/Py as a function of CTAC (+), SDS (-), and Brij 35 (◆) concentration in deionized water. pH: 7.

In mixed solutions of AMSA/Py and an anionic surfactant (SDS) or nonionic surfactant (Brij 35 ($C_{12}H_{25}(OCH_2CH_2)_{23}OH$)), I_E/I_M displays a maximum (Figure 4.10). Micellar bridging through hydrophobic associations has been proposed for solutions of hydrophobically modified poly (sodium acrylate)s with nonionic[31] or anionic[32] surfactants. AMSA/Py bridging and aggregate breakup with SDS and Brij 35 would affect the photophysical response. As interpolymer associations are created and then broken up by excess surfactant, I_E/I_M would increase, then decrease. Similar results have been reported in studies of the interactions of surfactants and phospholipids with pyrene-labeled poly (acrylic acid)s[33] and poly (N-isopropylacrylamide)s.[34,35]

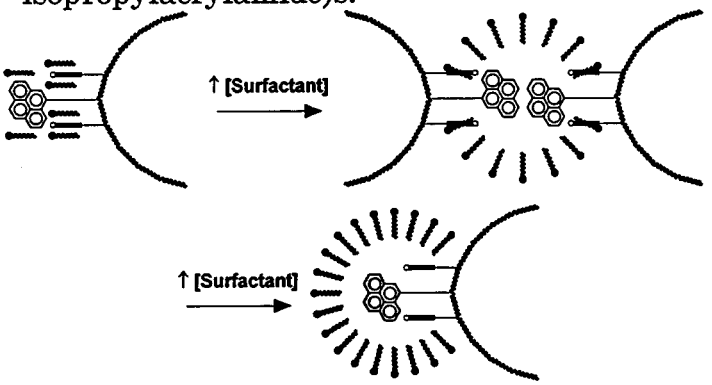

Figure 4.11. Proposed mechanism of polymer-surfactant crosslinking and subsequent aggregate disruption

Conclusions

A high molecular weight terpolymer of acrylamide (AM), 5 mole % sodium 11-acrylamidoundecanoate (SA) and 0.6 mole % 2-(1-pyrenylsulfonamido)ethyl acrylamide (Py) synthesized by micellar polymerization has been found to exhibit associations dependent upon ionic strength and pH. In deionized water, intermolecular hydrophobic associations through pyrene groups cause a significant viscosity increase. Pyrene-pyrene association is also observed as an enhancement in the degree of excimer emission. The acrylamidoundecanoate group imparts considerable salt and pH-responsiveness. As electrolyte concentration increases or pH decreases, the shielding or elimination of electrostatic repulsions between carboxylate groups shrinks the polymer chain. As the coil dimensions shrink, pyrene groups on the same polymer chain approach one another, and excimer emission increases relative to monomer emission. The variability in the photophysical response indicates a salt and pH-"triggered" mechanism. Interpolymer associations are predominant at low ionic strength and neutral pH. Fluorescence quenching studies reveal that salt-driven coil shrinkage may impart a more restricted, less fluid micellar environment. Maxima in I_E/I_M values are observed when nonionic or anionic surfactant is added to aqueous AMSA/Py solutions. The addition of cationic surfactant increases I_E/I_M prior to phase

separation. This observation alludes to the presence of a polymer-micelle bridging mechanism proposed by our research group and others.

References and Notes

1. McCormick, C.L.; Nonaka, T.; Johnson, C.B. *Polymer* **1988**, *29*, 731.
2. Ezzell, S.A.; McCormick, C.L. *Macromolecules* **1992**, *25*, 1881.
3. Ezzell, S.A.; Hoyle, C.E.; Creed, D.; McCormick, C.L. *Macromolecules* **1992**, *25*, 1887.
4. McCormick, C.L.; Middleton, J.C.; Cummins, D.F. *Macromolecules* **1992**, *25*, 1201.
5. Yeoh, K.W.; Chew, C.H.; Gan, L.M.; Koh, L.L.; Teo, H.H. *J. Macromol. Sci.-Chem.* **1989**, *A26*, 663.
6. Yeoh, K.W.; Chew, C.H.; Gan, L.M.; Koh, L.L.; Ng, S.C. *J. Macromol. Sci.-Chem.* **1990**, *A27*, 711.
7. Kramer, M.C.; Welch, C.G.; McCormick, C.L. *Polym. Prepr. (Am. Chem. Soc. Div. Polym. Chem.)* **1993**, *34 (1)*, 999.
8. Laschewsky, A.; Zerbe, I. *Polymer* **1991**, *32*, 2070.
9. Laschewsky, A.; Zerbe, I. *Polymer* **1991**, *32*, 2081.
10. Sprague, E.D.; Duecker, D.C.; Larrabee, C.E. *J. Am. Chem. Soc.* **1981**, *103*, 6797.
11. Paleos, C.M.; Malliaris, A. *J. Macromol. Sci.-Rev. Macromol. Chem. Phys.* **1988**, *28*, 403.
12. Chu, D.Y.; Thomas, J.K. *Macromolecules* **1991**, *24*, 2212.
13. McCormick, C.L.; Chang, Y. *Macromolecules* **1994**, *27*, 2151.
14. McCormick, C.L.; Hoyle, C.E.; Clark, M.D. *Macromolecules* **1991**, *24*, 2397.
15. McCormick, C.L.; Hoyle, C.E.; Clark, M.D. *Macromolecules* **1990**, *23*, 3124.
16. Peer, W.J. *Proc. Am. Chem. Soc. Div. Polym. Mat.: Sci. Eng.* **1987**, *57*, 492.
17. Turner, S.R.; Siano, D.B.; Bock, J. U.S. Patent 4520182, 1985
18. Branham, K.D.; Davis, D.L.; Middleton, J.C.; McCormick, C.L. *Polymer* **1994**, *35*, 4429.

19. *Polymer Handbook, Second Edition*; Brandrup, J.; Immergut, E.H. Eds.; Wiley: New York, 1975. II-47.

20. Biggs, S.; Hill, A.; Selb, J.; Candau, F. *J. Phys. Chem.* **1992**, *96*, 1505.

21. Cochin, D.; Candau, F.; Zana, R. *Macromolecules* **1993**, *26*, 5755.

22. Cochin, D.; Zana, R.; Candau, F. *Macromolecules* **1993**, *26*, 5765.

23. Kramer, M.C.; Steger, J.R.; McCormick, C.L. *Proc. Am. Chem. Soc. Div. Polym. Mat.: Sci. Eng.* **1994**, *71*, 413.

24. Lacowicz, J.R. *Principles of Fluorescence Spectroscopy*; Plenum: New York, 1983. Chapter 9.

25. Morishima, Y; Ohgi, H.; Kamachi, M. *Macromolecules* **1993**, *26*, 4293.

26. Manning, G.S. *Acc. Chem. Res.* **1979**, *12*, 443.

27. Goddard, E.D. *Coll. Surf.* **1986**, *14*, 301.

28. Goddard, E.D.; Pethica, B.A. *J. Chem. Soc.* **1951**, 2659.

29. Magny, B.; Iliopoulos, I.; Zana, R.; Audebert, R. *Langmuir* **1994**, *10*, 3180.

30. Chang, Y.; Lochead, R.Y.; McCormick, C.L. *Macromolecules* **1994**, *27*, 2145.

31. Iliopoulos, I.; Olsson, U. *J. Phys. Chem.* **1994**, *98*, 1500.

32. Iliopoulos, I.; Wang, T.K.; Audebert, R. *Langmuir* **1991**, *7*, 617.

33. Arora, K.S.; Hwang, K.-C.; Turro, N.J. *Macromolecules* **1986**, *19*, 2806.

34. Winnik, F.M.; Ringsdorf, H.; Venzmer, J. *Langmuir* **1991**, *7*, 912.

35. Ringsdorf, H.; Venzmer, J.; Winnik, F.M. *Angew. Chem. Int. Ed. Eng.* **1991**, *30*, 315.

Chapter 5: Stimuli-Responsive Associations Probed by Nonradiative Energy Transfer Studies of Naphthalene and Pyrene-Labeled Poly (Acrylamide-*co*-Sodium 11-(Acrylamido)Undecanoate

Synopsis

The synthesis and photophysical characterization of terpolymers of acrylamide (AM) with the surface-active monomer sodium 11-(acrylamido)undecanoate (SA) and either [(1-naphthyl)methyl]acrylamide or 2-[(1-pyrenylsulfonamido) ethyl] acrylamide are reported. The pronounced spectral overlap between the excited state of the naphthylmethyl group and the ground state of the pyrenylsulfonamido group allows analysis by nonradiative energy transfer (NRET) studies. Pyrene-labeled AM/SA copolymers exhibit strong associative behavior in aqueous solution, as evidenced by the viscosity profile as a function of polymer concentration. The concurrent increase in excimer emission with polymer concentration is reflective of interpolymer association between pyrene groups to form the dimeric excited state. NRET analysis of mixed solutions of naphthalene (NRET donor)- and pyrene (NRET acceptor)-labeled copolymers indicate sensitization of pyrene emission by naphthalene labels. The enhancement in acceptor emission at low polymer concentrations implies that intermolecular associations occur at polymer concentrations where association-driven viscosification is not observed. Open, intermolecular associations and interpolymer NRET are controllable by pH and electrolyte concentration. As ionic strength increases or pH decreases, open associations are broken up. This response had previously been reported as a macroscopic phenomenon by viscosity changes at higher polymer concentrations, but NRET studies confirm that the pH- and salt-responsiveness inherent to AMSA-based materials is also a molecular-level event.

Introduction

Our research group continues to investigate the photophysical properties of fluorescently labeled, hydrophobically modified, water-soluble polymers.[1,2,3,4] Amphiphilic polymers functionalized with hydrophobic groups are of considerable technological interest since micelle-like microdomains can be formed that dissolve small molecule hydrophobes in aqueous media.[5,6,7,8] These materials are also known to exhibit strong interactions with a variety of surfactants[9,10,11,12,13,14] and phospholipids[15,16]

More recently, studies have focused on fluorescently labeled water-soluble polymers in order to correlate the microscopic, photophysical response with a macroscopic event such as phase separation,[17] aggregation,[18,19] or latex film formation.[20] Nonradiative energy transfer (NRET) is a useful technique for probing associations and structural changes in polymer solutions. The photophysical phenomenon of NRET between a donor and an acceptor covalently attached to a

polymer has been termed "photon harvesting" by Webber[21] and the "antenna effect" by Guillet.[22]

In this study, naphthalene and pyrene labels are incorporated into acrylamide/sodium 11-(acrylamido)undecanoate (AMSA) copolymers.[23,24] Comparison of results from dilute solution NRET studies with data from viscosity and other fluorescence emission studies[25,26] provides a more detailed description of the nature of the associations exhibited by these materials in aqueous media. Photophysical analysis of these fluorescently labeled polyelectrolytes has shown that pH- and salt-dependent intermolecular (open) and intramolecular (closed) associations are both macroscopic and microscopic in nature. NRET between naphthalene and pyrene labels on separate AMSA polymer chains in dilute solution confirms significant variations in the degree of polymer-polymer aggregation as a function of polymer concentration, ionic strength, and pH. Environmental responsiveness measurable by macroscopic techniques is driven by angstrom-level interactions even in the dilute state.

The naphthalene/pyrene energy transfer pair has been employed by Winnik to investigate the effects of thermoreversible phase transitions on NRET in aqueous solutions of naphthalene- and pyrene-labeled poly (N-isopropylacrylamide).[17,18,27] NRET between terpolymers of acrylamide (AM), sodium 11-(acrylamido)undecanoate (SA), and a fluorescent comonomer is investigated as a function of polymer concentration and donor/acceptor ratio. The fluorescent monomer [(1-naphthyl)methyl]acrylamide (1) (Figure 5.1) is employed as energy transfer donor, and [2-(1-pyrenylsulfonamido) ethyl] acrylamide (3) (Figure 5.1) acts as energy transfer acceptor.

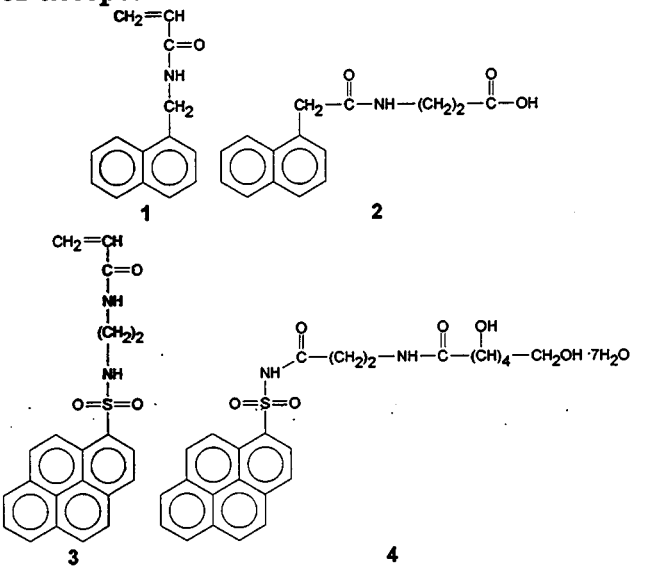

Figure 5.1. Nonradiative energy transfer donors: 1-naphthylmethyl acrylamide monomer (1) and 3-(1-naphthylmethyl-aminoacetyl) propionic acid model compound (2); nonradiative energy transfer acceptors: 2-(1-pyrenylsulfonamido) ethyl acrylamide monomer (3) and 2-(1-pyrenylsulfonamido) ethyl gluconamide heptahydrate model compound (4).

Experimental Section

Materials. All reagents and solvents were purchased from Aldrich Chemical Co. (Milwaukee, WI). Acrylamide was recrystallized twice from acetone. Other materials were used as received. Water for synthesis and solution preparation was deionized and possessed a conductance < 10^{-7} mho/cm.

Sodium 11-(acrylamido)undecanoate. The methods of Gan[23] were employed in the synthesis of SA monomer. Purity was confirmed via NMR and melting point determination.

[(1-Naphthyl)methyl]acrylamide (1). The structures of all fluorescent monomers and model compounds used in this study are shown in Figure 5.1. The procedure employed by Morishima[28] was followed. Acryloyl chloride was used instead of methacryloyl chloride for the acylation of [(1-naphthyl)methyl]amine. A yield of 70 % was obtained. Purity (> 99 %) was confirmed by HPLC and ^{1}H NMR.

Succinic acid N-[(1-naphthyl)methyl]monoamide (2). Into a 25 mL round-bottomed flask fitted with a magnetic stirring bar, N_2 inlet and bubbler, succinic anhydride (1.0 g, 10 mmol) dissolved in 10 mL DMF was added. A solution of [(1-naphthyl)methyl]amine (1.3 g, 8.3 mmol) in 3 mL of DMF was added after the succinic anhydride had dissolved. The reaction mixture was allowed to stir for 1 hr at room temperature. The off-white slurry was then precipitated in water, and the solids were recovered by vacuum filtration. The solid product was then recrystallized from boiling water after treatment with activated charcoal. HPLC indicated 99+% purity: m.p. 172-174 °C; ^{13}C NMR (DMSO-d_6) δ 29.2, 30.0, 40.2, 123.4, 125.3, 125.7, 126.1, 127.4, 128.4, 130.8, 133.2, 134.6, 171.0, 173.9.

2-[(1-Pyrenylsulfonamido)ethyl] acrylamide (3). The procedure employed by Ezzell and McCormick[1] was followed to give **3** in good yield and purity.

N-[2-(1-Pyrenylsulfonamido)ethyl]gluconamide heptahydrate (4). Model compound **3** was synthesized according to literature.[1]

Naphthalene- (5) and pyrene-labeled (6) poly(acrylamide-*co*-sodium 11-(acrylamido)undecanoate). A solution of sodium 11-(acrylamido)undecanoate (1.8 g, 6.5 mmol) and acrylamide (9.0 g, 127 mmol) in 340 mL H_2O was added to the reaction flask immersed in a 50 °C water bath. After 2-[(1-pyrenylsulfonamido)ethyl] acrylamide (0.51 g, 1.3 mmol) or [(1-naphthyl)methyl]acrylamide (0.27 g, 1.3 mmol) finely ground with a mortar and pestle was added to the flask, the solution was degassed with nitrogen. After one hour, sodium dodecyl sulfate (21.7 g, 75.2 mmol) was added. At this point direct bubbling of nitrogen through the solution was stopped to prevent excessive foaming. After stirring the solution under nitrogen for 3 hours, most of the fluorescent

comonomer had dissolved into SDS micelles. A degassed solution of potassium persulfate (50 mg, 0.19 mmol) in 5 mL H_2O was then injected into the monomer/surfactant solution. After stirring under nitrogen for three hours, the viscous polymer solution was added to 1400 mL acetone to yield an off-white rubbery precipitate. The polymer was washed with refluxing methanol for 16 hours in a Soxhlet extractor to remove residual monomer and surfactant. Yields of > 70 % are obtained in both syntheses.

Instrumentation. A Bruker AC-200 NMR spectrometer was used to obtain ^1H and ^{13}C NMR spectra. Molecular weights were determined with a Chromatix KMX-6 low angle laser light scattering photometer equipped with a 633 nm He/Ne laser. Refractive index increments (d*n*/d*c*) were measured with a Chromatix KMX-16 laser differential refractometer. UV-VIS spectra were recorded with a Hewlett Packard 8452A diode array spectrophotometer. HPLC was carried out on a Hewlett Packard 1050 Series chromatograph equipped with a photodiode array UV detector, an Alltech Versapak C_{18} reversed-phase column, and methanol as the mobile phase. Steady-state fluorescence spectra were measured on a Spex Fluorolog-2 fluorescence spectrometer and a DM3000F data system. Excitation and emission slit widths of 1 mm and right angle geometry were employed.

Sample Preparation. Polymer solutions were prepared by mixing stock solutions of naphthalene- and pyrene-labeled polymer in deionized water. For the salt studies, aqueous 5 M NaCl solution and deionized water were added to give the desired polymer and electrolyte concentrations. Solution pH was adjusted by dilution with its respective citric acid/disodium phosphate (Na_2HPO_4) buffer.[29]

For the three-dimensional surface plots, mixed solutions of naphthalene- and pyrene-labeled polymer were diluted with deionized water, NaCl solution, and buffer to give total polymer concentrations of 0.016 - 0.08 g/dL in 0.016 g/dL increments. A solution at each concentration was prepared with NaCl concentrations of 0 - 0.5 M in 0.1 M increments or pH 4 - 8 in increments of 1 pH unit.

Results and Discussion

Polymer Syntheses. The copolymerization of acrylamide (AM) with sodium 11-(acrylamido)undecanoate (SA) proceeds rapidly under micellar conditions. When a growing radical encounters a micelle that contains vinyl monomers, the localized monomer concentration is very high. High local monomer concentration and orientation lead to rapid propagation. Recruitment of additional monomer to polymerizing hemimicelles has also been proposed.[30,31] Thus, a rapid overall polymerization rate that yields high molecular weight polymer results. The molecular weights of terpolymers **5** and **6** (Figure 5.2) are reported in Table 5.1 Molecular weights are somewhat higher than that reported for SA homopolymer

and AM/SA copolymer;[23,24] this may result from the high purity of the monomers employed.

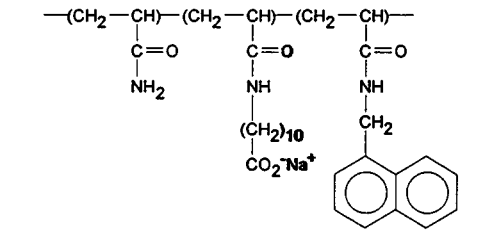

AMSA-Na (5)

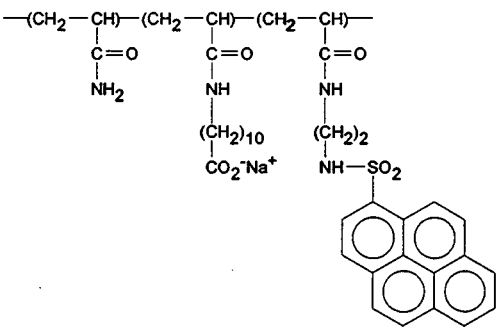

AMSA-Py (6)

Figure 5.2 Naphthalene-labeled polymer **5** and pyrene-labeled polymer **6**.

Table 5.1. Terpolymer Molecular Weight and Composition

Polymer	M_w (g/mol)	AM Content (Mol. %)[a]	SA Content (Mol. %)[a]	Label Content (Mol. %)[b]
5 (AMSA/Na)	2.7×10^6	≈ 94	5	0.6
6 (AMSA/Py)	1.8×10^6	≈ 94	5	0.6

[a] SA mole fraction in monomer feed.

[b] Determined from UV-Vis studies.

The label incorporation for both terpolymers is also shown in Table 5.1. Molar SA incorporation is assumed to equal SA mole fraction in monomer feed for this study. Gan has shown stoichiometric incorporation of SA repeat units into AM/SA copolymers,[24] and NMR analysis of a copolymer containing 10 mole % SA has supported this assumption.[26] When 5 mole % SA content was inferred, UV analysis indicated 0.6 mole % labeling of both naphthalene and pyrene onto their respective copolymers. This is calculated from the molar absorptivity, ε of model compounds **2** (6800 $M^{-1}cm^{-1}$ at 282 nm) and **4** (24,000 $M^{-1}cm^{-1}$at 350 nm). Both polymerizations utilized 1 mole % fluorescent monomer in the monomer feed, but only 60 % of the monomer is incorporated. This is not an unusual result. Ezzell and McCormick also reported low pyrene comonomer **3** content in acrylamide/**3**

copolymers synthesized by homogeneous and microheterogeneous techniques.[1] Pyrene and naphthalene labels may not be sufficiently soluble in SDS micelles, and incomplete dissolution in aqueous SDS would result.

Viscosity and Excimer Emission Studies. Our research group has utilized excimer emission studies of polyaromatic chromophores to probe the solution behavior of other amphiphilic polymers.[1-4] Naphthalene or pyrene groups bound to polymer interact in aqueous media to form a sandwich-like dimeric conformation (excimer). Hydrophobic association can drive these interactions; thus, changes in excimer relative to "monomer" emission parallel changes in macroscopic solution properties such as viscosity. A fluorescence emission spectrum of pyrene-labeled polymer **6** is shown in Figure 5.3. The peaks at 380, 400, and 420 nm correspond to the fluorescence emission of isolated pyrenes (monomer emission). The broad, structureless band centered at 520 nm results from excimer emission. Although we have previously noted naphthalene excimer emission in naphthyl-labeled acrylic acid and methacrylic acid copolymers,[3,4] naphthalene excimer does not form to any significant degree in these polymers. Other water-soluble polymers labeled with the naphthylmethyl moiety have also failed to form excimer in measurable amounts.[32] The proximity of the label to the polymer backbone may hinder the motion necessary for excimer formation.

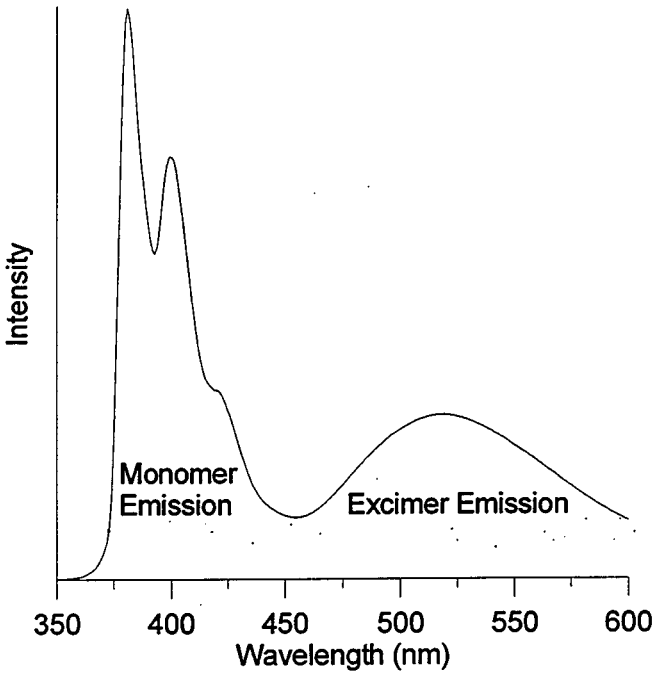

Figure 5.3 Fluorescence emission spectrum of pyrene-labeled polymer **6**. Polymer concentration: 0.052 g/dl in H_2O. Chromophore concentration: 3.3×10^{-5} M. Excitation wavelength: 340 nm. pH: 7.

If the intensity of pyrene excimer emission relative to that of the monomer emission (I_E/I_M; I_E = intensity at 519 nm, I_M = intensity at 400 nm) is measured as

a function of polymer concentration, an intermolecularly associating system may exhibit an increase in I_E/I_M. Both pyrene-labeled polyacrylamide and AMSA-Py obey this trend.[2,25,26] I_E/I_M and apparent viscosity of AMSA-Py are plotted as a function of polymer concentration in Figure 5.4. The apparent viscosity response displays an upwards curvature with an onset at about 0.3 - 0.4 g/dL; acrylamide homopolymer does not exhibit this response below 0.6 g/dL. I_E/I_M steadily increases as well, and interpolymer association appears to predominate in deionized H_2O.

Intramolecular associations are also reflected by changes in I_E/I_M. As NaCl is added to solutions of SA copolymers or pH is lowered, the shielding or elimination of electrostatic repulsions between carboxylate groups of the SA unit leads to coil shrinkage; viscosity decreases and I_E/I_M increases in these systems.[25,26,33] As coil dimensions shrink, intrapolymer associations between chromophores that drive excimer formation are augmented.

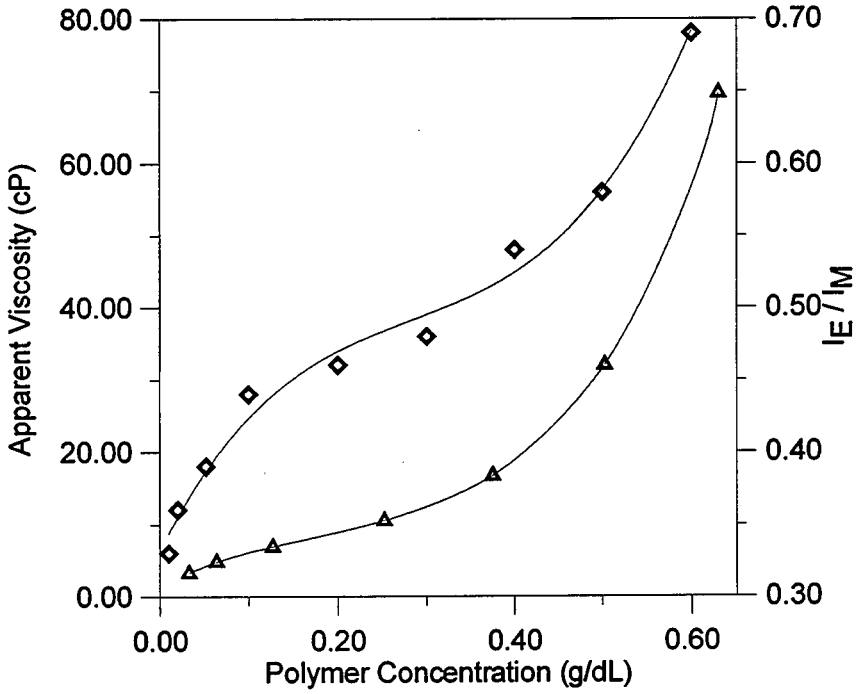

Figure 5.4 Apparent viscosity (▲) and excimer emission / monomer emission (I_E/I_M) (◆) as a function of polymer **6** concentration in H_2O. (I_E/I_M = intensity at 519 nm / intensity at 400 nm). pH: 7.

Nonradiative Energy Transfer Studies. According to Förster,[34] the probability of a nonradiative transfer of excitation energy from one chromophore to another (NRET) has a sixth power dependence expressed as Equation 1,

$$E = \frac{R_0^6}{R_0^6 + R^6} \qquad (1)$$

where E is the energy transfer efficiency, R_0 is the energy transfer donor/acceptor separation distance for which $E = 0.5$, and R is the donor/acceptor separation distance. The sixth power dependence arises from dipole-dipole interactions between chromophores participating in NRET. A simplified NRET mechanism is described in Equation 2.

$$D^* + A \rightarrow D + A^* \tag{2}$$

where D is the NRET donor, A is the NRET acceptor, and an asterisk denotes the excited state. For NRET to occur to any significant degree, the excited state energy of a NRET donor must approximate that of the ground state energy of the NRET acceptor; this is illustrated experimentally as the spectral overlap of donor fluorescence emission and acceptor UV-Vis absorbance, as shown in Figure 5.5.

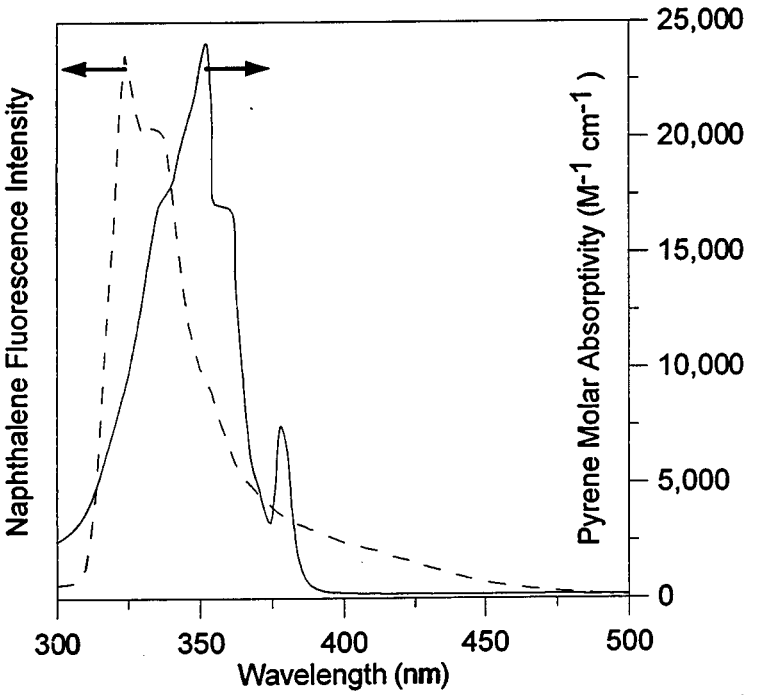

Figure 5.5 Spectral overlap of naphthalene model 2 fluorescence (-----) with pyrene model 4 UV absorbance (——). Excitation wavelength: 290 nm. [Naphthalene model 2] = 7×10^{-6} M. pH: 7.

Overlap occurs between 300 and 400 nm, and is readily quantitated as J, the overlap integral.

$$J = \int_0^\infty \lambda^4 \, I(\lambda) \, \varepsilon(\lambda) \, d\lambda \tag{3}$$

where λ is the wavelength, I is the fluorescence intensity of NRET donor and ε is the molar absorptivity of NRET acceptor. I is normalized such that

$$\int_0^\infty I(\lambda)\, d\lambda = 1 \tag{4}$$

If J is known, R_0 is readily calculated from Equation 5.

$$R_0^6 = \frac{9000\,(\ln 10)\,\kappa^2\,\Phi_D\,J}{128\,\pi\,n^4\,N} \tag{5}$$

where κ^2 is a function of the mutual orientation of donor and acceptor and is usually assumed to equal 2/3 for random orientation in fluid media, Φ_D is the emission quantum yield of the donor in the absence of NRET acceptor, n is the solvent refractive index, and N is Avogadro's number.

For the naphthylmethyl/pyrenylsulfonamido donor/acceptor pair, $J = 1.90 \times 10^{-14}$ cm^6 mol^{-1}, $\Phi_D = 0.11$, and $R_0 = 26.6$ Å.[32] These values are in agreement with other naphthalene/pyrene combinations.[17,18]

Webber has quantitated NRET as follows:[21]

$$\chi_{SS} = \frac{\left(\frac{I_A(\lambda)}{I_A(\lambda_A)}\right) f_A(\lambda_A) - f_A(\lambda)}{f_D(\lambda)} \tag{6}$$

where χ_{SS} is the steady state-derived NRET quantum efficiency. I_A is the fluorescence intensity of the acceptor; λ is the wavelength at which both donor and acceptor absorb light, and λ_A is the wavelength at which only acceptor absorbs light. f_A and f_D are the fractions of light that are absorbed by donor and acceptor, respectively, at wavelengths λ and λ_A. Because $f_A(\lambda_A) = 1$, and $f_A(\lambda) = 1 - f_D(\lambda)$, Equation 6 reduces to

$$\chi_{SS} = \frac{I_A(\lambda)}{I_A(\lambda_A)} \tag{7}$$

In this study, I_A represents the integrated fluorescence intensity from 360 to 600 nm, λ is 290 nm, and λ_A is 340 nm. Webber's expression does not hold if the optical density of the acceptor is much lower than that of the donor. The maximum naphthalene/pyrene ratio employed in our study is 5.25 to 1, and this equates to an optical density ratio of about 5. Overall optical density is still low, so any error introduced would be minimal.

If a constant naphthalene/pyrene ratio is employed, as in the salt and pH studies, changes in NRET are proportional to the ratio of pyrene emission to naphthalene emission.

$$\Delta NRET \propto \Delta \frac{I_{Py}}{I_{Na}} \tag{8}$$

where I_{Py} represents pyrene emission intensity and I_{Na} represents naphthalene emission intensity. In this study, fluorescence emission intensities at 340 and 400 nm were assigned to naphthalene and pyrene fluorescence, respectively. Morishima followed interpolymer NRET of fluorescently labeled amphiphilic polyelectrolytes by measuring the ratio of the fluorescence intensity of pyrenylmethyl emission relative to that of naphthylmethyl emission. I_{Py}/I_{Na} was then referenced to an I_{Py}/I_{Na} value where no measurable associations take place.[35]

Nonradiative Energy Transfer in Deionized Water. Qualitatively, NRET occurs as an increase in pyrene fluorescence in the presence of the naphthalene label, as shown in Figure 5.6. The spectrum represented by the dashed line depicts the fluorescence emission of a 0.01 g/dL solution of AMSA-Py, and the solid line spectrum is that of a 7/1 (w/w) mixed solution of AMSA-Na/AMSA-Py. Pyrene label concentration is the same in both solutions, yet the intensity of the characteristic pyrene emission bands increases considerably in the mixed solution. This result indicates a sensitization of pyrene emission by naphthalene labels in solution. This photophysical response may be attributable to interpolymer NRET between naphthalene and pyrene.

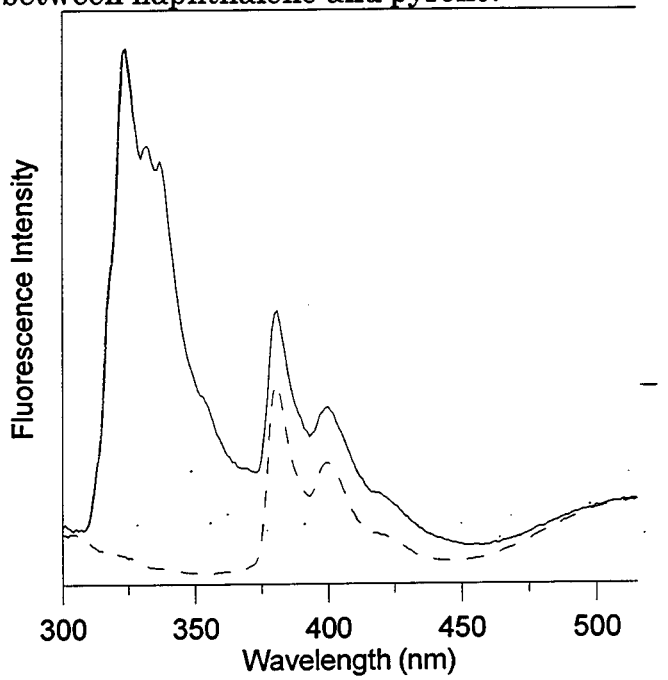

Figure 5.6 Fluorescence intensity of 0.01 g/dL pyrene-labeled polymer **6** (-----) and mixed solution of 0.01 g/dL pyrene-labeled polymer **6** with 0.07 g/dL added naphthalene-labeled polymer **5** (—). Excitation wavelength: 290 nm. pH: 7.

In 5. 7, NRET quantum efficiency is plotted vs. increasing polymer concentration and naphthalene/pyrene ratio ([Na]/[Py]). As polymer concentration

increases, so does [Na]/[Py]. This is accomplished by preparing samples of mixed polymer solutions of AMSA-Na and AMSA-Py. AMSA-Py concentration remains constant at 0.01 g/dL, and AMSA-Na concentration varies from 0.01 to 0.07 g/dL. In this manner, the total polymer concentration increases from 0.02 to 0.08 g/dL. It is quite apparent that an increase in polymer concentration (and in [Na]/[Py]) increases NRET. This results from a decrease in the average naphthalene/pyrene separation distance. The photophysical response may be explained by interpolymer aggregation via hydrophobic association between naphthalene and pyrene labels. This result is similar to that reported by Ringsdorf and Winnik in a study of naphthalene- and pyrene-labeled, hydrophobically-modified poly (N-isopropyl acrylamide) (PNIPAM).[18] As the naphthalene/pyrene ratio is increased with polymer concentration, pyrene emission increases and I_E/I_M decreases. This has been attributed to pre-C* interpolymer aggregation of naphthalene and pyrene-labeled polymer. Hydrophobic association of naphthalene-labeled polymer with pyrene-labeled polymer would result in the breakup of intermolecularly aggregated pyrene-labeled PNIPAM. Labeling in our systems may be sufficiently low such that association between hydrophobic groups on the same chain becomes less favorable than interpolymer chromophore aggregation. The local concentration of surfactant groups along the polymer chain is also probably not sufficiently high for extensive intramolecular, or closed association in deionized water. The polymer would then behave as an extended polyelectrolyte rather than as a compact, globular "polysoap" with water as a poor solvent,[36] and interpolymer association through naphthalene and pyrene labels becomes feasible.

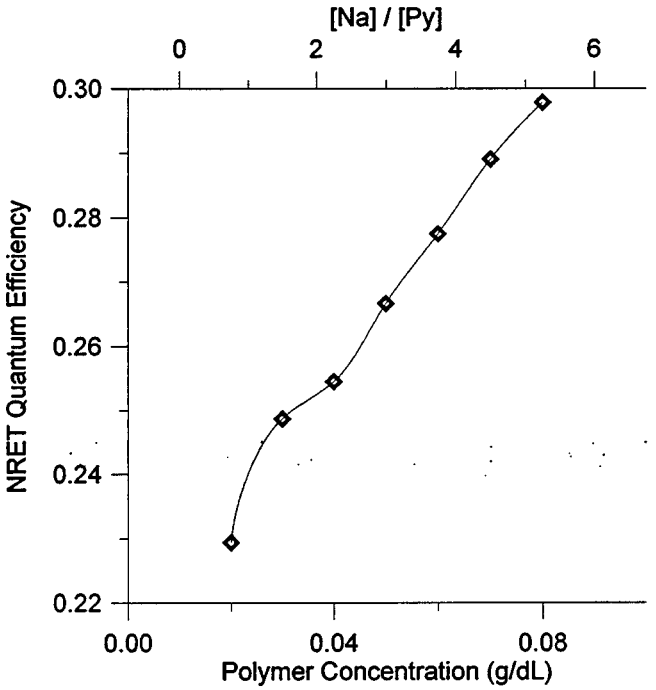

Figure 5.7 Nonradiative energy transfer quantum efficiency (calculated as Equation 7) of mixed AMSA-Na/AMSA-Py solutions as a function of polymer concentration and naphthalene/pyrene ratio. Excitation wavelength: 290 nm. pH: 7.

Electrolyte and pH Effects on Nonradiative Energy Transfer. It has been shown that the shielding or elimination of electrostatic repulsive forces in AMSA copolymers induces a pronounced coil contraction. In the labeled systems that we have investigated, this is observed as an increase in I_E/I_M.[25,26] The decrease in viscosity accompanied by an increase in intramolecular associations alludes to a mechanism whereby intramolecular interactions occur at the expense of intermolecular events. This proposed open-closed association transition is supported by data from fluorescence quenching studies of aqueous AMSA-Py solutions. Salt-induced reductions in quencher-label migration imply that mixed micelles formed by pyrene and SA repeat units become more organized as ionic strength increases.

As NaCl concentration increases, viscosity decreases, and excimer yield is enhanced in aqueous AMSA-Py solutions. If changes in the degree of interpolymer association are occurring on the molecular level, NRET should change as a function of electrolyte concentration. A three-dimensional polymer concentration - [NaCl] - I_{Py}/I_{Na} plot at a constant Na/Py ratio of 2.25 is shown in Figure 5.8. NRET increases slightly with polymer concentration for a given NaCl concentration. The weak response may be attributable to the low Na/Py ratio employed. The quantum yield of the naphthylmethyl group is low (0.11) even in the absence of pyrenylsulfonamido chromophores, and any detectable sensitization of pyrene emission by naphthalene would result from interaction between chromophores on different polymer chains. For a given polymer concentration, NRET drops considerably with increasing [NaCl]. The observed changes in NRET efficiency indicate that polymer chains aggregate in a concentration regime that is not detectable by macroscopic methods such as viscometry, and that these associations are broken up by salt-triggered coil shrinkage.

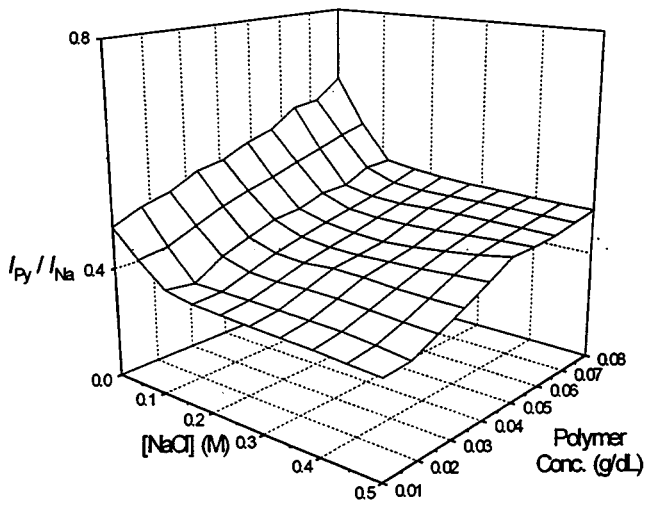

Figure 5.8. Pyrene emission/naphthalene emission ratio (I_{Py} = pyrene emission at 400 nm, I_{Na} = naphthalene emission at 340 nm) of 3/1 (w/w) AMSA-Na/AMSA-Py as

a function of polymer concentration and NaCl concentration. Excitation wavelength: 290 nm. pH: 7.

The effect of conformation-driven breakup of interpolymer association is even more pronounced with changes in pH. Previous studies of pyrene-labeled AMSA copolymer have shown that I_E/I_M increases dramatically as pH is lowered.[25,26] Viscosity also decreases through this pH range. The photophysical response suggests a compactness that brings pyrenes within a polymer chain in closer proximity to one another. However, the excimer yield studies do not specifically address the effects of acid on intermolecular aggregation.

A three-dimensional polymer concentration - pH - I_{Py}/I_{Na} plot is shown in Figure 5.9. NRET does not significantly increase for a given pH, but an appreciable transition in NRET efficiency occurs from pH 4 to 8 for a given polymer concentration. The change reflects a transition from intra- to interpolymer association as the polymer conformation changes from that of a compact structure stabilized by intramolecular micellization to a more open, random coil conformation.

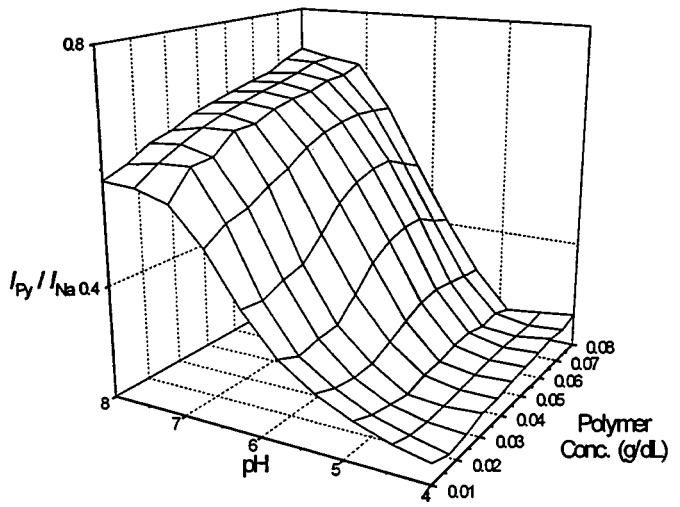

Figure 5.9. Pyrene emission/naphthalene emission ratio (I_{Py} = pyrene emission at 400 nm, I_{Na} = naphthalene emission at 340 nm) of 3/1 (w/w) AMSA-Na/AMSA-Py as a function of polymer concentration and pH. Excitation wavelength: 290 nm.

The photophysical response as a function of salt concentration and pH verifies that the degree and nature of intra- and interpolymer associations are controllable by environmental changes. The effects of acidic and saline media are conceptually illustrated in Figure 5.10. When a more open conformation is adopted, interpolymer hydrophobic associations between labels occur, and NRET increases in mixed solutions of singly labeled polymers. As the polymer chain contracts and labels sequester themselves within more organized micellar microdomains, donor-

acceptor interactions diminish. The pronounced pH- and salt-responsiveness has important ramifications with respect to the potential applicability of such materials as associative thickeners, and as vehicles for controlled release and sequestration.

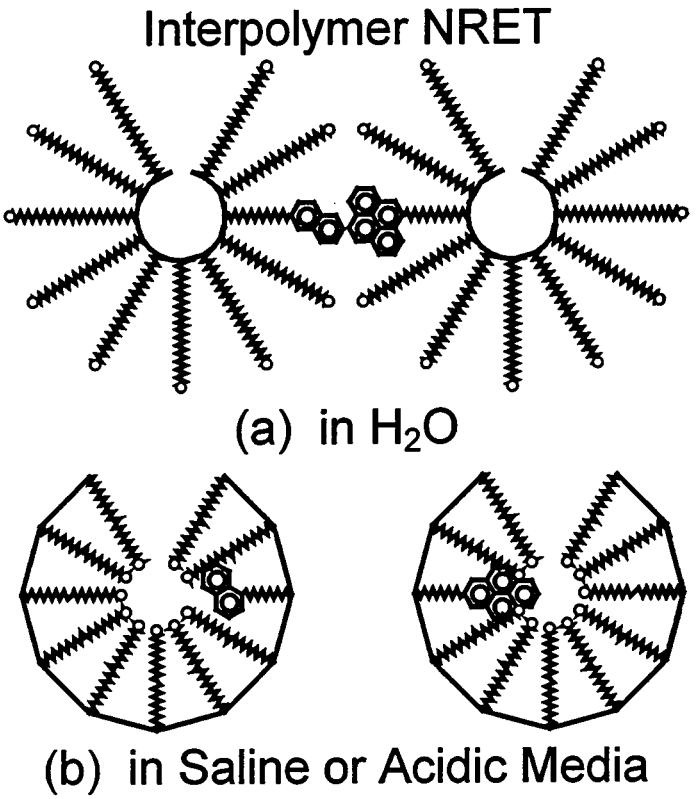

Figure 5.10. Proposed mechanism of inter/intramolecular association and effects on NRET response. (a) Intermolecular association in deionized water. (b) Intramolecular compartmentalization of surfactant groups and chromophores with added electrolyte or at low pH.

Conclusions

This study confirms the profound pH and salt-responsiveness of acrylamide polymers with a low substitution (5 mole %) of the surface-active monomer sodium 11-(acrylamido)undecanoate (SA). Viscosity studies had indicated that aqueous solutions of AM/SA copolymers labeled with pyrene exhibit extensive considerable viscosification relative to unmodified polymer. Concurrent increases in I_E/I_M with polymer concentration support an association mechanism involving chromophore groups on different polymer chains. Excimer yield is enhanced by the addition of electrolyte or acid.

Nonradiative energy transfer (NRET) studies of mixed solutions of naphthalene- and pyrene-labeled AMSA copolymer as a function of polymer concentration, electrolyte concentration, and pH support the mechanism of a salt- and pH-triggered transition from open to closed association. In deionized water and at high pH, interpolymer NRET between naphthalene and pyrene groups is much

higher than at low pH and high electrolyte concentration. The conformational changes that occur on the angstrom level are not observable by macroscopic techniques. However, the salt and pH-induced microdomain structuring reported by photophysical analysis is highly significant in the development of structure/property relationships for applications in aqueous media. NRET studies have effectively shown that changes in the medium which affect the macroscopic solution properties of AMSA copolymers also trigger changes in molecular-level microdomain organization.

References and Notes

1. Ezzell, S.A.; McCormick, C.L. *Macromolecules* **1992**, *25*, 1881.

2. Ezzell, S.A.; Hoyle, C.E.; Creed, D.; McCormick, C.L. *Macromolecules* **1992**, *25*, 1887.

3. McCormick, C.L.; Hoyle, C.E.; Clark, M.D. *Macromolecules* **1990**, *23*, 3124.

4. McCormick, C.L.; Hoyle, C.E.; Clark, M.D. *Macromolecules* **1991**, *24*, 2397.

5. Paleos, C.M.; Malliaris, A. *J. Macromol. Sci.-Rev. Macromol. Chem. Phys.* **1988**, *28*, 403.

6. Hurter, P.N.; Hatton, T.A. *Langmuir* **1992**, *8*, 1291.

7. Ito, K.; Ono, H.; Yamashita, Y. *J. Coll. Sci.* **1964**, *19*, 28.

8. Strauss, U.P.; Gershfeld, N.L. *J. Phys. Chem.* **1954**, *58*, 747.

9. Magny, B.; Iliopoulos, I.; Zana, R.; Audebert, R. *Langmuir* **1994**, *10*, 3180.

10. Iliopoulos, I.; Olsson, U. *J. Phys. Chem.* **1994**, *98*, 1500.

11. Iliopoulos, I.; Wang, T.K.; Audebert, R. *Langmuir* **1991**, *7*, 617.

12. Lundberg, D.J.; Brown, R.G.; Glass, J.E.; Eley, R.R *Langmuir* **1994**, *10*, 3027.

13. Winnik, F.M.; Ringsdorf, H.; Venzmer, J. *Langmuir* **1991**, *7*, 905.

14. Winnik, F.M.; Ringsdorf, H.; Venzmer, J. *Langmuir* **1991**, *7*, 912.

15. Ringsdorf, H.; Venzmer, J.; Winnik, F.M. *Angew. Chem. Int. Ed. Engl.* **1991**, *30*, 315.

16. Arora, K.S.; Hwang, K.; Turro, N.J. *Macromolecules* **1986**, *19*, 2806.

17. Winnik, F.M. *Polymer* **1990**, *31*, 2125.

18. Ringsdorf, H.; Simon, J.; Winnik, F.M. *Macromolecules* **1992**, *25*, 5353.

19. Winnik, F.M. *Macromolecules* **1989**, *22*, 734.

20. Zhao, C.; Wang, Y.; Hruska, Z.; Winnik, M.A. *Macromolecules* **1990**, *23*, 4082.

21. Webber, S.E *Chem. Rev.* **1990**, *90*, 1469.

22. Guillet, J.E.; Rendall, W.A. *Macromolecules* **1986**, *19*, 224.

23. Yeoh, K.W.; Chew, C.H.; Gan, L.M.; Koh, L.L.; Teo, H.H. *J. Macromol. Sci.-Chem.* **1989**, *A26*, 663.

24. Yeoh, K.W.; Chew, C.H.; Gan, L.M.; Koh, L.L.; Ng, S.C. *J. Macromol. Sci.-Chem.* **1990**, *A27*, 711.

25. Kramer, M.C.; Steger, J.R.; McCormick, C.L. *Proc. Am. Chem. Soc. Div. Polym. Mat.: Sci. Eng.* **1994**, *71*, 413.

26. Kramer, M.C.; Welch, C.G.; Steger, J.R.; McCormick, C.L. *Macromolecules*, in press.

27. Ringsdorf, H.; Simon, J.; Winnik, F.M. *Macromolecules* **1992**, *25*, 7306.

28. Morishima, Y.; Tominaga, Y.; Nomura, S.; Kamachi, M. *Macromolecules* **1992**, *25*, 861.

29. *Handbook of Chemistry and Physics, 41st Ed.*; Hodgman, C.D.; Weast, R.C.; Selby, S.M. Eds.; CRC: Cleveland, 1959. p. 1715.

30. Cochin, D.; Candau, F.; Zana, R. *Macromolecules* **1993**, *26*, 5755.

31. Cochin, D.; Zana, R.; Candau, F. *Macrolmolecules* **1993**, *26*, 5765.

32. Hu, Y.; Kramer, M.C.; Boudreaux, C.J.; McCormick, C.L. *Macromolecules*, submitted for publication.

33. Kramer, M.C.; Welch, C.G.; McCormick, C.L. *Polym. Prepr. (Am. Chem. Soc. Div. Polym. Chem.)* **1993**, *34 (1)*, 999.

34. Förster,T. *Discuss. Faraday Soc.* **1959**, *27*, 7.

35. Morishima, Y.; Nomura, S.; Ikeda, T.; Seki, M.; Kamachi, M. *Macromolecules* **1995**, *28*, 2894.

36. Strauss, U.P.; Gershfeld, N.L.; Cook, E.H. *J. Phys. Chem.* **1956**, *60*, 577.

CHAPTER 6: EFFECTS OF PH AND COMPOSITION ON ASSOCIATIVE PROPERTIES OF AMPHIPHILIC ACRYLAMIDE/ACRYLIC ACID TERPOLYMERS

Synopsis

Acrylamide (AM)/acrylic acid (AA) copolymers and AM/AA/N-[(4-hexyl)phenyl]acrylamide (HPAM, 0.5 mole%) terpolymers with varied AA content have been synthesized by micellar copolymerization. Co- and terpolymers with 5 - 37 mole% AA and similar hydrodynamic volumes were prepared. Solution viscosity studies of the copolymers as a function of pH and copolymer concentration in deionized water and NaCl solution indicate classical polyelectrolyte behavior. In aqueous solutions intra- or intermolecular hydrophobic associations may be favored by variation of terpolymer composition. Three dimensional plots of both I_3/I_1 (from pyrene probe fluorescence) and viscosity as functions of pH and terpolymer concentration demonstrate the responsive nature of associations in water and in 0.5M NaCl. Terpolymers containing approximately 9 and 21 mole% AA exhibit intermolecular (open) associations ≤ pH 5 and in the presence of NaCl. The terpolymer containing approximately 37 mole% AA, however, exhibits no intermolecular associations in deionized water even at low pH. Pyrene fluorescence studies of this terpolymer indicate a significantly apolar environment sensed by the probe at pH 4, suggesting that intramolecular (closed) microdomains are formed. Conceptual models based on hydrophobic, ionic, and hydrogen bonding interactions in these systems are presented.

Introduction

Water soluble acrylamide co- and terpolymers are appropriate for a variety of oil field applications.[1] Addition of small quantities (1 ≤ mole%) of hydrophobic groups via micellar copolymerization can lead to AM copolymers with enhanced solution properties[2-8] including viscosification due intermolecular associations above a critical overlap concentration (C^*). Importantly, this C^* is well below the entanglement overlap of the AM homopolymer[4-6] or random copolymers with similar hydrophobe content.[8,9] Fluorescence label studies on co- and terpolymers prepared by micellar polymerization indicate that the unique "blocky" microstructure which arises from the microheterogeneous nature of micellar polymerization is a determining factor for intermolecular associations.[8-10] Intermolecular aggregates formed by these "micro-blocky" copolymers have also been examined using external fluorescence probes and organized microdomains have often been compared to those of common surfactant micelles.[5,7]

Introduction of charged groups to hydrophobically-modified copolymers, either through hydrolysis or by copolymerizatiom with ionic

monomers, can increase solubility and provide systems responsive to changes in ionic strength and pH.[4,5,11-15] These polyelectrolyte systems exhibit decreased associative behavior and microdomain organization compared to their nonionic counterparts, often requiring higher levels of hydrophobe incorporation or addition of high concentrations of electrolyte to induce intermolecular aggregation.[4,5,11-14] Explanation of these properties has been incomplete. Increased polymer solubility and interchain ionic repulsions are speculated to be responsible for decreased intermolecular association.[4,13,14] One study[13] examined associative effects as a function of the level of hydrolysis in AM/ethylphenylacryamide copolymers through viscosity and fluorescence probe measurements. Differences in associative behavior as a function of degree of hydrolysis and NaCl concentration were reported, but the onset of aggregation in these systems was not explored; copolymer concentrations were well above C^*. Also lacking are studies that examine associative properties as a function of pH.

The purpose of this work is to investigate the viscosity and microdomain organization of hydrophobically-modified polyelectrolytes as a function of pH, salt concentration, polymer concentration, and polymer composition for a fixed level of hydrophobe. To facilitate these studies, we have synthesized two polymer series: control copolymers of AM and AA and terpolymers of AM, AA, and N-hexylphenylacrylamide (HPAM). Viscometric properties of the co- and terpolymers are examined as functions of polymer concentration and solution pH in the presence and absence of NaCl. To our knowledge, there have been no literature studies examining AM/AA copolymers utilizing such three dimensional topological plots. These studies provide useful data for interpreting the associative properties of hydrophobically-modified analogs. Topological investigations of viscosity as described above, and pyrene I_3/I_1 measurements are conducted on the terpolymers to examine the onset of intermolecular aggregation. These studies provide insight into the factors governing intermolecular associations and provide useful structure/property relationships for the design of pH or electrolyte responsive associations.

Experimental

Materials. All materials were purchased from either Aldrich or Fisher and used as received unless otherwise noted. 4-decylaniline (DA), acrylic acid (AA), and acryloyl chloride (AC) were distilled under vacuum prior to use. Acrylamide (Am) was recrystallized from acetone and potassium persulfate was recrystallized from water. Pyrene was recrystallized three times from absolute ethanol. *N*-[(4-hexyl)phenyl]acrylamide (HPAM) was synthesized by the same procedure as its butylphenyl[11] and decylphenyl[14] analogs, utilizing DA and AC in the presence of an acid scavenger. Analysis for HPAM - EA calc. for $C_{15}H_{21}NO$ (MW 231.33): %C, 77.88; %H, 9.15; %N, 6.05; %O, 6.92.

Found: %C, 77.78; %H, 9.16; %N, 6.06; %O (not anal.), 7.00. M.P. 95-96 °C. IR (KBr pellet): N-H 3285, vinyl and aromatic C-H 3133 and 3082, aliphatic CH_3 and CH_2 2957 and 2940, carbonyl 1665. ^{13}C NMR (d_6DMSO): aliphatic CH_3, 13.9; aliphatic CH_2, 22.1-34.6; vinyl carbons, 126.3 and 132.0; aromatic carbons, 119.3, 128.3, 136.7, 137.3; carbonyl, 162.9.

Terpolymer Synthesis and Purification. Terpolymers **P5-P8** were synthesized via the micellar polymerization method of Turner et. al.,[2] illustrated in Scheme II. Total monomer concentration was 0.44M. The HPAM content in the feed was held constant at 0.5 mole%, and AM:AA feed ratios were 94.5:5.0, 89.5:10.0, 79.5:20.0, and 69.5:30.0. SDS was used as the surfactant to solubilize the hydrophobic comonomer, and potassium persulfate was used as a free radical initiator. The surfactant to hydrophobe ratio, [SDS]/[HPAM], and the monomer to initiator ratio, [monomer]/[$K_2S_2O_8$], were held constant at 40 and 3000 respectively. Deionized water (240mL) was purged with N_2 for 30 minutes. SDS (6.3g) was added with stirring under N_2 purge. HPAM (0.13g) was then added with continued stirring for approximately one hour or until the solution cleared. The AM:AA ratio was varied as indicated in Table 6.1, and the pH of the reaction feed varied from 3.5 to 4.5 depending on the AA feed ratio. $K_2S_2O_8$ was dissolved into 10mL deoxygenated, deionized water and added to the solution. The reaction was allowed to proceed under N_2 for 6 hours. Polymers were precipitated into 1000-1200mL of acetone. The polymers were washed with fresh acetone and dried overnight. The terpolymers were ground to a fine powder and dissolved in water (approximately 0.25 g/dL) on an orbital shaker for 1-2 weeks. The pH of these solutions was adjusted to approximately 7.5, and samples were returned to the shaker for 1-2 days. The polymer solutions were dialyzed against deionized water in Spectra Por No. 4 dialysis tubing with a molecular weight cutoff of 12 000-14 000 for 8 days. The purified samples were then freeze-dried to a constant weight. Copolymers **P1-P4** were synthesized and purified by an identical procedure using no HPAM monomer.

Table 6.1. Compositional and Hydrodynamic Data for P1-P8.

Sample	AM:AA Feed Ratio[a]	Mole% AM[b]	Mole% AA[b]	Mole% HPAM[c]	%Conv.[d]	d_H (nm)[e]	d_H (nm)[f]
C1	95.0:5.0	91.7	8.3	-	81	45	21
C2	90.0:10.0	88.9	11.1	-	91	70	43
C3	80.0:20.0	75.8	24.2	-	83	71	60
C4	70.0:30.0	64.8	35.2	-	83	70	66
T1	94.5:5.00	94.5	4.9	0.6	58	67	-
T2	89.5:10.0	90.9	8.5	0.6	73	66	-
T3	79.5:20.0	78.4	21.0	0.6	67	67	-
T4	69.5:30.0	62.1	37.4	0.5	57	65	-

[a] Composition in reaction feed
[b] From ^{13}C NMR/elemental analysis
[c] From UV spectroscopy
[d] Estimated gravimetrically
[e] Hydrodynamic diameter from DLS in 1.0% SDS (±12 nm)
[f] Hydrodynamic diameter from DLS in 0.5M NaCl (±10 nm)

Structural Analysis. Co- and terpolymer compositions were determined by UV spectroscopy, elemental analysis, and/or ^{13}C NMR by methods discussed previously[14]. Elemental analyses were performed by M-H-W Laboratories, Phoenix AZ.

UV spectra were obtained with a Hewlett-Packard Model 8452A Photodiode-Array Spectrophotometer. A molar absorptivity of 10,700 M^{-1} cm^{-1} at 250 nm was used to calculate the composition of HPAM residues in the terpolymers.

^{13}C NMR spectra were obtained with a Bruker AC 200 spectrometer. Delay times of 5 - 6 s were used for gated-decoupled experiments. ^{13}C NMR spectra showed the expected chemical shifts for the backbone carbons at approximately 38-48 ppm as well as the two carbonyl resonances for acid (185.8 ppm) and amide (182.7 ppm) carbonyls.

IR spectra were obtained in KBr pellets with a Mattson Model 2020 FT-IR spectrophotometer.

Steady-state pyrene fluorescence studies were performed with an Edinburgh Analytical Instruments FS900CDT Steady-State T-Geometry

Fluorometer. Slit widths were maintained at ≤ 0.5 mm. An excitation wavelength of 338 nm was used. I_1 and I_3 were recorded at 372 and 384 nm, respectively. Steady-State spectra were analyzed using software provided by the manufacturer, and I_3/I_1 measurements were reproducible to ± 0.1 unit in the terpolymer solutions.

Viscosity measurements were conducted on a Contraves LS-30 low shear rheometer at 25 °C and a shear rate of 6 s^{-1}. At least three measurements were taken for each sample. An upper limit of 250 centipoise may be obtained on the Contraves LS-30 at this shear rate. This value was arbitrarily assigned to samples that exceeded this upper limit for means of comparison.

Dynamic light scattering studies were conducted with a Spectra-Physics 127 laser operating at 632.8 nm and a Brookhaven Instruments model BI-200SM automatic goniometer interfaced with a Brookhaven BI-2030AT autocorrelator and personal computer. Data were collected at an angle of 90° and effective hydrodynamic diameters (d_H) were calculated using the algorithm CONTIN and associated software provided by the manufacturer. Multiple analyses (3-5) were performed to insure reproducibility.

Sample Preparation. Samples for viscosity measurements and pyrene probe studies were made by preparing polymer stock solutions of 0.20 g/dL in deionized water and adjusting the pH to 4, 5, 6, and 7 ± 0.05 with μL amounts of concentrated HCl or NaOH solutions. The solutions were allowed to mix on an orbital shaker before dilutions were made. Dilutions of 0.16, 0.12, 0.08, 0.04, and 0.02 g/dL were made and the pH of each dilution adjusted to the desired value. Care was taken to insure a minimum amount of added acid or base was used to adjust the solution pH, since the neutralization process produces excess ions which may effect solution properties in deionized water. For salt studies, dry NaCl was added to each solution. Solutions for pyrene probe measurements were made by adding 1-2 μL of a concentrated stock solution of pyrene in methanol to each dilution. Final pyrene concentrations of approximately 1 x 10^{-6} mole/L were obtained.

Samples for dynamic light scattering measurements were prepared by dissolving the appropriate amount of polymer in the desired pre-filtered solvent (0.5M NaCl or 1.0% SDS) to give solutions of 2.0 x 10^{-4} g/mL polymer. After dissolution, the pH of the solution was adjusted to the proper pH (7.0 ± 0.05 in NaCl and 4.2 ± 0.1 in 1.0% SDS) using μL amounts of NaOH and HCl solutions. Polymer solutions were filtered passed through loops with Millipore 0.45μm filters to remove dust. Typical filtration times were 14-48 hours.

Results and Discussion

Terpolymer Composition. Hydrophobically modified polyelectrolytes, **T1-T4**, were synthesized via micellar polymerization as shown in Scheme I. The polymerization feed was varied as indicated in Table 6.1 to yield terpolymers of varying AA content. AM/AA copolymers of similar composition, **C1-C4**, were synthesized under identical conditions (Table 6.1).

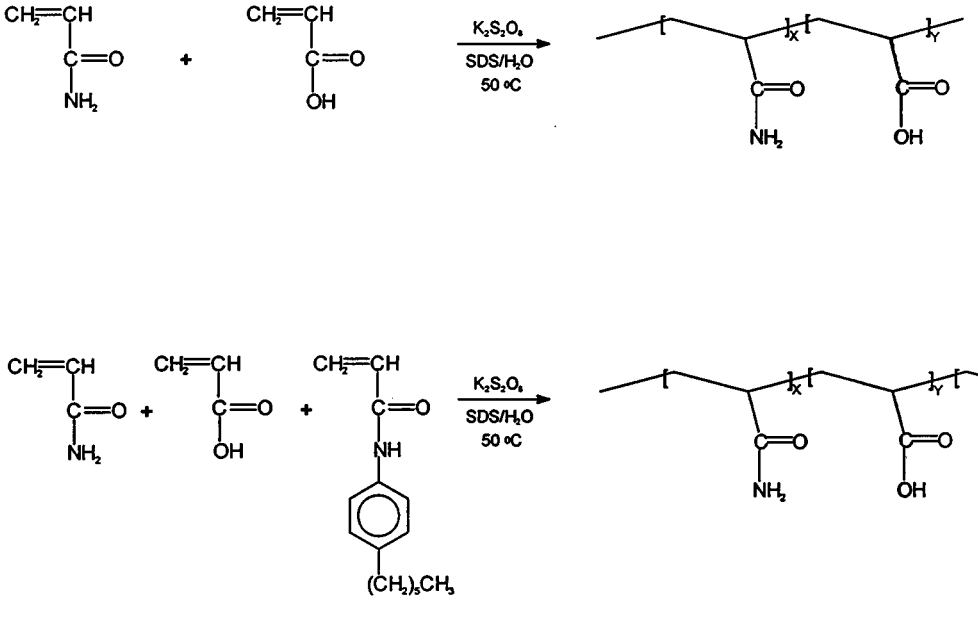

Scheme 6.1. Synthesis of copolymers **C1-C4** and terpolymers **T1-T4** by micellar polymerization at 50 °C.

Co- and terpolymer compositions were determined by UV spectroscopy, elemental analysis , and/or ^{13}C NMR as discussed previously.[14] HPAM incorporation in each terpolymer is consistent with the feed composition of HPAM (0.5-0.6 mole%). Under the conditions outlined in the Experimental Section, a level of approximately 1.6 HPAM monomers per SDS micella was maintained. Over the six hour reaction time, hydrophobe compositional drift[13b] should not be a concern; therefore, we expect similar hydrophobic "microblocks" to those previously reported for T_1 - T_4. AM:AA content in the co- and terpolymers agrees with values of the feed ratios within experimental error except for the 70:30 AM:AA polymers, **C4** and **T4**. The latter polymers have AA content consistent with previous studies on similar systems,[14-16] showing slightly higher AA incorporation.

Dynamic Light Scattering (DLS) Studies. DLS studies were first performed on copolymers **C1-C4** in 0.5M NaCl at 25 °C. Hydrodynamic

diameters (d_H) were determined from the limiting diffusion coefficients, D_o, using the Stokes equation:

$$D_0 = \frac{kT}{3\pi\eta_o d_H} \quad (1)$$

where k is the Boltzman constant, T is the absolute temperature and η_o is the viscosity of the solvent. Values of d_H appear in Table 6.1. These values scale with increasing charge density and are consistent with previous DLS studies on AM/AA co- and terpolymers.[16]

We have found that DLS in 1.0% SDS (w/v) is a useful method for comparison of molecular dimensions of hydrophobically-modified polyelectrolytes. The presence of SDS above its critical micelle concentration (CMC) prevents terpolymer aggregation and adsorption onto the micro-filter membranes that are utilized to remove dust from the sample.[14] DLS experiments on copolymers **C1-C4** in 1.0% SDS were performed and d_H determined for comparison with those for terpolymers **T1-T4**. These studies were performed at pH 4.2 ± 0.1 to minimize the effect of differing carboxylate compositions in the co- and terpolymers. Results for the copolymers appear in Table 6.1, and indicate similar hydrodynamic diameters for **C2-C4**. These data are consistent with measurements in 0.5M NaCl. The dimensions of **C1** appear to be the smallest of the series in both 0.5M NaCl and 1.0% SDS.

DLS studies on terpolymers **T1-T4** were not possible in 0.5M NaCl due to strong adsorption onto the microfilter membranes. We were also unable to use mixed solvents as water/dioxane or water/DMF for light scattering measurements as previously reported for other hydrophobically-modified associating systems[13] due to insufficient dn/dc values. Therefore, studies were carried out in 1.0% SDS. Hydrodynamic diameter values of 65-67 nm for **T1-T4** are similar to those of copolymers **C1-C4** (Table 6.1). Of course, hydrodynamic volume is affected by SDS, but we expect similar molecular weights and hydrodynamic volumes for the C1-C4 and T1-%4 series under the identical synthetic conditions. These values are in the same range as those previously reported for fluorescently labeled AM/AA copolymers.[10]

Viscometric Studies. Viscometric properties of the co- and terpolymer with the lowest AA contents (**C1** and **T1**) exhibited characteristics similar to AM homopolymer or copolymers with similar hydrophobic modification; little response to pH or electrolyte concentration is observed. Therefore, attention will be focused on the co- and terpolymers with higher AA content.

Effects of AA Content and Added Electrolyte. Since **C2-C4** and **T2-T4** possess different charge densities at high pH, the viscometric properties were examined as a function of ionic strength under dilute conditions. Therefore

reduced viscosity measurements were conducted on 0.05 g/dL solutions of **C2-C4** and **T2-T4** as a function of ionic strength $I^{-0.5}$ at pH 7.0.

Reduced viscosity of the copolymers is linear with $I^{-0.5}$ and the magnitudes of the slopes scale roughly with charge density (Figure 6.1, top). **C2** (11% AA) shows the smallest slope; **C3** (24% AA) and **C4** (35% AA) exhibit greater slopes. The terpolymers **T2-T4** (Figure 6.1, bottom)exhibit approximately the same slopes, however, indicating that hydrophobic modification may affect the polyelectrolyte nature of the chain in the presence of NaCl. Also, viscosity values for the terpolymers are higher than those for the copolymers, possibly attributable to intermolecular hydrophobic associations in solution.

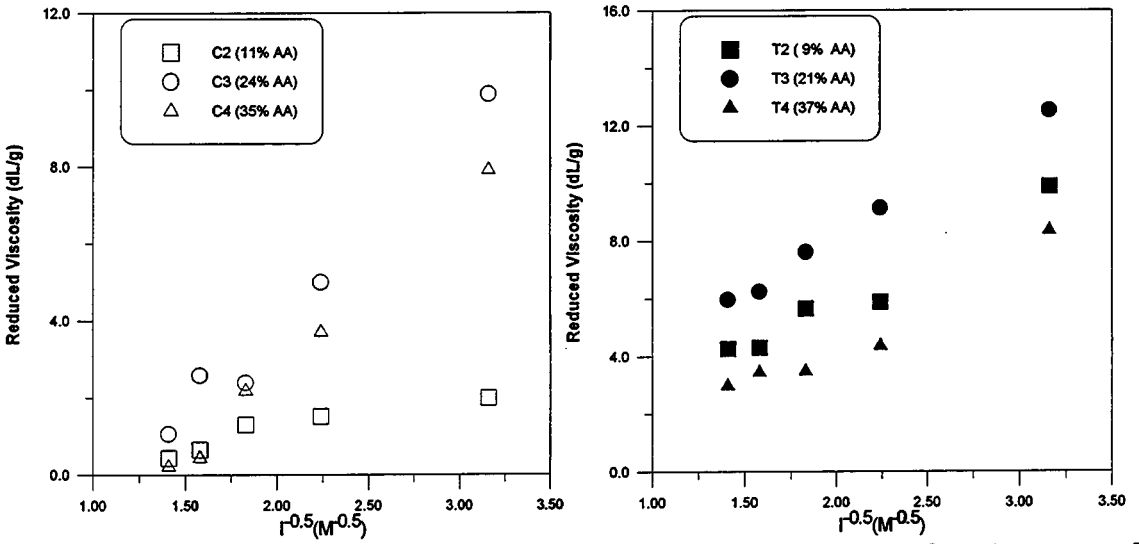

Figure 6.1. Reduced viscosity measurements as a function of ionic strength $I^{-0.5}$ at pH 7.0 for **C2-C4** (top) and **T2-T4** (bottom).Polymer concentration: 0.05 g/dL.

Effects of pH and Polymer Concentration. Viscometric studies were performed on each copolymer (**C2-C4**) and terpolymer (**T2-T4**) in deionized water and in 0.5M NaCl as a function of polymer concentration and solution pH. Polymer concentrations ranged between 0.20 and 0.02g/dL; pH values were 4.0, 5.0, 6.0 and 7.0 ± 0.05. A shear rate of 6 s^{-1} was employed and the temperature was maintained at 25 °C.

The topological features of the apparent viscosity-pH-polymer concentration relationships in deionized water are shown in Figures 6.2-6.4. Data for the unmodified copolymers are shown in the upper portion of each figure and for the terpolymers in the lower portion. Analogous topological data for the co- and terpolymers in 0.5M NaCl are shown in Figures 6.5-6.7.

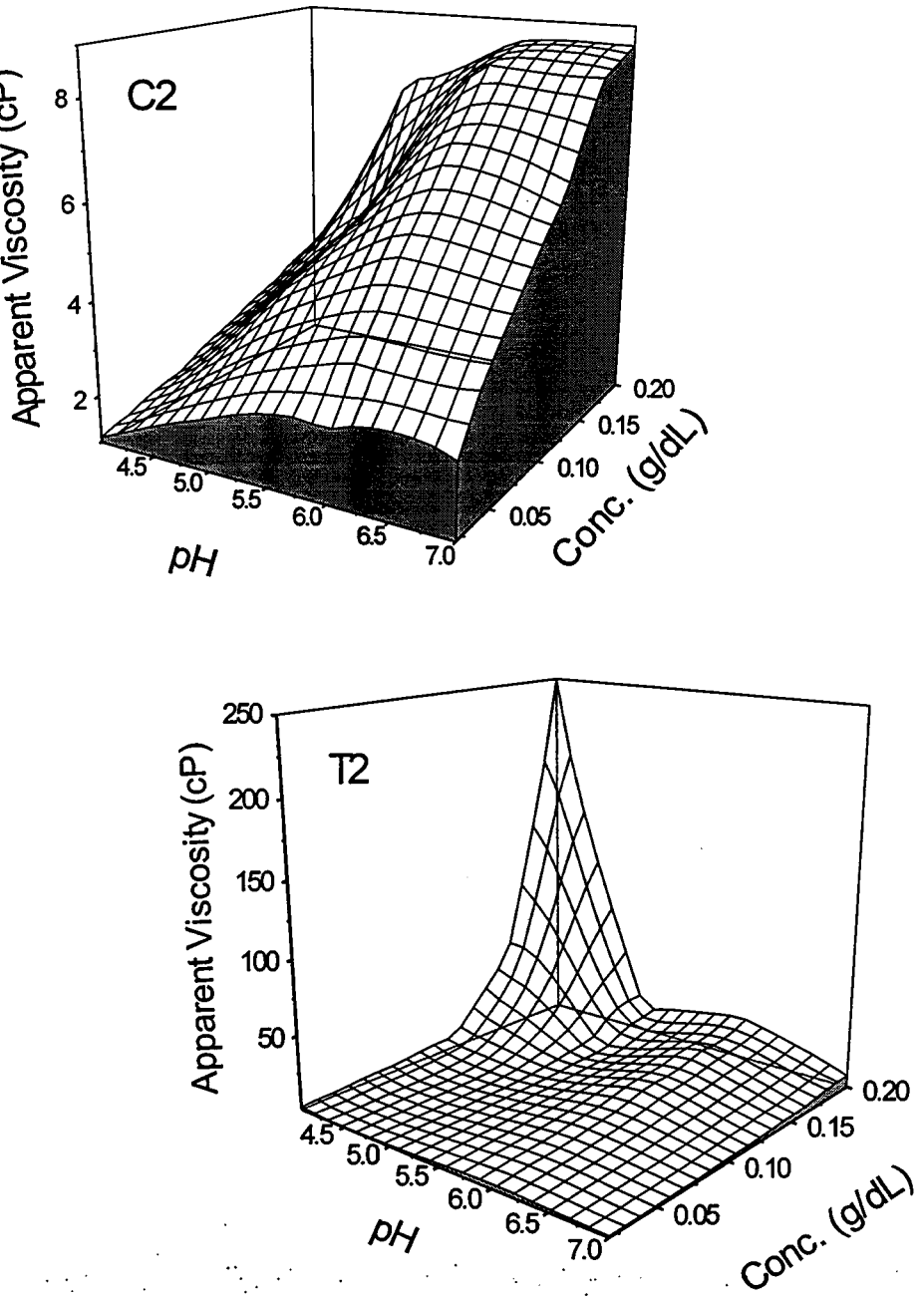

Figure 6.2. Apparent Viscosity of **C2** (11% AA, 89% AM, top) and **T2** (9%AA, 90%AM, 0.6%HPAM, bottom) as a function of solution pH and polymer concentration in deionized water. A shear rate of 6 s-1 was employed and the temperature was maintained at 25 °C.

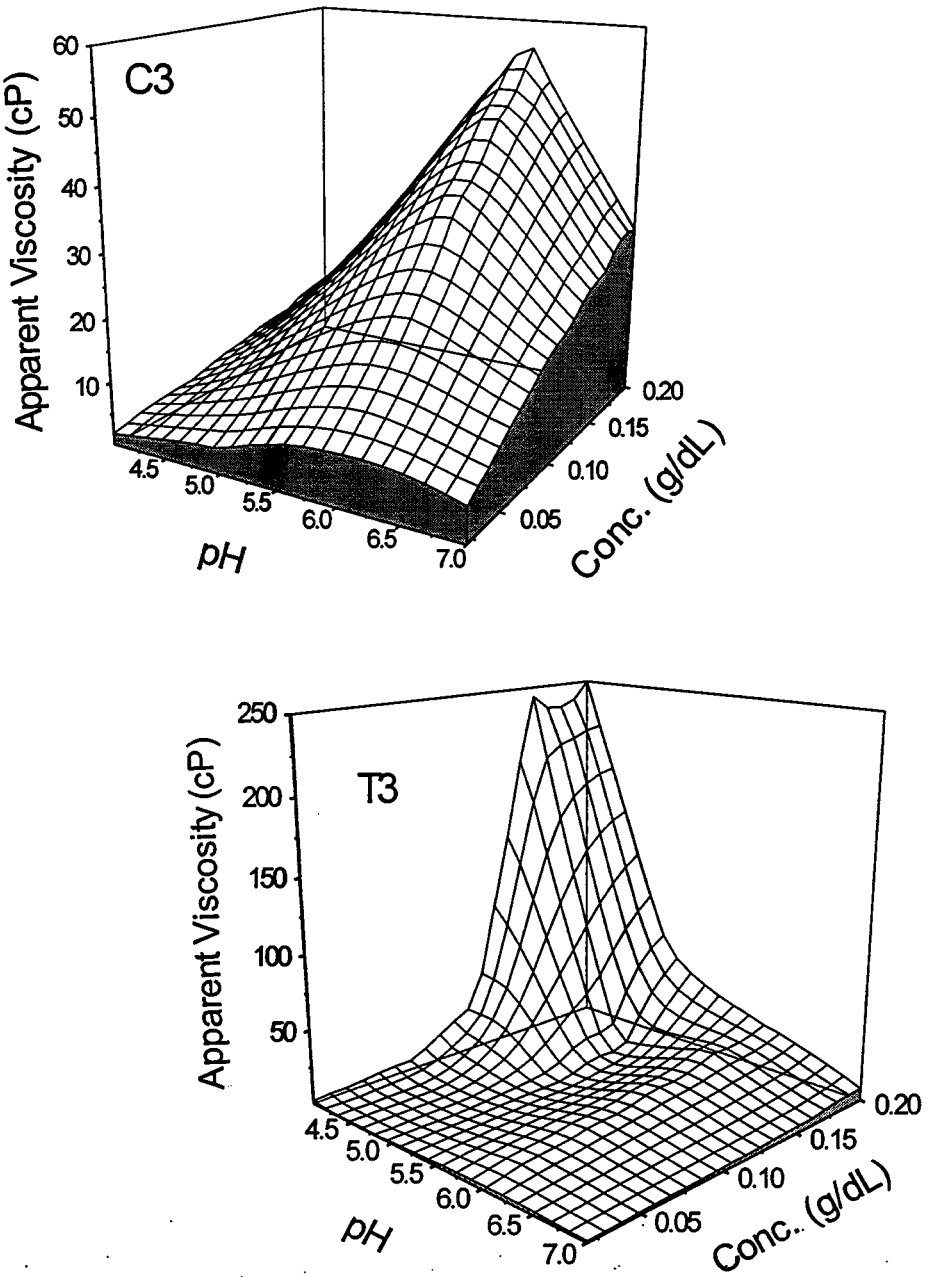

Figure 6.3. Apparent Viscosity of **C3** (24% AA, 76% AM, top) and **T3** (21%AA, 78%AM, 0.6%HPAM, bottom) as a function of solution pH and polymer concentration in deionized water. A shear rate of 6 s-1 was employed and the temperature was maintained at 25 °C.

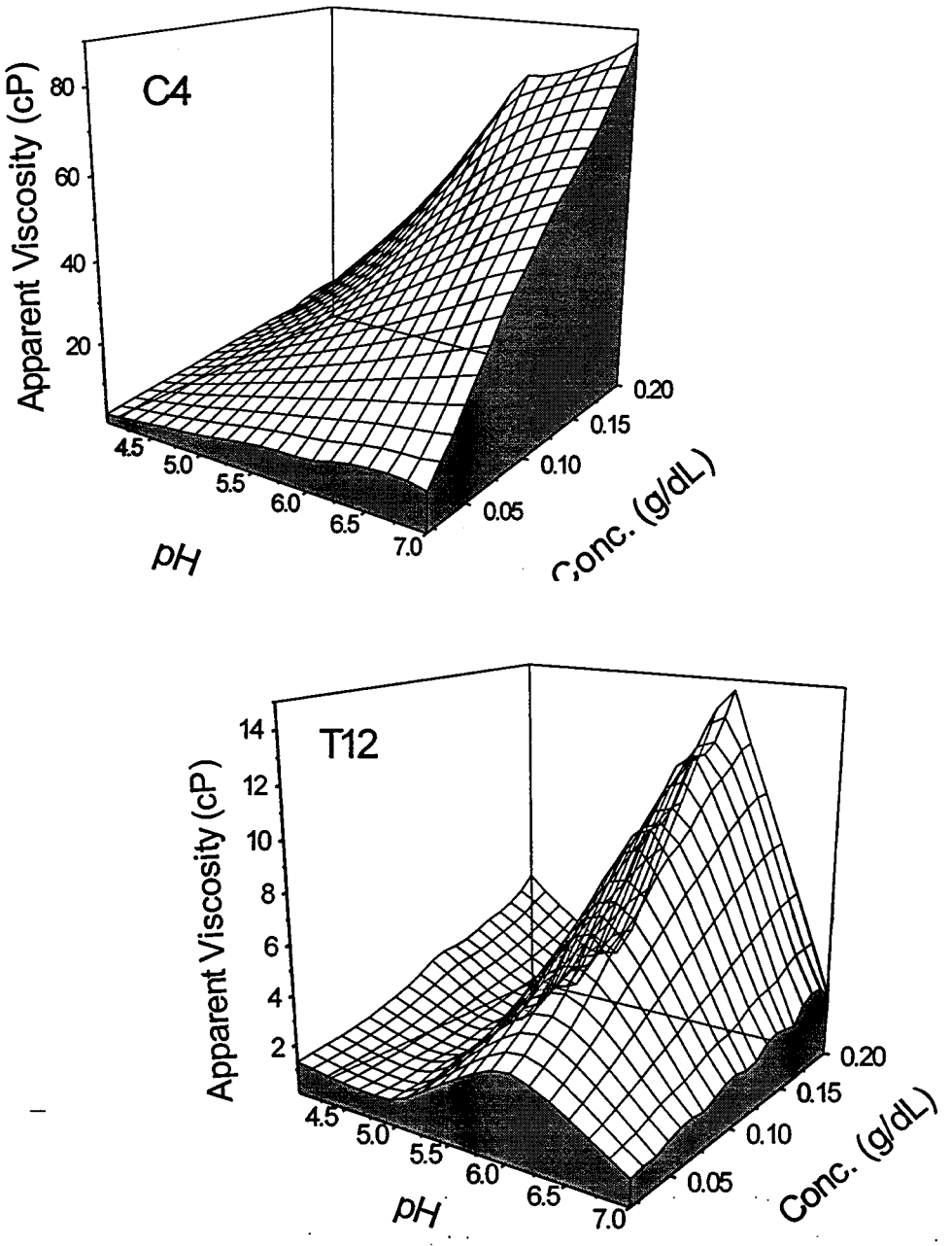

Figure 6.4. Apparent Viscosity of C4 (35% AA, 65%AM, top) and T4 (37%AA, 62%AM, 0.5%HPAM, bottom) as a function of solution pH and polymer concentration in deionized water. A shear rate of 6 s-1 was employed and the temperature was maintained at 25 °C.

The copolymers exhibit the expected viscosity behavior for polycarboxylic acids, revealing maxima in viscosity at high concentration and pH values. The magnitude of viscosity maxima in deionized water (at 0.20g/dL) scales with polyelectrolyte charge density. **C2** (11%AA) exhibits a maximum viscosity of approximately 8.5 cP at pH 7 (Figure 6.2), and **C3** (24%AA) exhibits a maximum viscosity of approximately 55 cP at pH 6 (Figure 6.3). The increase in viscosity from pH 7 to 6 may be due to intramolecular hydrogen bonding, which stiffens the polymer chain.[17,18] **C4** (35%AA) exhibits the highest viscosity maximum of approximately 85 cP at pH 7 (Figure 6.4). Viscosities for **C2**, **C3**, and **C4** in 0.5M NaCl (Figures 6.5-6.7) are lower by an order of magnitude due to electrostatic screening by the excess counterions; the viscosity increase with increasing pH is, therefore, much less dramatic. These studies provide a useful baseline by which to gauge the viscometric and associative behavior of the hydrophobically-modified terpolymers **T2-T4**.

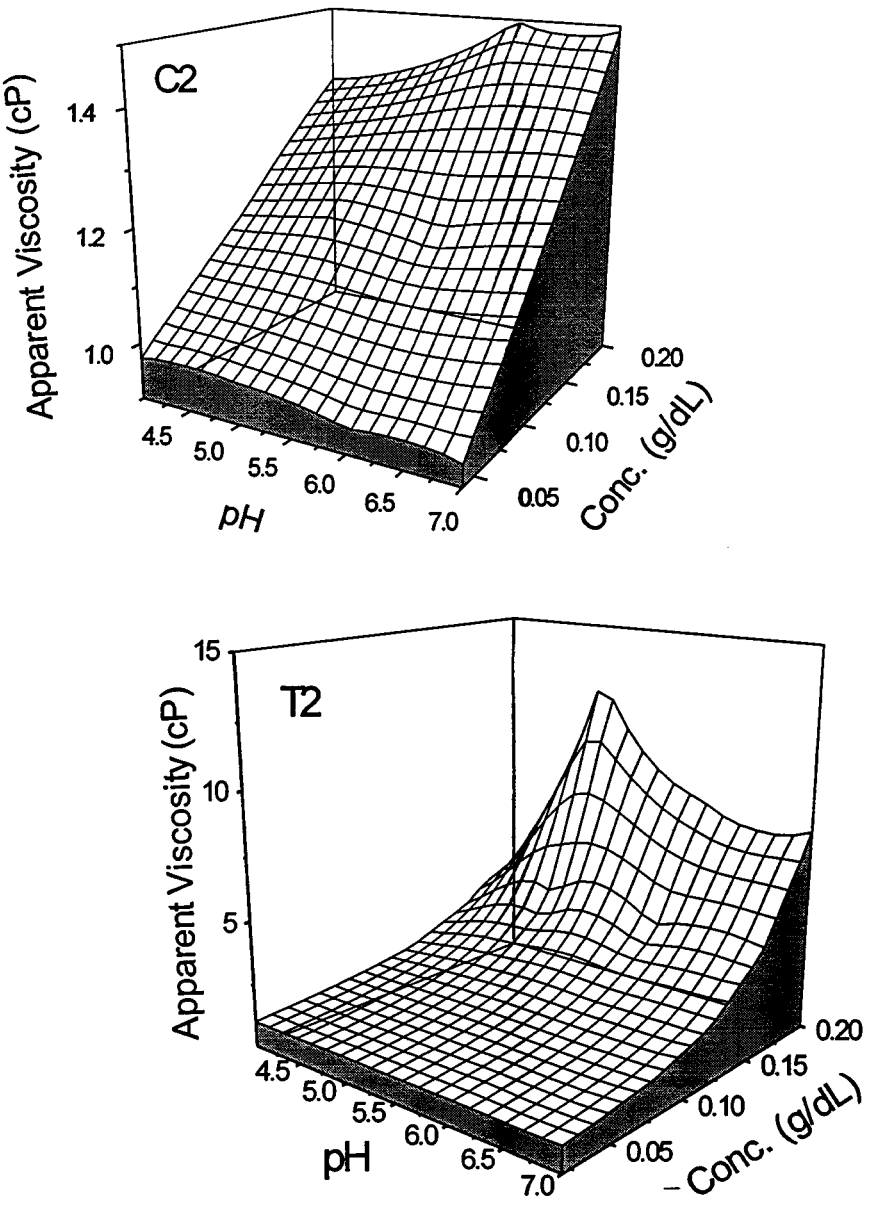

Figure 6.5. Apparent Viscosity of **C2** (11% AA, 89% AM, top) and **T2** (9%AA, 90%AM, 0.6%HPAM, bottom) as a function of solution pH and polymer concentration in 0.5M NaCl. A shear rate of 6 s-1 was employed and the temperature was maintained at 25 °C.

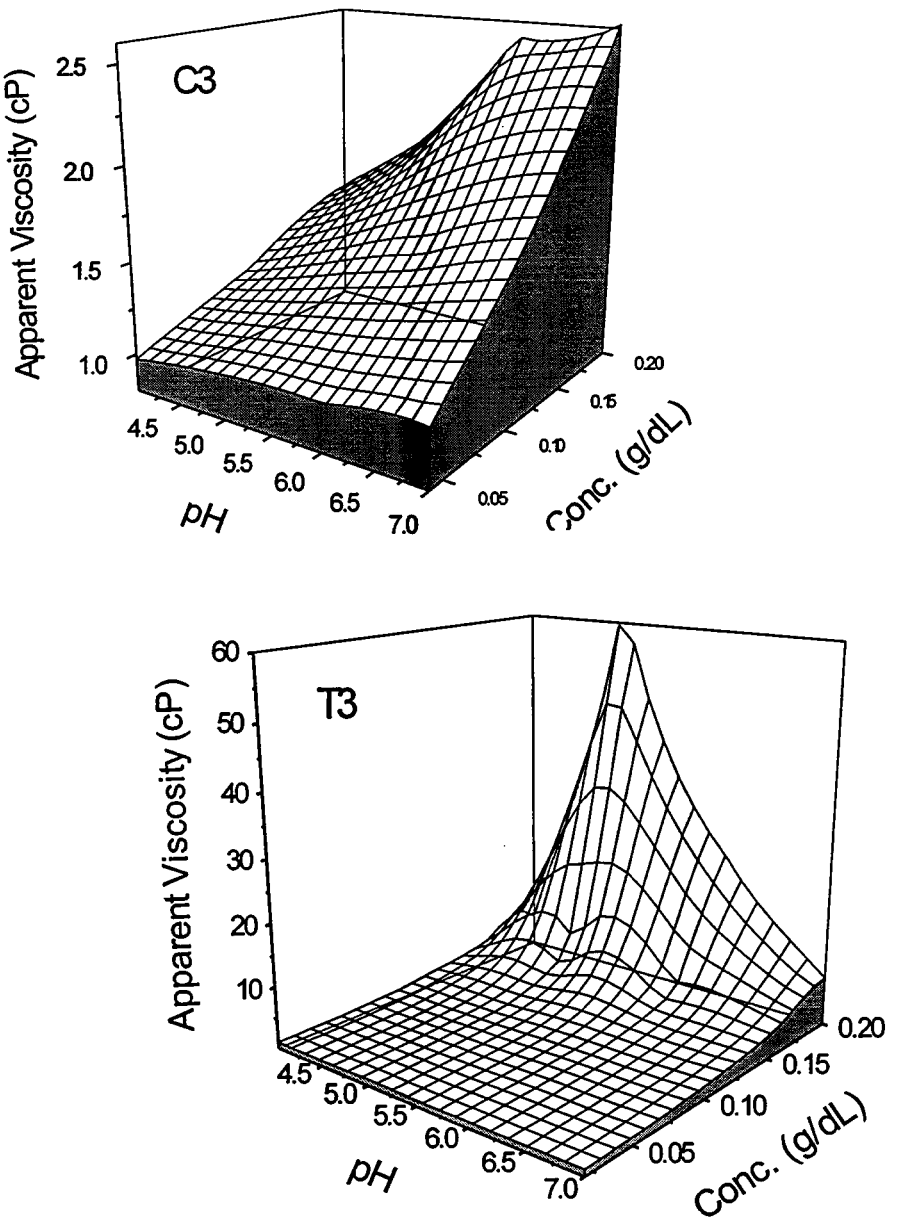

Figure 6.6. Apparent Viscosity of **C3** (24% AA, 76% AM, top) and **T3** (21%AA, 78%AM, 0.6%HPAM, bottom) as a function of solution pH and polymer concentration in 0.5M NaCl. A shear rate of 6 s-1 was employed and the temperature was maintained at 25 °C.

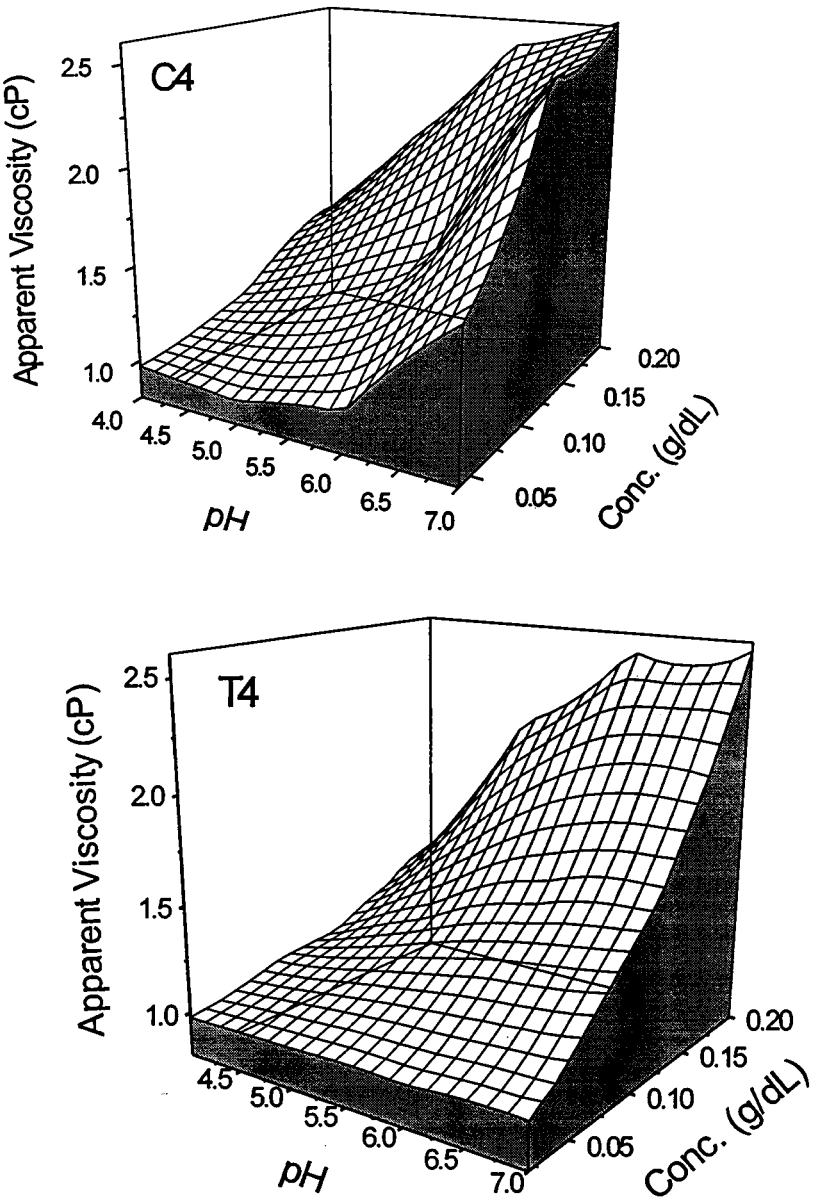

Figure 6.7. Apparent Viscosity of **C4** (35% AA, 65% AM, top) and **T4** (37%AA, 62%AM, 0.5%HPAM, bottom) as a function of solution pH and polymer concentration in 0.5M NaCl. A shear rate of 6 s-1 was employed and the temperature was maintained at 25 °C.

Topological apparent viscosity-pH-concentration data for **T2-T4** in deionized water (Figures 6.2-6.4) and 0.5M NaCl (Figures 6.5-6.7) exhibit some interesting features. Figures 6.2 and 6.3 show the topological data for

T2 (9% AA) and **T3** (21% AA), respectively, in deionzed water. Notable differences in viscosity behavior of these terpolymers and their respective control copolymers, **C2** (11%AA) and **C3** (24%AA), are observed. Large increases in apparent viscosity are observed with decreasing pH and increasing terpolymer concentration in both plots. No associative behavior is noted at pH 6 and 7 in both cases; viscosity increases in a linear fashion with terpolymer concentration. However, at pH 4 and 5, marked curvature in the viscosity-concentration dependence indicates intermolecular associations for both **T2** and **T3**. At pH 4, both terpolymers have viscosities surpassing 250 cP due to extensive intermolecular associations. The onset of association or critical overlap concentration, C^*, appears to be at a lower polymer concentration for **T3**, below 0.10g/dL. The onset of association for **T2** is at a concentration slightly greater than 0.10g/dL. The amount of HPAM in all the terpolymers was determined to be identical (0.5-0.6 mole%) within experimental error and data from DLS indicate similar dimensions for **T2** and **T3**. Therefore, the differences in C^* are likely due to compositional effects.

The viscosity-pH-concentration plot for terpolymer **T4** (37% AA) in deionized water is shown in Figure 6.4. Although some curvature in the apparent viscosity versus concentration dependence is present at pH 4, no notable increase in viscosity is evident at any of the pH values investigated, in contrast to data for **T2** and **T3**. If extensive hydrophobic associations are present in **T4** in deionized water, they are intramolecular (closed) in nature. This finding is consistent with studies by Klenina and Lebedeva[19] who noted poor solubility of AM/AA copolymers of greater than 30 mole% AA at low pH. These studies suggest that above this AA composition, intramolecular hydrogen bonding is stronger than the polymer-water interactions resulting in poor polymer solvation. Intermolecular association for **T4** at low pH may therefore be overwhelmed by intramolecular hydrogen bonding.

The concentration range studied in this work is identical to that of previous studies on hydrophobically-modified AM copolymers[2-7] in which the onset of intermolecular associations was noted. For the AA containing terpolymers **T2-T4**, no intermolecular association is evident in deionized water at pH 6 and 7. Intermolecular associations in **T2** and **T3** have apparently been disrupted by ionization of the carboxylic acid groups. Further discussion of the nature of these "pH-triggered" associations in solution is presented in subsequent sections.

Figures 6.5-6.7 show topological viscosity-pH-concentration data for **T2-T4** in 0.5M NaCl. Viscosities for each sample are lower at pH 6 and 7 as compared to values in deionized water due to the addition of NaCl. Electrostatic shielding of the polyeletrolyte charges causes collapse of the individual polymer coils, but intermolecular associations result at sufficient terpolymer concentrations for **T2** (Figure 6.5) and **T3** (Figure 6.6) at pH 5-7. Each polymer exhibits a C^* at approximately 0.15 g/dL (except at pH 4). The

induction of intermolecular associations at high pH by the addition of NaCl is consistent with results reported for N-[4-(decyl)phenyl]acrylamide modified terpolymers.[14] Associations may be more efficient at high pH in NaCl solutions as compared to deionized water due to the screening of inter- and intracoil polyelectrolyte charges as well as enhanced water structuring in the presence of NaCl. Also, collapse of the polymer coils may result in more hydrophobic groups at the surface which aggregate to minimize contact with water.

The lack of high viscosity for **T2** and **T3** at pH 4 in 0.5M NaCl is likely due to the collapse of the polymer coils due to protonation of the AA groups and increased hydrophobic associations due to the presence of NaCl. A "salting-out" effect on the terpolymers may prohibit bridging or open associations under these conditions. However, no precipitation is noted for these solutions. Alternatively, intramolecular hydrogen bonding, similar to that postulated for **T4**, could be promoted because of the compact nature of the polymer coils in 0.5M NaCl.

The topological data for **T4** in 0.5M NaCl (Figure 6.7) exhibit some curvature indicative of intermolecular associations at pH 5-7, but associative behavior is altered little by the presence of salt. The viscosity values are lower in general due to the presence of electrolyte. Although **T4** does not exhibit extensive associations in 0.5M NaCl, it should be noted that an identical terpolymer bearing the larger decylphenyl hydrophobe[14] showed significant associations at pH 7 in 0.5M NaCl.

Pyrene Probe Fluorescence Studies. In order to determine the extent and nature of the hydrophobic associations in **T2-T4**, pyrene probe fluorescence experiments were performed under conditions identical to those in the viscosity studies. The ratio of the fluorescence intensity of the third vibronic band to that of the first vibronic band (I_3/I_1) of pyrene is a useful indicator of the local dielectric constant surrounding the probe.[20] I_3/I_1 has values of approximately 0.5 in water, 0.7-0.9 in common short chain alcohols and ~1.5 in hydrocarbon media. I_3/I_1 values for pyrene solubilized in common surfactant micelles[20] or hydrophobic microdomains in amphiphilic polymer systems[21] are between those found in aqueous and hydrocarbon media.

The I_3/I_1-pH-concentration plot for **T2** in deionized water is shown in Figure 6.8. I_3/I_1 remains approximately equal, within experimental error, to its value in water from 0.02 to 0.20 g/dL concentration of terpolymer at pH 6 and 7. Below pH 5, I_3/I_1 increases significantly at high terpolymer concentration. A maximum value of ~ 0.85 is obtained at pH 4-0.20g/dL (comparable to I_3/I_1 of pyrene in common surfactant micelles). Comparison of these data (Figure 8.8) with viscosity data for **T2** in water (Figure 6.2) indicates that the increase in I_3/I_1 corresponds to C* at pH 4 (just above 0.10g/dL).

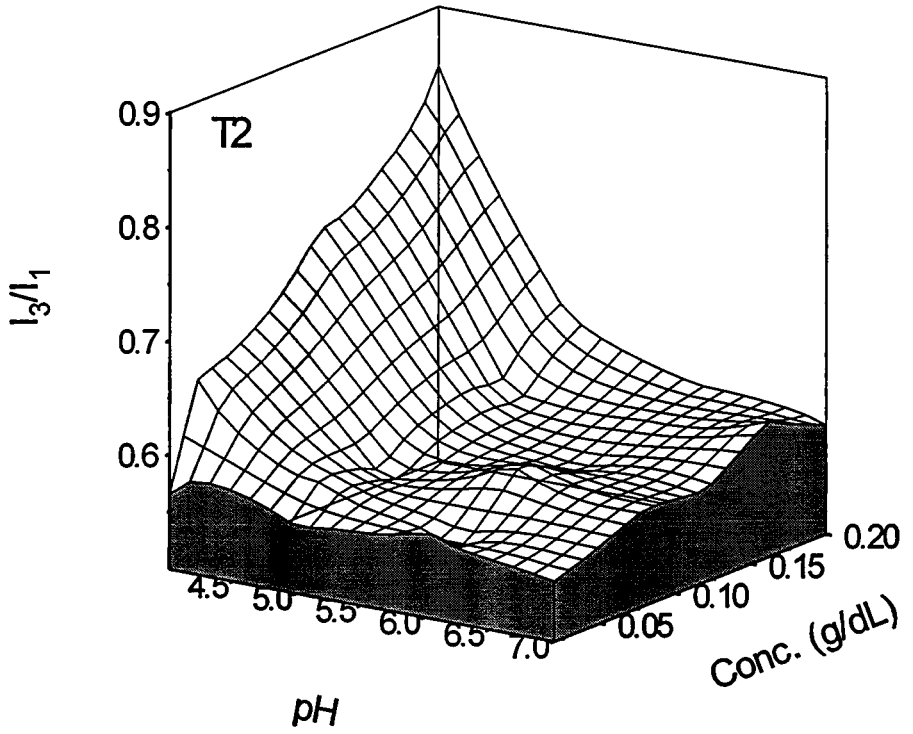

Figure 6.8. I_3/I_1 as a function of solution pH and terpolymer concentration in deionized water for **T2** (9%AA, 90%AM, 0.6%HPAM, bottom) at 25 °C.

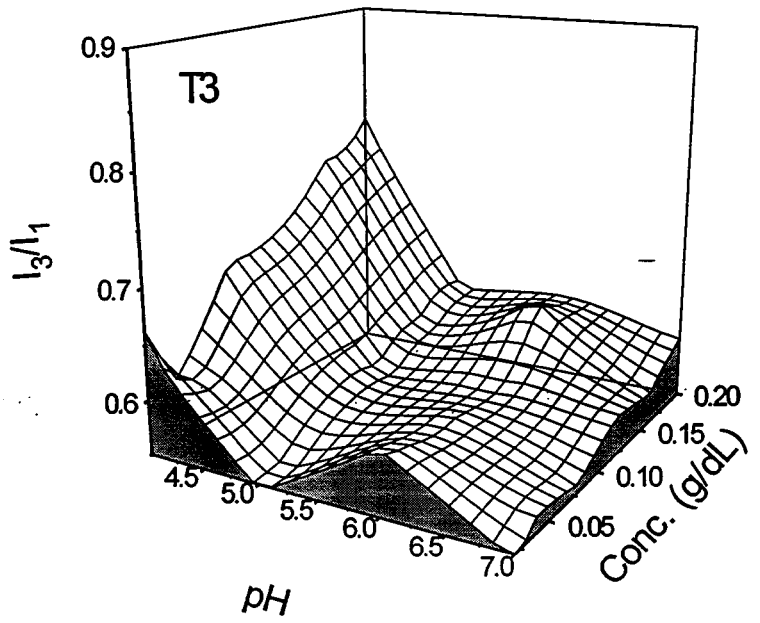

Figure 6.9. I_3/I_1 as a function of solution pH and terpolymer concentration in deionized water for **T3** (21%AA, 78%AM, 0.6%HPAM, bottom) at 25 °C.

I_3/I_1 data as a function of pH and terpolymer concentration for **T3** in deionized water (Figure 6.9) are similar to those of **T2**. The I_3/I_1 value above pH 5 remains close to that of water even at high terpolymer concentration. Below pH 5, I_3/I_1 approaches values found in surfactant micelles once sufficient terpolymer concentration is reached. Maximum values of I_3/I_1 of **T3** (0.80) and **T3** (0.85) are equal within experimental error, suggesting domain organization is similar under these conditions. Furthermore, these values are comparable to acrylamide polymers containing < 0.5 mole% lauryl methacrylate above C^*.[7] Increased domain organization with protonation of the carboxylate groups is addressed below.

I_3/I_1-pH-concentration plots for **T4** in deionized water appear in Figure 6.10. The features of I_3/I_1 as a function of pH and terpolymer concentration are similar to those exhibited by **T2** and **T3** below pH 5. I_3/I_1 reaches a value of 0.8 just below 0.10 g/dL terpolymer and increases to ~1.0 at 0.20 g/dL. This indicates a more hydrophobic environment at low pH, despite the fact that no C* was evident from viscosity studies (Figure 6.4). Therefore, the hydrophobic microdomains sensed by the pyrene probe are likely of an intra- rather than an intermolecular nature. The higher values of I_3/I_1 at low pH may indicate stabilization of intramolecular associations by hydrogen bonding[19] and the drop in I_3/I_1 with decreasing terpolymer concentration at pH 4 and 5 in water is likely due to significant partitioning of the probe into the aqueous phase as the concentration of intramolecular hydrophobic domains is decreased.[20]

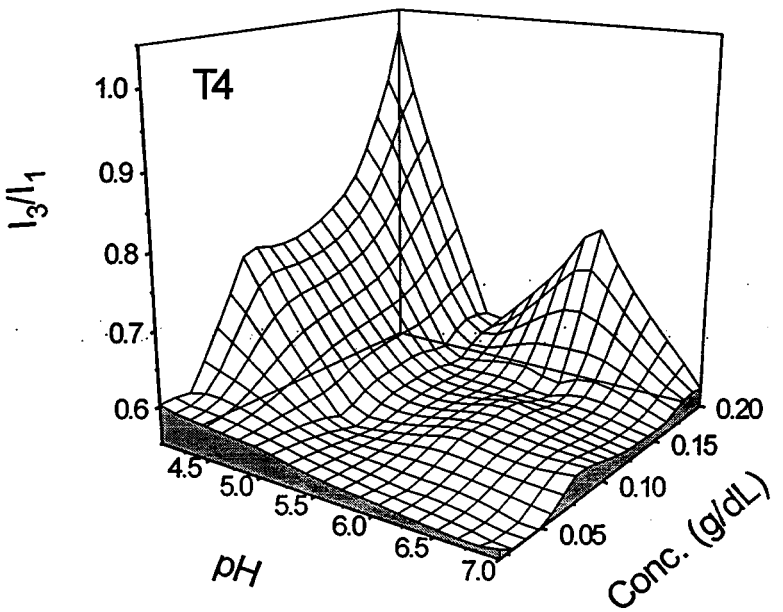

Figure 6.10. I_3/I_1 as a function of solution pH and terpolymer concentration in deionized water for **T4** (37%AA, 62%AM, 0.5%HPAM, bottom) at 25 °C.

Also, the I_3/I_1 value of pyrene in solutions of **T4** increases between pH 7 and 5 as long as a terpolymer concentration exceeds 0.15g/dL. This behavior mirrors the viscosity increase under the same conditions (Figure 6.4). The origin of the increase in both viscosity and I_3/I_1 under these conditions is unclear at present, but is likely related to hydrogen-bonding and the exclusion of water from the probe.

Topological data of I_3/I_1-pH-terpolymer concentration in 0.5M NaCl for **T2** is shown in Figure 6.11. Data for terpolymers **T3** and **T4** show similar features. First, the dependence of I_3/I_1 on pH at high terpolymer concentration is less pronounced in NaCl solution, compared to deionized water (Figures 6.8-6.10). This is expected since the polyions are in a less extended conformation in the presence of excess counterions.

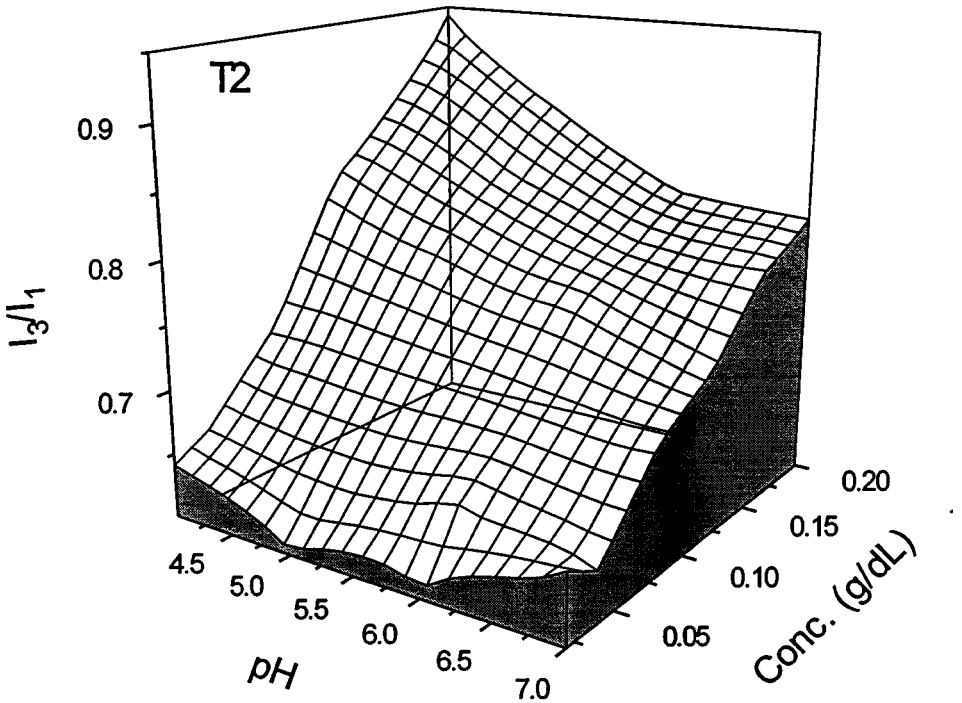

Figure 6.11. I_3/I_1 as a function of solution pH and terpolymer concentration in 0.5M NaCl for **T2** (9%AA, 90%AM, 0.6%HPAM, bottom) at 25 °C.

Also, I_3/I_1 is higher at pH 6 and 7 in 0.5M NaCl than in water. This is significant in light of the fact that **T2** and **T3** exhibit intermolecular associations in 0.5M NaCl even at high degrees of ionization. These results suggest perturbation of hydrophobic associations due to increasing ionization of the polymer chain may be overcome by addition of NaCl.

Terpolymer Solvation and Microdomain Organization. The remarkable effect of 0.5 mole percent incorporation HPAM on solution

properties that we observe experimentally by comparing the T and C series is attributable to macromolecular concentration and solvation. The presence of polymer sequences along the amphiphilic macromolecule which are "water averse" allows for long-range intra- and/or inter-molecular microdomain formation. Such interactions have been extensively reviewed in both synthetic[22,23] and biological[22,24,25] amphiphilic polymers.

For both synthetic[23] and biopolymer systems[24,25] it has been proposed that two modes of hydration of the amphiphilic polymer are operative: one is due to water restructuring as hydrophobic moieties release ordered water back into the bulk on aggregation; the second is due to hydration of polar or ionic entities along the macromolecular backbone. It is hypothesized that water molecules cannot participate in both modes of hydration and that increasing hydration of the hydrophilic portion of the chain results in disruption of nearby hydrophobic aggregates. Urry[24] has elegantly demonstrated this behavior by measuring the resulting changes in the lower critical solution temperature (LCST) for polypeptides with controlled changes in amino acid sequence and thus polarity, solvation, and hydrogen bonding. Similar changes in LCST have been observed for copolymers of N-isopropylacrylamide with acrylamide in our laboratories and others.

The seemingly complex of the BPAM/AM/AA (T series) of terpolymers as followed by viscosity/pH/concentration or I_3/I_1-pH-concentration plots can be readily interpreted in terms of the above by examining high ($\geq$0.1 g/dl) and low (<0.1g/dl) terpolymer concentrations at high (pH>75) and low (pH<5) values.

In general, little inter-molecular (open) association is observed at high pH in deionized water. Only T2 and T3 exhibit a C* in deionized water at low pH. I_3/I_1 measurements support the presence of intermolecular microdomains. T4, on the other hand exhibits no C*, but I_3/I_1 studies reveal well organized intramolecular (closed) microdomains in aqueous solution. Addition of 0.5M NaCl shifts C* for T_2 and T_3 to higher concentrations. T4 exhibits both closed and open association in 0.5M NaCl at low pH and high terpolymer concentration.

The above concepts are illustrated conceptually in Scheme 2. At high pH the terpolymers are depicted as rod-like entities due to intra-coil charge-charge repulsions of the carboxylate ions.

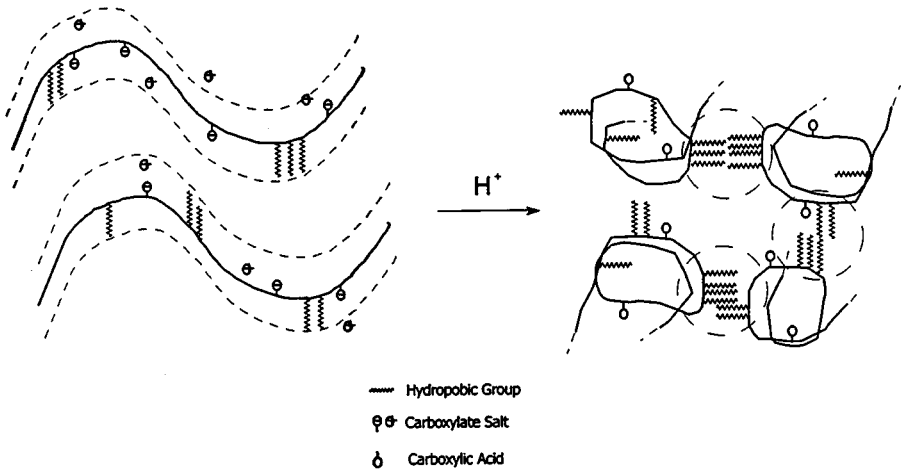

Scheme 6.2. Conceptual model for the pH-responsive intermolecular associations of **T2** and **T3**.

Intermolecular hydrophobic associations are prohibited by hydration of the polymer backbone and/or interchain ionic repulsions of the charged groups. As acid is added the system, the carboxylate groups are masked, reducing hydrophilic hydration of the chain and intercoil ionic repulsions. The restructuring of water forces the hydrophobes from individual polymer chains into intermolecular (open) microdomains resulting in viscosification of the solution.

Viscosity and I_3/I_1 studies of **T3** and **T4** indicate, that intermolecular associations may result at high pH in the presence of electrolyte (0.5M NaCl). At comparable pH values, **T3** and **T4** show increased I_3/I_1 at high terpolymer concentration as compared to deionized water. This may be due to enhanced organization of the hydrophobic domains in solution brought about by the water structuring effect of NaCl,[25] and/or removal of conformational restraints by collapse the polymer coils due shielding of polyelectrolyte charges. Apparently, these factors allow intermolecular hydrophobic association at sufficient terpolymer concentration, in spite of the hydration of the carboxylate groups at high pH. Note that I_3/I_1 data indicate that the aggregates at high pH are more hydrated than at low pH.

Viscosity is at a minimum for **T2** and **T3** at pH 4 in 0.5M NaCl (Figures 6.5 and6.6) but at a maximum in deionized water (Figures 6.2 and 6.3). One might expect that hydrophobic associations would be at a maximum at pH 4 in 0.5M NaCl for reasons stated above. The lack of high viscosity for **T2** and **T3** at pH 4 in 0.5M NaCl is unclear since I_3/I_1 values are actually enhanced under these conditions (Figure 6.11). One possibility is a "salting-out" effect on the terpolymers as they approach the uncharged state.

However, no precipitation is noted for these solutions. Alternatively, intramolecular hydrogen bonding, similar to that postulated for **T4**, could be promoted due to the compact nature of the polymer coils in 0.5M NaCl. In this case, water would be excluded from the hydrophobic domains.

In the case of **T4**, significant intermolecular associations may be ruled out from viscosity data; I_3/I_1 data suggest intramolecular hydrophobic associations at low pH. Values of ~ 1.0 at low pH and high terpolymer concentration in deionized water and in 0.5M NaCl are measured. This value equals or exceeds the highest value of I_3/I_1 for pyrene in the hydrophobic interior of surfactant micelles, suggesting a high degree of microdomain organization. The drop in I_3/I_1 with decreasing terpolymer concentration at pH 4 and 5 in water (Figure 6.10) is likely due to significant partitioning of the probe into the aqueous phase as the concentration of intramolecular hydrophobic domains is decreased.[20] I_3/I_1 data under these conditions in 0.5M NaCl show a similar decrease.

Conclusions

AM/AA/HPAM **T2-T4** terpolymers with identical HPAM content, sequence distribution, and molecular size but varying AA content were synthesized by micellar polymerization. Associative properties were investigated at pH 4.0, 5.0, 6.0, and 7.0 by low shear viscosity and pyrene probe fluorescence studies in deionized water and 0.5M NaCl. At pH 6 and 7 in deionized water, no hydrophobic associations are noted for any of the terpolymers due to hydration of the carboxylate residues in solution. Apparently, hydration of the carboxylate residues disrupts the structuring of water that drives hydrophobic associations. At pH 4 and 5, two copolymers containing 9 and 21 mole% AA show extensive intermolecular hydrophobic associations. Masking of the carboxylate charges at low pH allows the natural structuring of water around the hydrophobic HPAM residues, thus driving intermolecular association.

No intermolecular associations for a terpolymer containing 37% AA are noted even at pH 4. However, well-organized hydrophobic microdomains are indicated at low pH by pyrene I_3/I_1 measurements. This leads to the conclusion that intramolecular hydrophobic associations are stabilized by strong hydrogen bonding. These intramolecular hydrophobic microdomains appear to be unaltered in the presence of 0.5M NaCl.

Addition of NaCl to solutions of the terpolymer containing 9 and 21 mole % AA results in intermolecular associations even at high pH. Collapse of the polymer coils and screening of intra- and intercoil electrostatic repulsions by excess electrolyte and/or the water structuring effect of NaCl allow hydrophobic association even though hydration of the carboxylate residues remains high. Finally, loss in viscosity is noted at pH 4 for these two terpolymer systems in 0.5M NaCl. This is thought to occur by either a

"salting out" effect on the terpolymers or the promotion of intramolecular hydrophobic associations stabilized by hydrogen bonding.

These studies clearly demonstrate how controlling composition, solution pH, ionic strength, and terpolymer concentration can lead to materials with pH-and electrolyte-responsive associations.

References and Notes

1. McCormick, C. L., Bock, J. and Schultz, D. N., In *Encyclopedia of Polymer Science and Engineering*, **17**, John Wiley & Sons, Inc., New York, **1989**, 730-784.

2. Turner, S. R.; Siano, D. B. and Bock, J., U. S. Patent, 4,520,182.

3. Valint, P. L.; Bock, J.; Ogletree, J.; Zushuma, S.; Pace, S. J., *Polym. Prepr.*, **1990**, *31*, 67.

4. Bock, J., Siano, D. B., Valint, P. L., Pace, S. J., in *Polymers in Aqueous Media*, **1989**, Glass, J. E. (Ed.), ACS Advances in Chemistry Series No. 223, The American Chemical Society, Washigton, D. C., 411.

5. Siano, D. B., Bock, J., Myer, P., Valint, P. L., in *Polymers in Aqueous Media*, **1989**, Glass, J. E. (Ed.), ACS Advances in Chemistry Series No. 223, The American Chemical Society, Washington, D. C., 425.

6. McCormick, Nonaka, T. and Johnson, C. B., *Polymer*, **1988**, *29*, 731.

7. Flynn, C. E. and Goodwin, J.W., in *Polymers as Rheological Modifiers*, Schultz, D. N. (Ed.), **1991**, ACS Symposium Series No. 462, The American Chemical Society, Washington D. C., 190.

8. Ezzell, S. A. and McCormick, C. L., *Macromolecules* **1992**, *25*, 1881.

9. Ezzell, S. A.; Hoyle, C. E.; Creed, D.; McCormick, C. L., *Macromolecules* **1992**, *25*, 1887.

10. Branham, K. D. and McCormick, C. L. in *Multi-Dimensional NMR, FT-IR/Raman, and Fluorescence Spectroscopy of Polymers,* ACS Symposium Series No. 598, The American Chemical Society, Urban, M. and Provder, T. (Ed.s), Chatper 32, p 1994.

11. McCormick, C. L.; Middleton, J. C. and Cummins, D. F., *Macromolecules*, **1992**, *25*, 1201-1206

12. McCormick, C. L.; Middleton, J. C. and Grady, C. E., *Polymer*, **1992**,*33*, 4184.

13a. Biggs, S., Selb, J., and Candau, F., *Polymer*, **1993**, *34*, 580.

13b. Biggs, S., Hill, A., Selb, J., and Candau, F.; J. Phys. Chem. 1996, 1505 1992.

14. Branham, K. D.; Davis, D.L. Middleton, J. C., and McCormick, C.L., *Polymer*, **1994**, *35*, 4429.

15. Mortimer, D. A., Polymer International, 1991, **25**, 29.

16. Branham K., D., Shafer, G., S., Hoyle, C. E., and McCormick, C. L., *Macromolecules*, accepted for publication, June 1995.

17. Klein, J. and Heitzmann, R., *Makrolmol. Chem.*, **1978**, *179*, 1895.

18. Kulicke, W.-M. and Horl, H.-H., *Colloid & Polymer Sci.*, **1985**, *263*, 530.24)

19. Klenina, O. V. and Lebedeva, L. G., *Polym. Sci., U.S.S.R.*, **1983**, *25*,2380.

20. Kalyanasundarum, K., *Photochemistry in Microheterogeneous Systems*, **1987**, Academic Press, Inc., Orlanda, Fl.

21. Varadaraj, R., Branham, K. D., McCormick, C. L., and Bock, J., in *Macromolecular Complexes in Chemistry and Biology*, **1993**, Springer Verlag, New York, 15.

22. Tanford, C., *The Hydrophobic Effect: Formation of Micelles and Biological Membranes*, **1973**, Wiley & Sons, New York.

23. Urry, D. W., *Scientific American*, **1995**, *Jan.*, 64.

24. Urry, D. W., *Angew. Chem. Int. Engl. Ed.*, **1993**, *32*, 819.

25. Collins, K. D. and Washabaugh, M. W., *Quart. Rev. of Biophys.*, *18*, **1985**, *18*, 323.

CHAPTER 7: DILUTE POLYMER SOLUTIONS IN EXTENSIONAL FLOW THROUGH POROUS MEDIA - THEORETICAL CONSIDERATIONS

Polymer Flooding

Water soluble polymer molecules are used to make the displacing fluids that are employed during reservoir flooding. To be economical, the polymers must increase the flow resistance of the displacing fluid even when added at very low concentrations, usually at the parts per million level. During flooding, oil recovery is maximized when the mobility of the displacing fluid or polymer solution is equal to or less than the mobility of the residual fluids existing within the reservoir. The mobility of a polymer solution decreases as the fluid shear and extensional viscosities increase.

Shear viscosities characterize the flow resistance created when a fluid experiences a shearing flow field. In shearing flow the fluid velocities are changing with respect to a direction perpendicular to the flow direction. However, because the polymer concentrations used for displacing fluids are very low, the solution shear viscosity is almost the same as the solvent, water. Therefore, the very small increase in solution shear viscosity due to the presence of the polymer molecules has a minor effect in decreasing the displacing fluid's mobility.

In contrast, the extensional viscosity of a dilute polymer solution flowing through a reservoir can significantly contribute to the flow resistance of the displacing fluid. Extensional viscosities characterize the flow resistance created when a fluid experiences an extensional flow field. In extensional flow the fluid velocities are changing with respect to the direction parallel to the flow direction. This type of flow field exists during reservoir flooding because the displacing fluid is constantly being accelerated and decelerated as it progresses through the interstitial passages within the porous media. Thus, an understanding of which macromolecular parameters enhance solution extensional viscosity is important in the development of more effective polymers.

Dilute Polymer Solutions

A high molecular weight polymer molecule in solution interacts with many low molecular weight solvent molecules. Because most polymers are rope like and have a large degree of flexibility, solvent - polymer interactions cause the polymer macromolecules to expand and form random coils. See Figure 7.1. Each coil is roughly spherical and contains not only the coiled polymer molecular mass but also a much larger solvent mass. The bound solvent within a polymer coil volume has been altered because of the interaction with the macromolecule and is thermodynamically different than unbound solvent. When the coil is extended in a flow field both the polymer macromolecule and the associated solvent molecules are disordered from their unperturbed state. This coil deformation converts fluid kinetic energy into heat which lowers the solution's mobility.

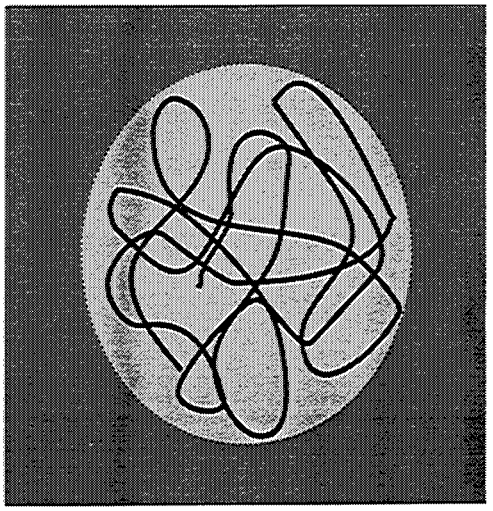

Figure 7.1 Coiled polymer macromolecules in solvent.

The volume of a mole of coils is equal to the product of the solution's intrinsic viscosity, η_{intr}, (a measurable parameter that is the coil volume per unit polymer mass) and the polymer molecular weight, M. The volume fraction of polymer coils in a dilute solution is equal to the product of the intrinsic viscosity and the mass concentration of polymer in the solution, c. The solution is considered dilute when the volume fraction of polymer coils is less than unity. Therefore, the polymer solution is considered dilute when $c\,\eta_{intr} < 1$. For dilute solution conditions each polymer coil responds to the fluid flow field independently of adjacent coils.

Flow of Dilute Polymer Solutions Through Porous Media

All porous media contain many fluid passages that are composed of converging and diverging channels. As fluids travel through these converging and diverging channels, alternating extensional and compression flow fields develop. In an extensional flow field, the fluid velocities are increasing in the direction of flow. In a compression flow field, fluid velocity are decreasing in the flow direction.

In a converging channel, the fluids surrounding a polymer coil will produce frictional drag forces on the coil that are proportional to the velocity acceleration of the surrounding fluid. The drag forces are larger at the forward end of the coil than at the rear because fluid velocities are larger at the forward end of the coil. When the difference in drag forces across the polymer coil is sufficiently large, the coil will elongate. After coil elongation, coil compression occurs due to a reversal of drag forces as the coil passes into a diverging channel.

Kinetic energy is converted into heat as the coils are cyclically strained. The polymer macromolecule and bound solvent within each coil are perturbed with each cycle of extension and compression. This repeated change of molecular order due to the extensional strain introduced into the polymer molecule and bound solvent will produce a degradation of fluid kinetic energy into heat. This results in a decrease in the solution's mobility as it flows through a porous medium.

Polymer Coil as a Kelvin Mechanical System

The simplest way to model the extensional flow behavior of a polymer solution is to first assume that the polymer molecules within a dilute solution act as a collection of independent but identical coils[1]. Next each polymer coil is considered to react to extensional fluid flow forces as a strain lock and dashpot connected in parallel. This arrangement of a dashpot and lock will be referred to as a Bingham mechanical system. Refer to Figure 7.2.

The lock prevents polymer coil deformation or strain until the fluid extensional stress is greater than a specific yield stress, σ_{yield}. Note that the lock will reset when the coil strain is returned to zero. The dashpot provides the coil with a energy conversion property. When the dashpot is deformed or strained, fluid kinetic energy is transformed into heat by the dashpot. The dashpot's viscous resistance to strain is characterized by a coil viscosity, η_c. The apparent polymer coil extensional viscosity, η_e, is the ratio of coil extensional stress, σ_{coil}, to the coil extensional rate, $\dot{\varepsilon}_{coil} = d\varepsilon_{coil}/dt$, which is the change in the coil extensional strain, ε_{coil}, with respect to time, t. Thus, $\eta_e = \eta_c = \sigma_{coil}/\dot{\varepsilon}$ *when* $\sigma_{fluid} > \sigma_{yield}$. No coil extensional strain will develop until the applied extensional stress, σ_{fluid}, equals or exceeds the coil yield extensional stress, σ_{yield}. If the yield stress is zero, coil strain will develop when any extensional stress is applied. Under these conditions the mechanical system can be considered as only a dashpot.

The coil viscosity is expected to be a function of the extensional strain developed within the polymer coil. As a first approximation, it is assumed that this function is a polynomial.

$$\eta_c = \eta_{c0} + \eta_{c1}\,\varepsilon + \eta_{c2}\,\varepsilon^2 + \cdots \quad (3)$$

In Equation (3), the coefficients, η_{c0}, η_{c1}, and η_{c2}, will have constant values that depend upon polymer and solvent molecular properties. However at low extensional coil strains, the higher order terms in the above equation are probably not significant. Otherwise, in the limit of low extensional coil strains, the coil viscosity is expected to be a constant.

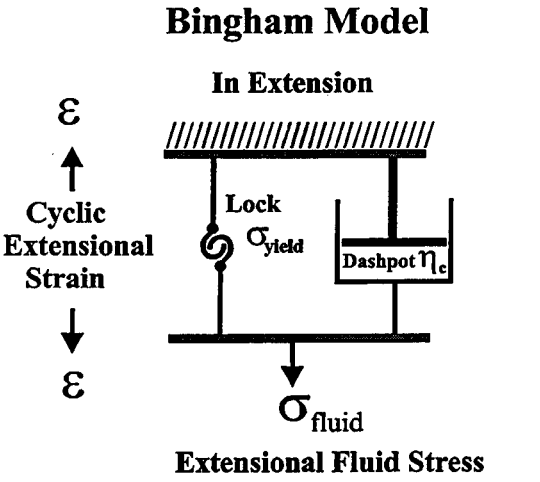

$$\eta_e = \eta_c \quad \text{for } \sigma_{fluid} > \sigma_{yield} \quad (1)$$

$$\varepsilon = 0 \quad \text{for } \sigma_{fluid} \leq \sigma_{yield} \quad (2)$$

Figure 7.2. Bingham Model

The above mechanical model for polymer coil extensional flow in a porous media suggests that for a polymer to be a good candidate as a mobility control agent in oil recovery (it forms a dilute solution that gives high resistance to flow within a reservoir) the polymer should have: 1) a large coil volume that maximize extensional fluid stress on the coil; 2) a coil viscosity that is low so coil strain can be experienced at low extensional stresses; and 3) no significant yield stress. These properties will enable polymer coil extension and contraction at the low displacing fluid flow rates experienced during reservoir flooding. Enablement of coil extension and contraction will decrease the displacing fluids mobility and thereby improve polymer flooding efficiency.

Extensional Flow of Polymer Solutions Through Screens

Several investigators have used fiber beds[2, 3] and arrays of cylinders[4] to study the extensional flow behavior of polymer solutions. Screens can also be used to simulate the extension-compression fluid flow fields found in porous media. Very restricting screens are available and sets of these screens placed in series will produce a cyclic extension-compression flow pattern similar to that found when flooding oil reservoirs. Screens have a thickness of three wire or thread diameters. See Figure 8.3 and Figure 8.4.

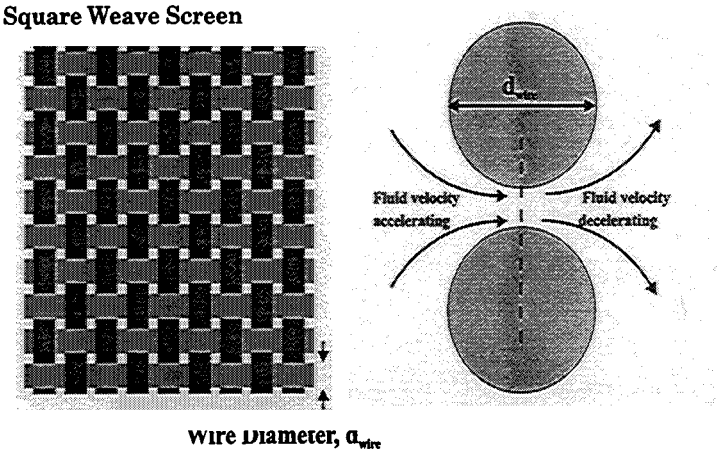

Figure 7.3. Wire screen.

The acceleration of the fluid velocity across a screen can be used to estimate the average fluid extensional rate, $\dot{\varepsilon}_{fluid}$. This is the change in fluid velocity over a distance of 1.5 screen wire diameters. The fluid reaches its maximum velocity when passing through the throat formed by adjacent wire threads. Using these criteria, the average extensional rate of a fluid passing through a plain square mesh screen made using wires of diameter d_{wire} and having a fractional free projected area, f, can be estimated by:

$$\dot{\varepsilon}_{fluid} = \frac{16Q}{3\,\pi\,D_s^2 d_{wire}} \frac{1-f}{f} \qquad (4)$$

where Q is the fluid volumetric flow rate through a circular screen of diameter D_s.

The average polymer coil extensional strain can be approximated from fluid flow conditions and screen geometry. In addition it is assumed that at low fluid extensional rates slippage between a polymer coil and its surrounding fluid will not develop or be a minimum after the yield point for coil extension is exceeded. Thus, $\dot{\varepsilon}_{coil} = \dot{\varepsilon}_{fluid}\, k_s$ where k_s is the slippage factor. A k_s value of unity signifies that no slippage develops between coil and surrounding fluid after the yield point for coil extension is exceeded. A lower value of the factor would indicate slippage, i.e., the coil extensional rate would be less than the surrounding fluid extensional rate.

$$\varepsilon_{coil} \approx \int_0^{t_{ext}} \dot{\varepsilon}_{fluid}\, k_s\, dt \approx \int_0^{t_{ext}} \frac{16\, k_s\, Q}{3\,\pi\,D_s^2 d_{wire}} \frac{1-f}{f} dt \approx \frac{2\, k_s [1-f]}{[1+f]} \quad for \quad Q \succ Q_{yield} \qquad (5)$$

If $Q < Q_{yield}$ then $\varepsilon_{coil} = 0$. In Equation (5), the time of coil extension was approximated as the average time for the fluid to traverse a distance equal to 1.5 screen wire diameters. Thus,

$$t_{ext} = 3\,\pi\,d_{wire}\,D_s^2\,f\,/\,[8\,Q\,(1+f)\,].$$

It was assumed that the coil extensional strain developed in passing through the first half of the screen passage of distance 1.5 d_{wire} is completely recovered over the second half of the screen passage that is also equal to 1.5 d_{wire}. This assumption of complete coil recovery after passage through each screen is probably valid if coil extensions are small.

At higher fluid volumetric flow rates, the polymer coils may retain some extensional strain after passage through each screen due to insufficient recovery time. They will not recover to an unperturbed coil state. Coil recovery will become restrictive when the time available for recovery (equal to the time of extension, t_{ext}) is much less than the characteristic recovery time for the polymer coil, λ_c. This recovery time is probably similar to the Zimm response time which can be estimated from the polymer molecular weight, M, solvent viscosity, μ_o, temperature, T, polymer intrinsic viscosity, η_{intr}, and gas law constant, R.

$$\lambda_c \approx \frac{25\,M\,\eta_{intr}\,\mu_o}{6\,\pi^2\,R\,T}$$

Past studies[7] suggest that coil extension will start when the coil extensional rate, $\dot{\varepsilon}_{coil}$, *equals* λ_c.

Power Usage During Flow Through Screens

If the fluid extensional stress is greater than the coil yield stress then the polymer coils within the solution are extended and thereafter compressed as they pass through a set of n screens connected in series. Power is required because of a cyclic strain introduced into the coils. At a volumetric flow rate of Q, the total power, Z_{total} across each screen due to the presence of polymer within the solution is given by

$$Z_{total} = \frac{(\Delta P_{solution} - \Delta P_o\,[1 + c\,\eta_{intr}]\,[1 - c\,\eta_{intr}])\,Q}{n} \qquad (6a)$$

$$Z_{total} = \frac{(\Delta P_{solution} - \Delta P_o\,[1 - (c\,\eta_{intr})^2])\,Q}{n} \qquad (6b)$$

As the volume fraction of polymer coils in the solution, $c\,\eta_{intr}$, becomes small then $1 - (c\,\eta_{intr})^2 \cong 1$.

Thus, in the limit of low $c\,\eta_{intr}$, $Z_{total} \cong \frac{(\Delta P_{solution} - \Delta P_o)\,Q}{n}$ (6c)

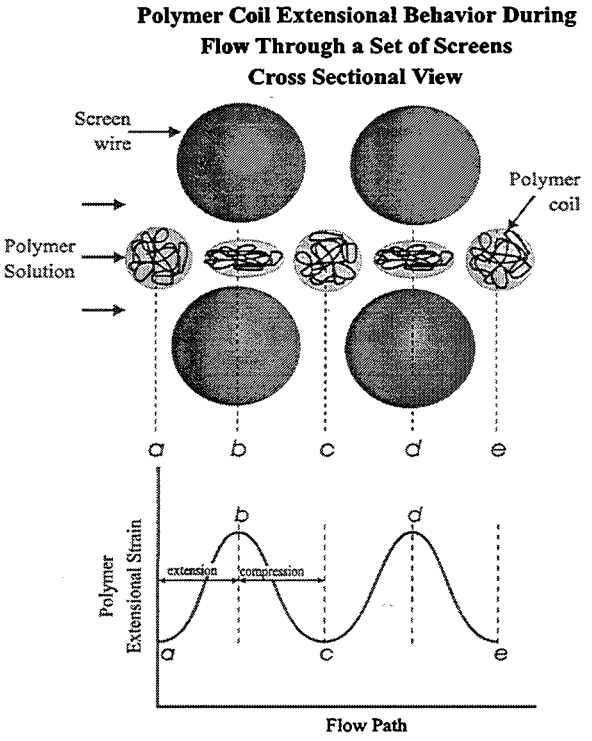

Figure 7.4. Polymer coil extensional behavior.

In Equation (6), $\Delta P_{solution}$ is the solution pressure drop across the set of screens and ΔP_o is the pressure drop across the screens of the solvent at the same flow rate, Q. The volume fraction of polymer in the solution is $c\,\eta_{intr}$ where c is the polymer concentration and η_{intr} is the polymer's intrinsic viscosity. The quantity $\Delta P_o [1 + c\,\eta_{intr}][1 - c\,\eta_{intr}]$ is the fluid pressure drop due to the volume fraction of solvent present in the polymer solution. Note that $\Delta P_o [1 + c\,\eta_{intr}]$ is the solvent pressure drop that would occur if polymer coils were present but did not experience extension or compression.

Each dashpot extension-compression cycle occurs over a distance of $3\,d_{wire}$. The fluid volume experiencing this cyclic strain over each screen is $3\,\pi\,\phi\,D_s^2\,d_{wire}/4$ where ϕ is the porosity of the screen. The number of polymer coils within this volume is $3\,\pi\,\phi\,D_s^2\,d_{wire}\,c\,N_A/(4M)$ where N_A is Avogadro's number and c is the mass concentration of polymer having a viscous average molecular weight of M. Therefore, the power required by each coil to pass through each screen, Z_{coil}, is the total power divided by the number of polymer coils within the fluid volume experiencing extension.

$$Z_{coil} = \frac{Z_{total}}{3\,\pi\,\phi\,D_s^2\,d_{wire}\,c\,N_A/(4M)} = \frac{4\,Q\,M(\Delta P_{solution} - \Delta P_o)}{3\,\pi\,\phi\,n\,D_s^2\,d_{wire}\,c\,N_A} \qquad (7)$$

Power Usage by a Kelvin System

The above power can also be equated to the strain developed in the Bingham system that is used to model a single polymer coil as it is extended and compressed in passing through a screen. In a complete cycle of extension and compression only the dashpot requires power. Power for this strain, Z_{coil}, is 2 times the product of the extensional force on the dashpot, F, times the extensional coil strain distance produced per unit time, dl/dt. The 2 is introduced because a power for coil compression is also needed in each strain cycle and this power is equivalent to the power for dashpot extension. The extensional force on the dashpot is the product of the stress on the dashpot, $\eta_c \dot{\varepsilon}_{coil}$ times the cross sectional coil area, $\pi d_{coil}^2/4$ where d_{coil} is the coil diameter.

$$F = \eta_c \dot{\varepsilon}_{coil} \pi d_{coil}^2/4 \qquad dl/dt = \dot{\varepsilon}_{coil} d_{coil}$$

$$Z_{coil} = 2F(dl/dt) = \frac{\pi d_{coil}^3 \eta_c}{2} (\dot{\varepsilon}_{coil})^2 \qquad (8)$$

The cube of the coil diameter can be estimated from a measurement of the polymer's intrinsic viscosity, η_{intr}. The intrinsic viscosity is the volume of coils per unit mass of polymer in solution. Thus, if each coil is a sphere of diameter d_{coil}, then $d_{coil}^3 = 6\eta_{intr} M/(\pi N_A)$. Introducing this into Equation (8) gives

$$Z_{coil} = \frac{3\eta_{intr} M \eta_c}{N_A} (\dot{\varepsilon}_{coil})^2 \qquad (9)$$

It is assumed that at low fluid extensional rates and low coil extensional strains slippage between a polymer coil and its surrounding fluid will not develop or will be at a minimum after the yield point for coil extension is exceeded. After the yield point is exceeded, $\dot{\varepsilon}_{coil} = \dot{\varepsilon}_{fluid} k_s$, where k_s is the slippage factor. A value close to one is expected. Slippage should increase with higher fluid extensional rates and larger polymer coil extensions. After substitution of $\dot{\varepsilon}_{coil} = \dot{\varepsilon}_{fluid} k_s$, Equation (9) becomes

$$Z_{coil} = \frac{3\eta_{intr} M k_s^2 \eta_c}{N_A} (\dot{\varepsilon}_{fluid})^2 \qquad (10)$$

Working Equation to Analyze Extensional Flow Data

Equation (7) can be combined with equation (10) to give

$$\frac{4Q(\Delta P_{solution} - \Delta P_o)}{9\pi\phi n D_s^2 d_{wire} c \eta_{intr}} = k_s^2 \eta_c (\dot{\varepsilon}_{fluid})^2 \quad for \quad Q > Q_{yield} \qquad (11)$$

Equation (4) can be used to express the extensional rates of Equation (11) in terms of screen geometry and fluid volumetric flow rates.

$$\frac{4Q(\Delta P_{solution} - \Delta P_o)}{9\pi\phi n D_s^2 d_{wire} c \eta_{intr}} = k_s^2 \eta_c \left[\frac{16(1-f)}{3\pi D_s^2 d_{wire} f}\right]^2 Q^2 \qquad (12)$$

Substitution into Equation (12) of $\beta = \dfrac{\pi D_s^2 d_{wire} f^2}{64 n \phi c \eta_{intr}(1-f)^2}$ and a subsequent rearrangement yields

a working equation that can be used to analyze polymer solution flow data.

$$(\Delta P_{solution} - \Delta P_o) = \frac{k_s^2 \eta_c}{\beta} Q \quad for \quad Q > Q_{yield} \qquad (13)$$

This relationship can be used to examine the fluid pressure data collected using a screen extensional rheometer. Plots of the values of the left side of Equation (13), the pressure drops across the screens due to the polymer versus values of the fluid volumetric flow rate, Q, should be a straight line with a zero intercept and have a slope, b, equal to $\eta_c k_s^2 / \beta$. Note that all the parameters needed in Equation (13) are known or can be measured. Thus, the Kelvin system dashpot or coil viscosity can be determined from plots of flow data using Equation (13) because $\eta_c = \beta b / k_s^2$. Recall that at low coil extensional strains it is expected that slippage is minium and thus $k_s \approx 1$.

The flow rate at which the polymer coils start to extend, Q_{yield}, can be determined by comparing a plot of solution pressure drop across the screens, $\Delta P_{solution}$, versus the solution volumetric flow rate with a plot of solvent pressure drop across the screens, ΔP_o, versus solvent volumetric flow rate. The flow rate at which the solution pressure drop deviates upward from the solvent pressure drop is Q_{yield}. The coil yield stress, σ_{yield}, is approximated as the product of the coil extensional viscosity, η_c, and the fluid extensional rate corresponding to Q_{yield}.

$$\sigma_{yield} = \eta_c \dot{\varepsilon}_{yield} = \eta_c \frac{16 Q_{yield}}{3\pi D_s^2 d_{wire}} \frac{1-f}{f} \qquad (14)$$

Fluid Extensional Rates in Sandstone

We can use the information developed by the screen rheometer to predict polymer solution flow behavior in oil bearing reservoirs. Sandstones have porosities,

ϕ, which range from 0.1 to 0.4 and permeabilities, $k_{sandstone}$, which vary from 1.0×10^{-10} to 3.0×10^{-8} cm^2 (10 to 3000 md). For many sandstone reservoirs, ϕ, can be related to $k_{sandstone}$ as shown in Equation (15).

$$\phi = A_{sand} + B_{sand} \log (k_{sandstone}) \quad (15)$$

The parameters, a and b, vary with the particular reservoir. Woodbrine sandstone values for A_{sand} and B_{sand} are 0.465 and 0.025, respectively, where $k_{sandstone}$ is expressed in cm^2 dimensions.[5]

$$d = \frac{1 - \phi}{\phi} \sqrt{\frac{180\, k_{sandstone}}{\phi}} \quad (16)$$

Although a sandstone reservoir is composed of compressed or consolidated sand particles, this porous media can be roughly characterized by an average sand sphere diameter, d. This diameter can be estimated from ϕ and $k_{sandstone}$ values of the reservoir using the Kozeny-Carman relationship, Equation (16).[6]

$$\dot{\varepsilon} = \frac{\sqrt{2}}{\phi} \frac{v}{d} \quad (17)$$

The reservoir characteristic particle diameter, d, can be used to estimate the extensional rate, $\dot{\varepsilon}$, for a fluid forced through the media at velocity, v.[7] See Equation (17).

The fluid velocity in the porous media, v, decreases as the distance from the injection wellhead increases. At large distances from the injection well, a typical displacing fluid velocity is about 1.0 ft per day.

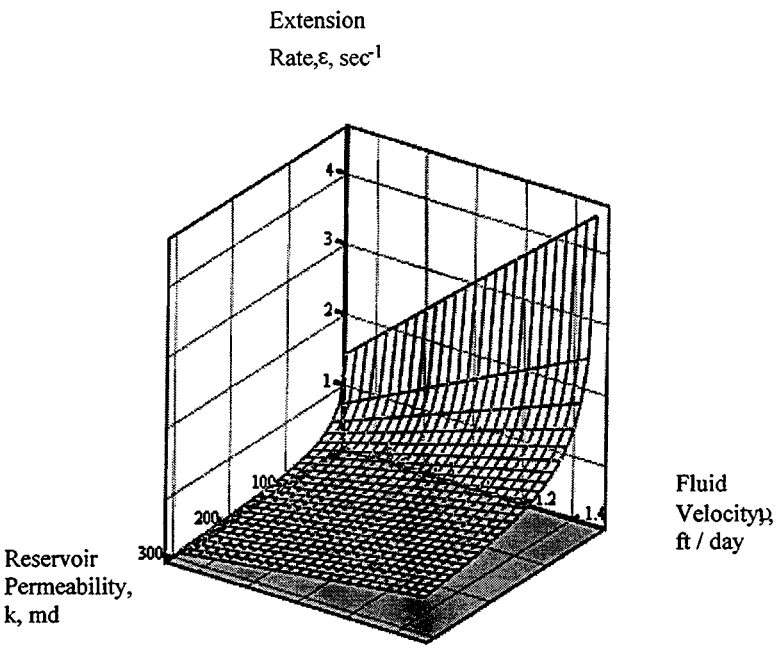

Typical Fluid Extension Rates in Woodbrine Sandstone

$(k, \upsilon, \varepsilon)$

Figure 7.5. Fluid extensional rates plot.

Fluid extensional rates can be calculated using the above information. Figure 8.5, shown above, gives a 3D plot of calculated fluid extensional rates for typical polymer flooding conditions in Woodbrine sandstone. These fluid extensional rates range from 0.5 to 5.0 sec^{-1}. Fluid extensional rates near the injection wellhead are much higher and vary from 50 to 500 sec^{-1}.

Therefore, for polymers to be effective in decreasing the mobility of a displacing fluid they must elongate at the low extensional rates of 0.5 to 5.0 sec^{-1} experienced during reservoir flooding. In addition, the polymers must not be over extended and broken into smaller molecular weights by the large fluid extensional rates developed at the wellhead.

Permeability of Polymer Solutions

As previously explained, the pressure drop of a polymer solution flowing through a porous media, $\Delta P_{solution}$, can be considered as the sum of pressure drop due to the solvent, $\Delta P_o (1 - c\,\eta_{intr})(1 + c\,\eta_{intr}) \approx \Delta P_o$, and the pressure drop due to the polymer, $\Delta P_{polymer}(c\,\eta_{intr})$. Examination of Equation (13) shows that for polymer solutions having no extensional yield point:

$$\frac{\eta_c}{\beta} Q = \Delta P_{polymer}(c\,\eta_{intr}) \qquad (18)$$

After inserting the definition of β, this equation can be rearranged as a Darcy equation[8].

$$Q = \frac{k_{polymer} A}{\eta_c L} \Delta P_{polymer} \qquad (19)$$

where $k_{polymer}$ is the polymer permeability when flowing through a porous media of cross sectional area, A, and length, L. When the porous media is a set of n screens placed in series as they exist in the screen rheometer then:

$$A = \frac{\pi D_s^2}{4} \qquad x = 3 \qquad \delta = x\, d_{wire} \qquad L = \delta\, n \qquad k_{polymer} = \frac{3\,\delta\, d_{wire}}{64\,\phi}\left(\frac{f}{1-f}\right)^2$$

As shown in the above equations, the length, L, can be considered as the product of the number of extension-compression cycles, n, and the distance between cycles, δ. For the screen rheometer,

$$x = 3 \text{ and } \delta = 3\, d_{wire}.$$

Applying the same logic used to develop the polymer permeability expression for flow through screens, polymer permeability can also be determined for solution flow through a bed packed with uniform spheres of diameter d_{sphere}. For beds of spheres, Equation (19) is valid when

$$A = \frac{\pi D_{bed}^2}{4} \qquad x = 1 \qquad \delta = x\, d_{sphere} \qquad L = \delta\, n \qquad k_{polymer} = \frac{\delta\, d_{sphere}\, \phi^3}{8}$$

The above relationships apply to polymer solution flow through a bed of solid spheres having diameter d_{sphere} with a porosity ϕ. The bed has a diameter of D_{bed} and a length L. The distance between extension-compression cycles, δ, is about one sphere diameter for beds of uniform spheres. Comparisons of the permeability expressions for screens and beds of packed spheres show that, as expected, the polymer permeability is strongly dependent upon the pore geometry. Pore geometry determines the number of extension-compression cycles per unit length of porous media, the fluid extensional rate developed each cycle, and the time fluid extensional forces are applied to the polymer coil during each cycle. Thus, the extent of polymer extensional strain each cycle is controlled by both pore geometry and the extensional force response properties of the polymer coil.

The flow of solvent through a porous media can also be expressed as a Darcy equation.

For any porous media $$Q = \frac{k_{solvent} A}{\mu_o L} \Delta P_o \qquad (20).$$

The solvent permeability, $k_{solvent}$, can be theoretically estimated or experimentally determined. For porous media made from stacks of screens[9] or beds of

uniform spheres[10] the theoretical solvent permeabilities at low fluid volumetric flow rates are:

$$\textit{Screens} \qquad k_{solvent} = \frac{d_{wire}\,\delta f^2}{50\,(\sqrt{f} - f)\,(1 - f^2)} \qquad \textit{Spheres} \qquad k_{solvent} = \frac{d_{sphere}^2\,\phi^3}{\psi\,(1 - \phi)^2}$$

From past work, the constant ψ is expected to be 175; however, our experimentation shows ψ to be approximately 225. Equations (19) and (20) can be used to determine the pressure drop of a polymer solution through any porous media.

$$\Delta P_{solution} = \Delta P_o + (c\,\eta_{intr})\,\Delta P_{polymer} = \frac{Q L}{A}\left[\frac{\mu_o}{k_{solvent}} + \frac{\eta_c}{k_{polymer}}\right] \qquad (21)$$

Rearrangement of Equation (21) gives the Darcy equation for a polymer solution.

$$Q = \frac{k_{overall}\,A}{\mu_o\,L}\,\Delta P_{solution} \qquad (22a) \qquad \textit{where} \quad k_{overall} = \frac{k_{solvent}}{1 + \dfrac{k_{solvent}}{k_{polymer}}\dfrac{\eta_c}{\mu_o}\,(c\,\eta_{intr})} \qquad (22b)$$

Equation (22b) defines an overall permeability, $k_{overall}$, for a polymer solution flowing through a porous media. Reducing the overall permeability directly decreases the mobility of the polymer solution in the porous media. Polymer solution flooding of oil reservoirs improves when the displacing solution mobility is lowered to values approaching the displaced fluid.

Equation (22b) shows that the overall permeability decreases as either coil viscosity increases or the volume fraction of polymer in the solution increases. The overall permeability also decreases when the ratio of solvent permeability to polymer permeability increases. This permeability ratio is only a function of reservoir pore geometry and therefore has a fixed value for each type reservoir. When this ratio approaches small values the overall permeability will approach the solvent permeability. This implies that only selective reservoirs that have favorable pore geometries ($r = k_{solvent} / k_{solvent} > 1$) are suitable for polymer flooding.

Mobility of Polymer Solutions in Porous Media

Fluid Mobility in Screens. If the porous media could be characterized as a set of screens, then the ratio of solvent permeability to polymer permeability, r, can be defined by the screen fractional free projected area, f, and the screen porosity, ϕ.

$$\textit{Screens} \qquad r = \frac{k_{solvent}}{k_{polymer}} = \frac{d_{wire}\,\delta f^2}{50\,(\sqrt{f} - f)\,(1 - f^2)}\,\frac{64\,\phi\,(1 - f)^2}{3\,\delta\,d_{wire} f^2} = \frac{64\,\phi\,(1 - f)^2}{150\,(\sqrt{f} - f)\,(1 - f^2)} \qquad (23)$$

For example if screens were used such that f = 0.16 and ϕ = 0.515 then from Equation (23), r = 0.67.

Using these screens and applying Equation (22) to a copolymer solution of $c\,\eta_{intr}$ = 0.1 and a coil viscosity η_c = 0.58 poise enables calculation of a mobility ratio, MR, where $MR = k_{solvent} / k_{overall}$. Water, the solvent, has a shear viscosity, μ_o, of 0.0089 poise at 25 °C.

$$Screens \quad MR = \frac{k_{solvent}}{k_{overall}} = 1 + \frac{k_{solvent}}{k_{polymer}} \frac{\eta_c}{\mu_o} (c\,\eta_{intr}) = 1 + (0.67)\left(\frac{0.58\,poise}{0.0089\,poise}\right)(0.1) = 5.36$$

This calculation shows that the copolymer solution would have a mobility through the screens that is 436% less than the solvent, water. In other words, the copolymer solution will require 5.36 times the pressure needed to force the same volumetric flow rate of solvent through the screens.

Fluid Mobility in Packed Beds of Uniform Spheres. If the porous media could be characterized as a packed bed of uniform spheres, then the ratio of solvent permeability to polymer permeability, r, can be defined by the porosity, ϕ.

$$Sphere\ Beds \quad r = \frac{k_{solvent}}{k_{polymer}} = \frac{d_{sphere}^2\,\phi^3}{255\,(1-\phi)^2} \frac{8}{d_{sphere}^2\,\phi^3} = \frac{8}{225\,(1-\phi)^2} \qquad (24)$$

For example, if sandstone had porosity, ϕ, equal to 0.367, then from Equation (24), r = 0.089. Using this bed and the same copolymer solution having a volume fraction polymer of 0.1 enables calculation of a mobility ratio for the polymer flowing through the bed of packed spheres. If the copolymer has the same coil viscosity as found for the screens then,

$$Sphere\ Beds \quad MR = \frac{k_{solvent}}{k_{overall}} = 1 + \frac{k_{solvent}}{k_{polymer}} \frac{\eta_c}{\mu_o} (c\,\eta_{intr}) = 1 + (0.089)\left(\frac{0.58\,poise}{0.0089\,poise}\right)(0.1) = 1.58$$

The above calculations indicate that when flowing through a bed of spheres the copolymer solution has a mobility that is only 58% less than that of the solvent.

This result is in contrast to the much larger decrease in the same copolymer solution mobility experienced when flowing through screens. The difference in the interstitial channel geometries between screens and sphere beds has altered the ability of the polymer solution to propagate through the porous media.

Conclusions on Fluid Extensional Viscosity in Flow Through Porous Media

Experimental results and theoretical analysis of the flow of polymer solutions through screens and packed beds of uniform solid spheres indicate that to reduce fluid mobility the polymer molecules in solution must experience cyclic extension and compression strain as they travel through the porous media. Polymer extensional

strain is maximized and solution mobility is minimized when three conditions are present: 1) the volume fraction of polymer coils in the solution is large, 2) the extensional rheology of the polymer is favorable and, 3) the porous media geometry can develop a fluid extensional flow field that exceeds the coil yield stress. If any single condition is not present, the desired reduction of solution mobility due to polymer extension will be nonexistent.

Only conditions 1 and 2 can be controlled when flooding an oil reservoir with a polymer solution. For oil reservoirs, the porous media geometry varies considerably from field to field and also at locations within a given field. Thus, the success of any oil reservoir polymer flooding is strongly dependent upon the geometry of the porous media. No polymer solution can be successful during reservoir flooding unless the porous media geometry can develop a fluid extensional flow field.

In the next chapter the relationships developed in this chapter will be used to characterize the extensional flow behavior of several polymer systems.

References and Notes

1. Hester, R. D. & L. M. Flesher, *Proceedings of the American Chemical Society, Div. of Polymer Materials: Science & Engineering*, 73, 486, 1995
2. Skartsis, L., B. Khomami and J. L. Kardos, *J. Rheol.*, 36(4), 581, 1992
3. Skartsis, L., *Polym. Eng. Sci.*, 32(4), 221, 1992
4. Jones, D. M. and K. Walters, Rheol. Acta, 28, 482, 1989
5. Collins, R. E., *Flow of Fluids Through Porous Materials*, Petroleum Pub. Co., Tulsa, OK (1976).
6. Scheidegger, A. E., *The Physics of Flow Through Porous Media, 3rd Ed.*, University of Toronto Press, Toronto, Canada (1974).
7. Durst, F. and R. Haas, *Rheol. Acta 20*, 179-92 (1981).
8. Amyx, J. W., D. M. Bass, R. L. Whiting, *Petroleum Reservoir Engineering - Physical Properties*, McGraw-Hill Book Co., New York, NY (1960).
9. Perry, R. H., D. W. Green, J. O. Maloney, *Perry's Chemical Engineers' Handbook*, 6th Ed., McGraw-Hill Book Co., New York, NY (1984).
10. Bird, R. B., W.E. Stewart, E. N. Lightfoot, *Transport Phenomena*, John Wiley & Sons, New York, NY (1960).

Nomenclature

The nomenclature for Chapter 7 is found at the end of Chapter 8.

CHAPTER 8: DILUTE POLYMER SOLUTIONS IN EXTENSIONAL FLOW EXPERIMENTAL OBSERVATIONS

Construction of a Screen Rheometer

A screen extensional rheometer (SER), designed to study the extensional flow characteristics of dilute polymer solutions, was constructed in the Polymer Science Department's Fabrication Center. Figure 8.1 shows a cross sectional drawing of the screen extensional rheometer. Also the three photographs, show below in Figure 8.2, displays the rheometer components and a fully assembled instrument. The rheometer uses a minimum internal fluid volume to direct fluids across a set of inexpensive and commercially available nylon screens (Small Parts Inc., Miami Lakes, FL). The 0.5 inch diameter screens can be obtained in various sizes and can be easily changed. Up to 150 screens can be placed in series within the housing. If desired, spacers can be placed between adjacent screens to increase the residence time between screens. Increased residence time between screens will allow more time for polymer coil strain recovery between cycles of coil extensional strain. As show by Figure 8.3, fluids are forced through the SER using an ISCO, model 500D syringe pump.

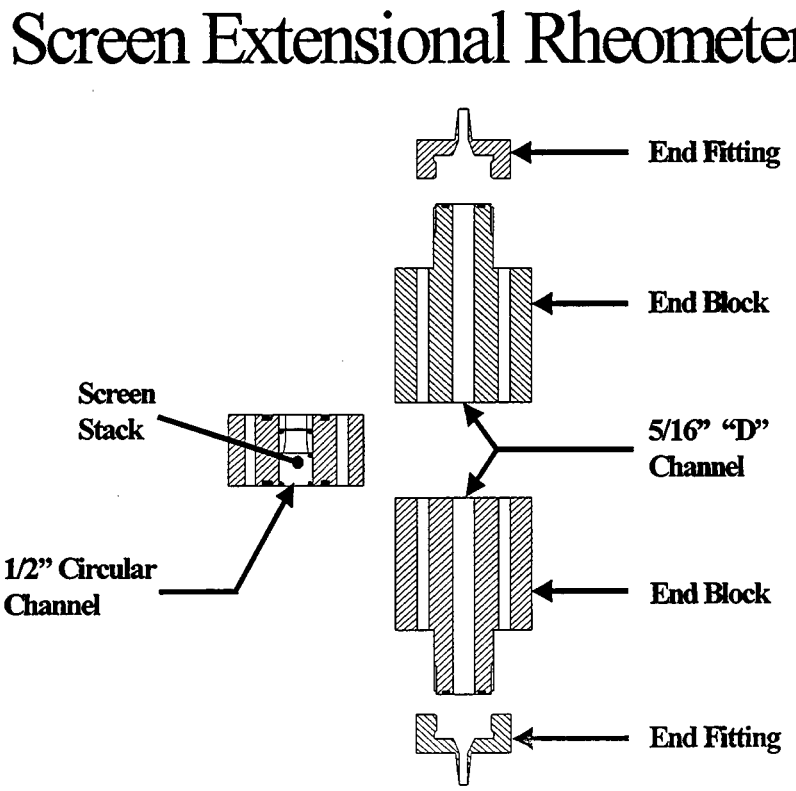

Figure 8.1. Screen Rheometer.

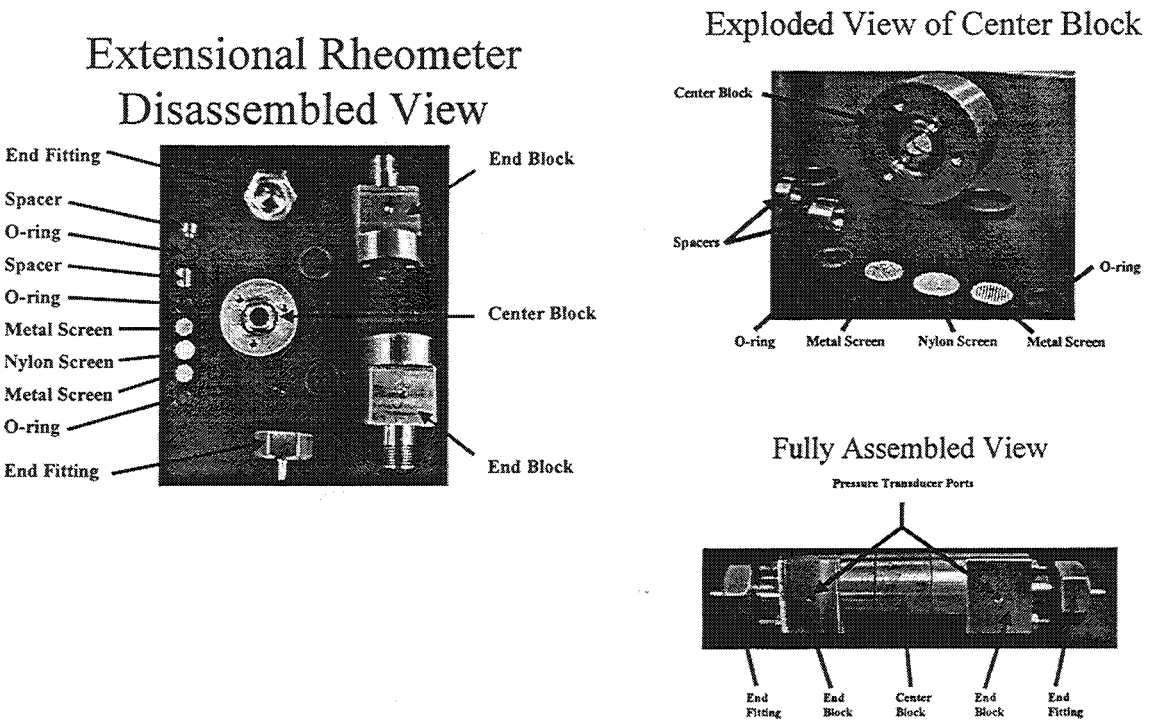

Figure 8.2. Extensional Rheometer components.

Two pressure transducers (Entran Devices, Inc., Fairfield, NJ) are used to measure fluid pressures before and after the screens. A transducer calibration technique was developed so that the screen rheometer can be used to accurately measure the extensional properties of dilute polymer solutions.

Transducer Calibration

The two transducers being used with the SER are rated to provide a linear response over the range of 0 to 10 psia. Because of the low pressure range, it was decided that a column of mercury would be the most accurate and rapid method for producing known pressures to calibrate the transducers. Transducer calibration followed the sequence outlined below. See Figure 8.3.

1. The SER was filled with water until the exit port to atmospheric pressure contained fluid.
2. The secondary outlet valve ② was closed.
3. Valve ① was opened to connect the SER to a mercury manometer.
4. The secondary outlet valve ② was thereafter opened to allow the mercury manometer to equilibrate to a height equal to atmospheric pressure. The

height was recorded.

5. Next, the primary outlet valve ④ was closed.
6. The transducer output voltages at the atmospheric pressure conditions were recorded.
7. The mercury injection valve ③ was opened and mercury was injected until the high pressure (before the screens) transducer output voltage increases to about 0.75 volt.
8. The two transducer output voltages were recorded.
9. Steps 7 and 8 were repeated until the mercury height was approximately 25 inches.
10. Mercury heights were converted into pressures and pressure vs. voltage data was plotted for each transducer. A linear calibration line was fitted to each set of data.

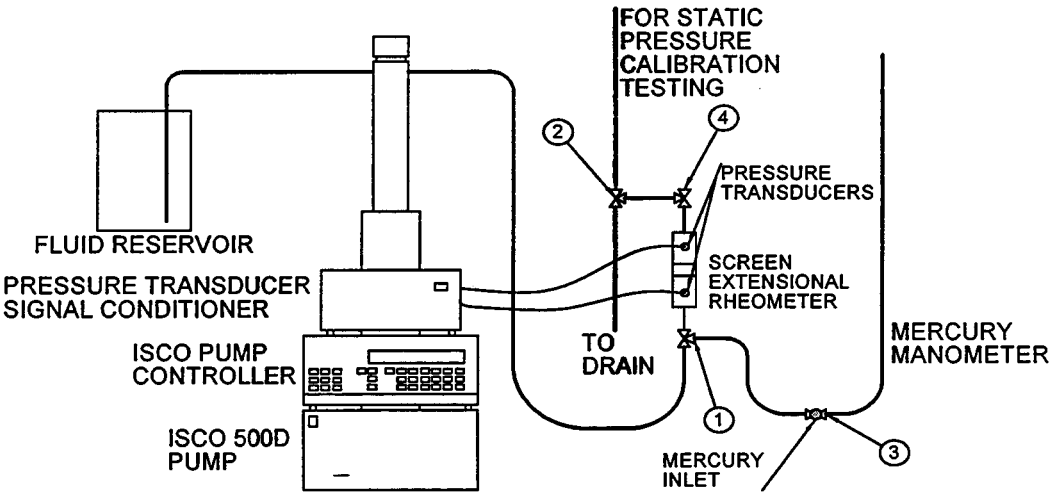

Figure 8.3. Screen Extensional Rheometer Calibration Schematic.

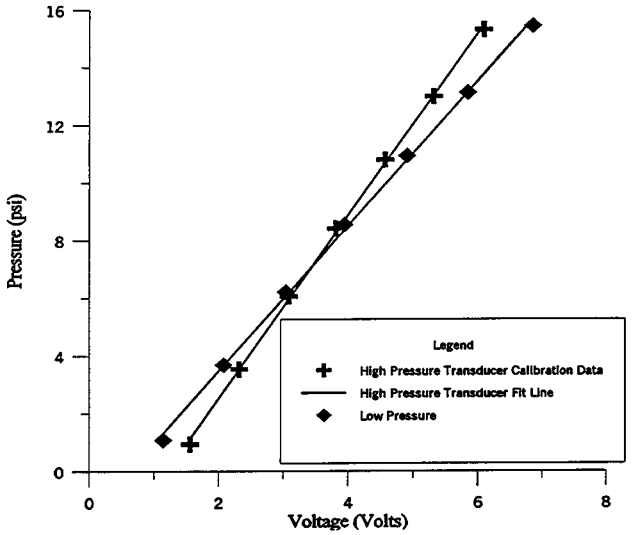

Figure 8.4. Typical Calibration Plot

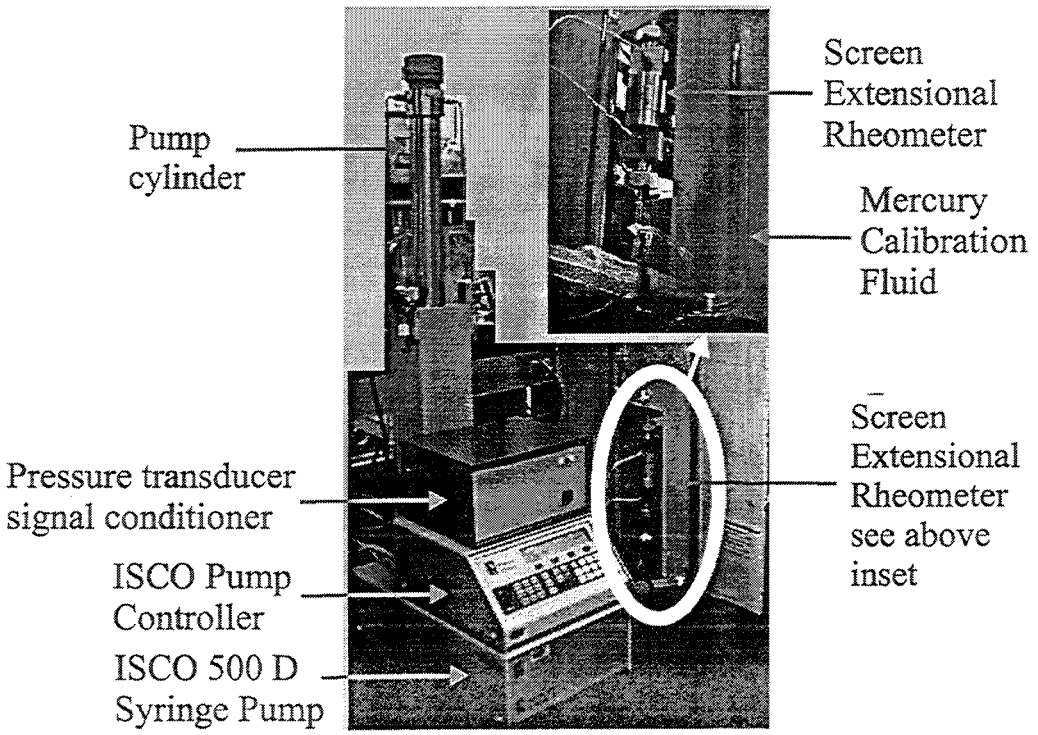

Figure 8.5: Screen Extensional Rheometer Photographs

Figure 8.4 shows a typical plot of calibration data. The data for each transducer was regressed to give a linear function fit. These fit functions were used to relate fluid pressures to transducer output voltages. A photograph of the extensional rheometer and its associated equipment is shown below in Figure 8.5.

Screen Rheometer Configuration

The 0.5 inch diameter screens used in the rheometer were obtained from Small Parts Inc., of Miami Lakes, FL. Each screen was made from a square mesh overlapping weave of small nylon filaments having a wire diameter, d_{wire}. Scanning electron micrographs were taken of several nylon screens so that the wire diameter and the fraction of free projected area located between nylon wires, f, could be directly measured from photographs of the highly magnified screens. These measurements confirmed that the wire diameter, 0.020 mm, and the fraction of free projected area, 0.16, were correctly specified by the vendor.

The material volume of a screen was determined by weighing a screen and then dividing by the density of nylon, 1.14 g / mL. The spacial volume of a screen is product of the area of the screen, $\pi D^2/4$, and the screen thickness. The screen thickness is three wire diameters, 3 d_{wire}. The screen open volume is the spacial volume less the material volume. The porosity, ϕ, is the ratio of the screen open volume to the spacial volume. Table 8.1 list the parameters defining the screens used in this study.

Table 8.1. Screen Rheometer Parameter Values

Screen Rheometer Parameter Description	Symbol	Value
screen diameter	D_s	1.27 cm
screen wire diameter	d_{wire}	0.020 mm
fractional free projected area of screen	f	0.16
porosity	ϕ	0.515
number of screen in series	n	30

Polymer Solution Description

Dilute solution flow properties of several acrylamide based polymers, polyacrylamide (PAM), a tetrapolymer, ATABAM 5-5, and diacetone acrylamide (DAAM 35), and a molecular weight range of poly(ethylene oxide) were investigated using the screen rheometer. Extensional flow curves for each of the acrylamide based copolymers and PEO homopolymers were generated. Polymer solutions were prepared

so that the volume fraction of polymer coils, $C^* = c\,\eta_{intr}$, equaled 0.1. Table 8.2 shows the chemical structure of the polymers used in this study.

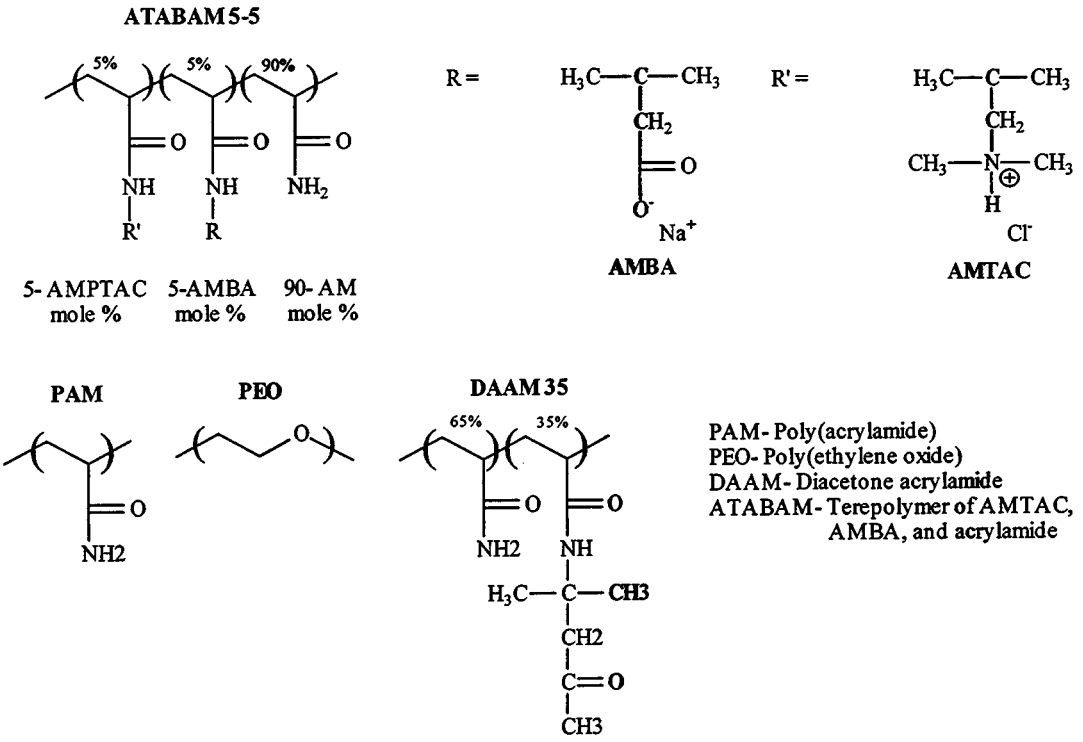

Table 8.2. Polymer Repeat Structures

To confirm that a polymer solution was truly dilute at a dimensionless concentration, C*, of 0.1, several polymer solutions were prepared at dimensionless concentrations lower than 0.1. Solution pressure drop measurements across the screens made on the same polymer at lower concentrations were always lower in direct proportion to the polymer concentration. This behavior is what is expected if all solutions are dilute. Therefore, a C* equal to 0.1 gives dilute conditions and thus no interaction exists between polymer coils. However, as the polymer concentration decreased, the noise associated with pressure data acquisition significantly increased. Thus, a dimensionless concentration of 0.1 was considered optimal with regard to both maintaining dilute solution conditions and minimizing noise.

Analysis of Extensional Flow Behavior of Dilute Aqueous Polymer Solutions

Poly(ethylene oxide) Solutions. Poly(ethylene oxide) homopolymers (PEO) having molecular weights of 0.9, 2 and 4 million molecular weight were purchased from Union Carbide of Danbury, CT. Dilute aqueous solutions of these polymers were

prepared such that all solutions concentrations, c, were $C^* / \eta_{intr} = 1 / (10\,\eta_{intr})$. The intrinsic viscosities of the 0.9, 2 and 4 million molecular weight polymers were measured as 5.5, 10.1 and 18.6 dL/g, respectively, using a Contraves, model 30, rheometer operating at a steady shear rate of 5.96 Hz. Therefore, the solution concentrations equivalent to a C* of 0.1 are 182, 99 and 54 ppm for the 0.9, 2 and 4 million molecular weight PEO polymers, respectively.

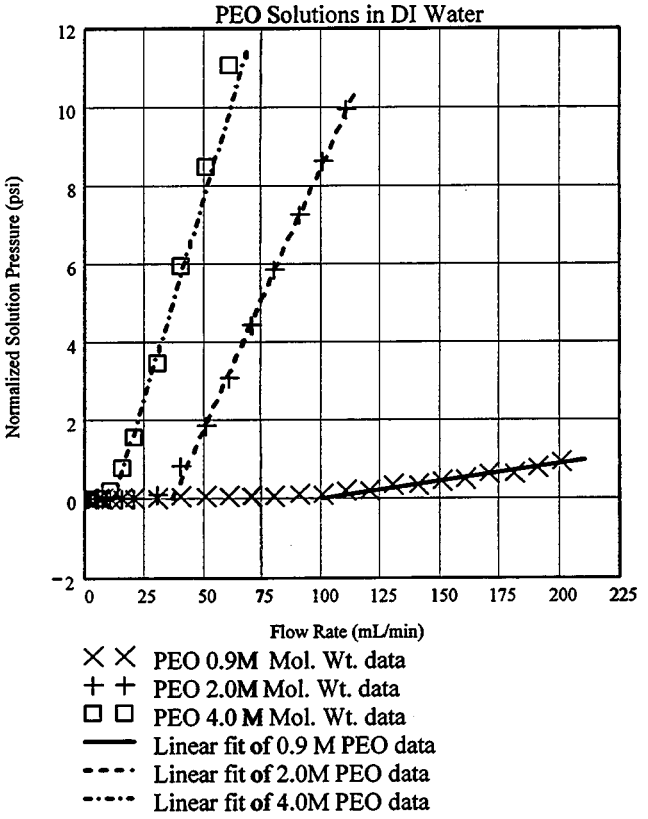

Figure 8. 6.: PEO Solutions

Solvent and all polymer solutions were forced through the SER at several volumetric flow rates using a set of 30 screens connected in series. The pressure drop across the screens was measured at each flow condition. Figure 8.6 shows the flow data plotted as suggested by Equation (13) of Chapter 7 ,i.e., $(\Delta P_{solution} - \Delta P_{solvent})$ *versus* Q. The value of $(\Delta P_{solution} - \Delta P_{solvent})$ is referred to as the normalized solution pressure and is the pressure drop across the screens that is due only to the presence of polymer in the solvent.

Note in Figure 8.6 that the normalized solution pressure (NSP) of the 0.9M mol. wt. PEO solution deviates upward from a value of zero at a flow rate of about 100 mL/min. This is the fluid flow rate, Q_{yield}, at which these polymer coils start to extend. This coil extension converts some of the fluid kinetic energy into heat. This energy transformation produces a solution pressure drop across the screens that is greater

than that for the solvent flowing through the screens at the same volumetric rate as the solution.

The NSP of the 2.0M mol. wt. PEO solution deviates upward at a flow rate of about 36 mL/min. The 4.0M Mol. Wt. PEO solution has a Q_{yield} that equals 12 mL/min. After identifying the Q_{yield} values for each polymer solution, Equation (14) of Chapter 7 was used to calculate the polymer coil extensional yield stresses, σ_{yield}, associated with each polymer. See Table 8.3, a summary of polymer properties, for the yield stress values.

At flow rates greater than the yield point, the initial NSP versus flow rate data for each polymer solution was fitted to a straight line. As explained in Chapter 7, the slope of each line was used to calculate the coil extensional viscosity, η_c, of each polymer Results are listed in Table 8.3.

Acrylamide Homopolymer Solution. The intrinsic viscosity of this 4 million molecular weight polyacrylamide homopolymer (PAM) was measured as 15.2 dL/g. The flow properties of an aqueous solution of the PAM were determined with the SER using a dimensionless concentration, C*, equal to 0.10. Figure 8.7 shows the flow data plotted as suggested by Equation (13) of Chapter 7. The PAM coil parameters, listed in Table 8.3, were calculated from the flow data as described for the PEO solutions.

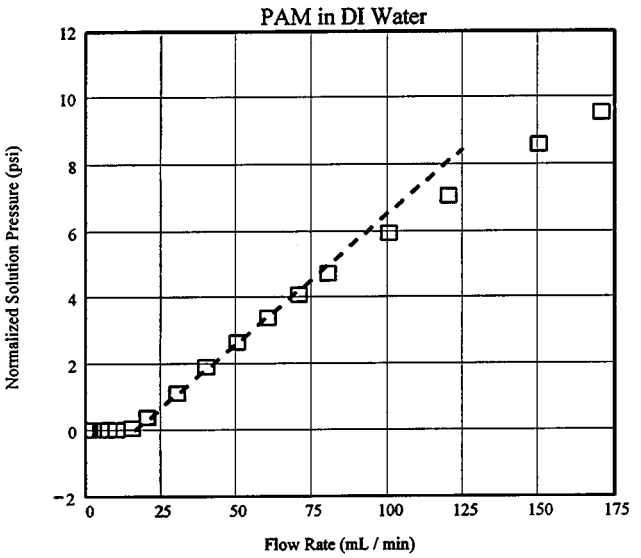

Figure 8.7. PAM Solution

The flow properties of dilute aqueous solutions of a ATABAM5-5 polymer, two AMBA25 copolymers, and a DAAM35 polymer were evaluated using the screen rheometer. All solutions were prepared such that the volume fraction of polymer coils in the solution, $C^* = c\,\eta_{intr}$, was always 0.1. The DAAM35 terpolymer was placed in three solvents, deionized water, NaCl (0.514M), and urea (6.0M). These solvents were chosen to study the effects of environment on polymer extensional flow behavior of the

DAAM35 terpolymer solutions.

The flow data for all polymer solutions were plotted as suggested by Equation (13) of Chapter 7. The data for all solutions were fitted to straight lines. See Figures 8.8 and 8.9. The slopes of the lines were used to calculate the coil viscosity of each polymer. Results are listed in Table 8. 3. Unlike the solutions of PEO, PAM, and ATABAM5-5, the two AMBA25 and the three DAAM35 solutions, regardless of solvent, had no measurable yield flow rate. If yield flow rates exists for these solutions, they must be less than 0.5 mL/min, the lower limit of the SER measurement resolution.

Table 8.3. Polymer & Solution Properties

Polymer & Mol. Wt.	Solvent	Intrinsic Viscosity dL / g	Polymer Coil Characteristic Time λ_c msec	Yield Flow Rate Q_{yield} mL / min	Extensional Yield Rate ε_{yield} kHz	Polymer Coil Extensional Viscosity η_c dyne sec / cm^2	Polymer Coil Extensional Yield Stress, σ_{yield} dyne / cm^2
0.9M PEO polyox WSR-1105	DI Water	5.5	0.075	100	4.61	0.12	550
2.0M PEO polyox WSR-N-60K	DI Water	10.1	0.31	36	1.66	1.72	2850
4.0M PEO polyox WSR-301	DI Water	18.6	1.13	12	0.55	2.65	1460
4.0M PAM	DI Water	15.2	0.93	16	0.74	1.01	750
ATABAM 5-5	DI Water	11.6	Mol. Wt. Not Measured	45	2.07	0.39	810
AMBA25 (4015-84)	DI Water	13.4	Mol. Wt. Not Measured	<0.5	<0.02	0.29	<6
AMBA25 (4015-86)	DI Water	9.2	Mol. Wt. Not Measured	<0.5	<0.02	0.10	<2
DAAM35	DI Water	8.4	Mol. Wt. Not Measured	<0.5	<0.02	0.017	<0.3
DAAM35	0.514 M NaCl	6.4	Mol. Wt. Not Measured	<0.5	<0.02	0.0025	<0.05
DAAM35	6 M Urea	7.6	Mol. Wt. Not Measured	<0.5	<0.02	0.024	<0.5

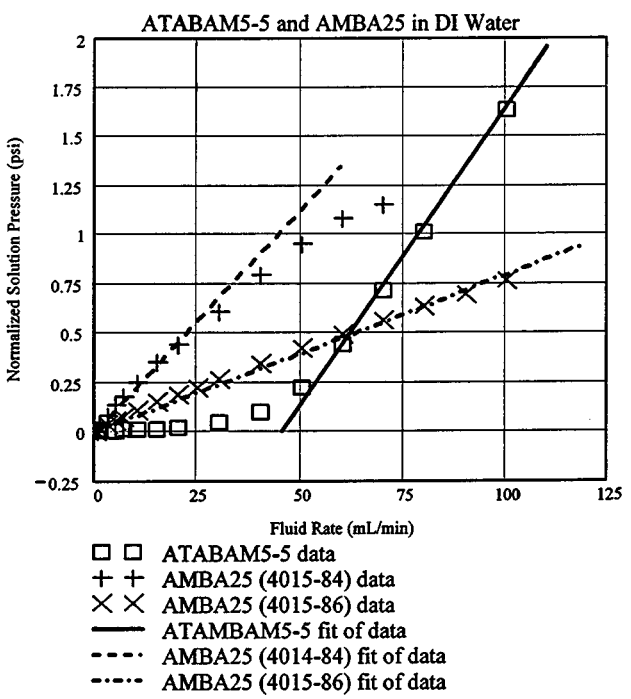

Figure 8. 8. ATABAM & AMBA Solutions

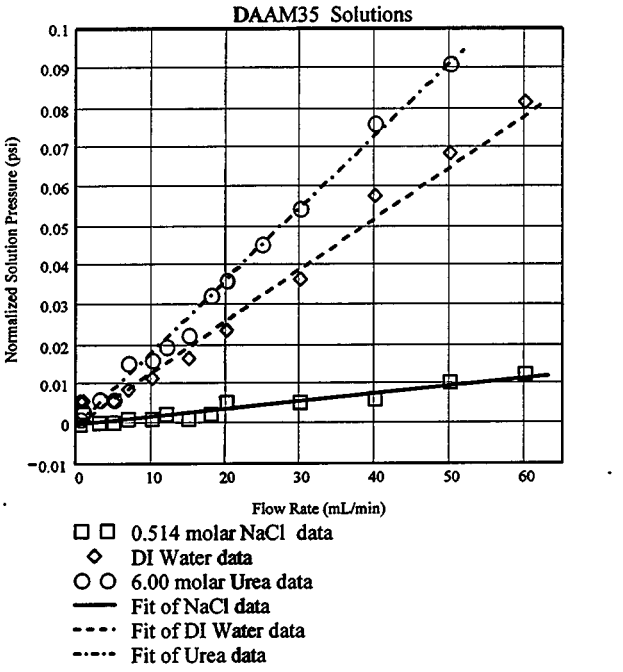

Figure 8.9. DAAM Solutions

Discussion of Results

As shown in Figure 8.9, the normalized solution pressures of the DAAM35 terpolymer solutions are solvent dependent. Table 8.3 reveals that the coil viscosity was a minimum in 0.514 molar NaCl, increased 700% in deionized water, and then increased 40% more in 6 molar urea. Solvents containing NaCl enhance polymer intra coil secondary bonding associations. In contrast, solvents containing urea diminish polymer intra coil secondary bonding associations. Thus for this polymer, larger coil extensional viscosities are developed by solvent additives that break up intra macromolecular structure.

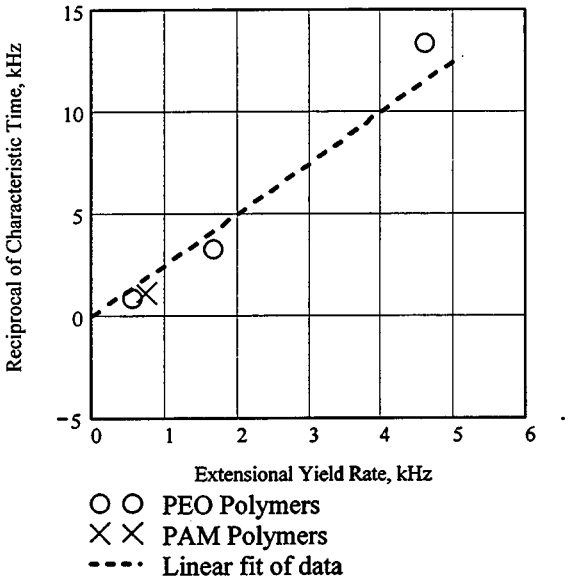

Figure 8.10.
Reciprocal of Polymer Coil
Characteristic Time Compared
To Observed Extensional Yield Rate

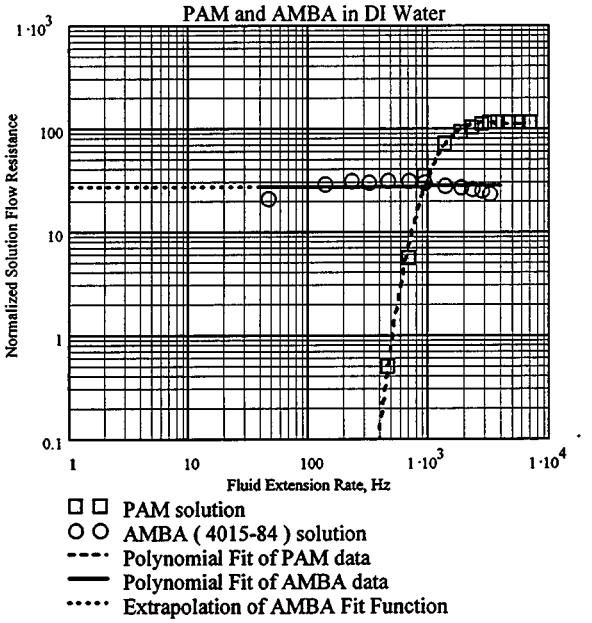

Figure 8.11.
Comparison of AMBA and PAM
Normalized Solution Flow Resistance

Table 8.3 shows that the polymer coil extensional yield rate is much lower for the higher molecular weight PEO than the lower molecular weight PEO. This suggests that lower molecular weight polymers having smaller coil diameters do not extend as easily as higher molecular weight polymers. For linear polymers it is expected that coil extension will begin when the fluid extensional rate approaches the reciprocal of the polymer coil characteristic time. Figure 10 indicates that the PEO and PAM polymers tend to follow this relationship. The polymer coil yield extensional rate is almost directly proportional to the reciprocal of the characteristic time, i.e., $\dot{\varepsilon}_{yield} \approx 2/(5\,\lambda_c)$. In contrast, the AMBA25 and DAAM35 copolymers do not follow this relationship and appear to have a zero coil yield extensional rate.

Table 8.3 also indicates that larger molecular weight polymer coils have larger coil extensional viscosities than smaller molecular weight polymers. Thus, when larger polymers extend they will convert more fluid kinetic energy to heat and thereby reduce fluid mobility to a greater extent than a smaller polymer.

In polymer flooding, fluid extensional rates and stresses within a reservoir become lower as the distance from the injection well increases. Therefore, for a polymer solution to be effective in decreasing fluid mobility at large distances from the injection well, it must be able to extend at very low fluid extensional rates, viz., 0.5 to 5 Hz. As shown by Figures 8.8 and 8.9, polymers such as AMBA25 and DAAM35 that apparently have no coil yield extensional rate would be more efficient in flooding than

the PAM or PEO polymers. These polymers appear to expand regardless of the displacing fluid flow rates. In contrast, the PAM and PEO polymers extend only at fluid flow rates that are much higher than typically found during reservoir flooding.

A more effective comparison of the flow resistance between polymer solutions can be made by defining the normalized solution flow resistance, NSFR[1,2]. The NSFR is the increase in solution flow resistance, $\Delta P_{solution} - \Delta P_{solvent}$, as compared to solvent flow resistance, $\Delta P_{solvent}$, per unit volume fraction of polymer coils in solution, $c\,\eta_{intr}$.

$$NSFR = \frac{\Delta P_{solution} - \Delta P_{solvent}}{\Delta P_{solvent}(c\,\eta_{intr})} \quad or \quad \frac{\Delta P_{solution}}{\Delta P_{solvent}} = 1 + (NSFR)(c\,\eta_{intr})$$

A polymer solution is more effective at reducing fluid mobility ($\Delta P_{solution} >> \Delta P_{solvent}$)when it has a high NSFR value and a large volume fraction of polymer coils in the solution. The NSFR is expected to be related to the ratio of coil extensional viscosity, η_c, to solvent viscosity, μ_o, i.e., $NSFR \cong (\eta_c / \mu_o) - 1$. In general, a polymer solution should have large NSFR values at the fluid extensional rates experienced when flooding the reservoir, typically 0.5 to 5 Hz. This condition should maximize oil displacement from the porous media.

As shown by Figure 8.11, the NSFR varies with the fluid extensional rate and type of polymer solution. For the PAM solution, the NSFR is zero at fluid extensional rates less than the coil extensional yield rate of about 3000 Hz. At the extensional yield rate the NSFR has a step change and suddenly increases to a value of 110. Above the extensional yield rate the NSFR remains at a nearly constant value of 110. This PAM solution would not be an acceptable displacing fluid for oil reservoirs because its NSFR is near zero at the fluid extensional rates experienced during flooding.

The AMBA solution NSFR values are almost constant at 30, regardless of the fluid extensional rate. Extrapolation of the AMBA solution behavior into the fluid extensional rate range typically experienced during flooding, 0.5 to 5 Hz, shows that the NSFR values are expected to be about 30. Thus, this AMBA solution would have good performance during flooding because the polymer coils of this solution extend even at very low fluid extensional rates.

Conclusions

This study suggests that for a polymer to be an acceptable mobility control agent the polymer should have

1) a large intrinsic viscosity - this minimizes the quantity of polymer needed for a given level of mobility control;

2) a coil viscosity that is high - this maximizes the NSFR and thus minimizes solution mobility; and

3) a coil extensional yield stress that is zero or very low - this insures that polymer coils will extend even at the low fluid flow rates experienced during reservoir flooding.

These desirable polymer properties will enable polymer coil extension in oil recovery

at the extremely low displacing fluid flow rates experienced during reservoir flooding and thereby improve flooding efficiency. Future copolymers designed for use in reservoir flooding should be synthesized with an effort directed at producing and controlling these desirable macromolecular properties.

References and Notes

1. Durst, F. and R. Hass, *Rheol. Acta. 20*, 179, 1981.
2. Hester, R. D. and C. L. McCormick, SPE/DOE 27823, *Proceedings of the Ninth Symposium on Improved Oil Recovery*, Tulsa, OK, 447, 1994.

Nomenclature

Symbol	Description
A	cross sectional area of a porous media
A_{sand}	intercept value for Equation (15) of Chapter 7
B_{sand}	slope value for Equation (15) of Chapter 7
b	slope, see Equation (13) of Chapter 7
C*	dimensionless concentration, $C^* = c\,\eta_{intr}$
c	mass concentration of polymer coils in solution
D_{bed}	diameter of packed sand bed
D_s	screen diameter
d	average sand diameter, see Equation (16) of Chapter 7
d_{sphere}	solid sphere diameter
d_{wire}	screen wire diameter
f	fractional free projected area of a screen
$k_{overall}$	overall fluid permeability
$k_{polymer}$	permeability of polymer coils
$k_{sandstone}$	permeability of sandstone
$k_{solvent}$	permeability of a Newtonian solvent
L	total length of the porous media
M	viscous average polymer molecular weight
MR	mobility ratio or ratio of solvent permeability to overall fluid permeability
N_A	Avogadro's number
NSFR	normalized solution flow resistance, $NSFR = NSP / [\Delta P_{solvent}(c\,\eta_{intr})]$
NSP	normalized solution pressure, $NSP = \Delta P_{solution} - \Delta P_{solvent}$